INFORMATION TO USERS

This dissertation was produced from a microfilm copy of the original document. While the most advanced technological means to photograph and reproduce this document have been used, the quality is heavily dependent upon the quality of the original submitted.

The following explanation of techniques is provided to help you understand markings or patterns which may appear on this reproduction.

1. The sign or "target" for pages apparently lacking from the document photographed is "Missing Page(s)". If it was possible to obtain the missing page(s) or section, they are spliced into the film along with adjacent pages. This may have necessitated cutting thru an image and duplicating adjacent pages to insure you complete continuity.

2. When an image on the film is obliterated with a large round black mark, it is an indication that the photographer suspected that the copy may have moved during exposure and thus cause a blurred image. You will find a good image of the page in the adjacent frame.

3. When a map, drawing or chart, etc., was part of the material being photographed the photographer followed a definite method in "sectioning" the material. It is customary to begin photoing at the upper left hand corner of a large sheet and to continue photoing from left to right in equal sections with a small overlap. If necessary, sectioning is continued again — beginning below the first row and continuing on until complete.

4. The majority of users indicate that the textual content is of greatest value, however, a somewhat higher quality reproduction could be made from "photographs" if essential to the understanding of the dissertation. Silver prints of "photographs" may be ordered at additional charge by writing the Order Department, giving the catalog number, title, author and specific pages you wish reproduced.

University Microfilms

300 North Zeeb Road
Ann Arbor, Michigan 48106

A Xerox Education Company

DIFFERENTIAL THERMAL ANALYSIS AND HIGH TEMPERATURE X-RAY DIFFRACTION OF THE LEAD SULFANTIMONIDES AND OTHER SELECTED SULFOSALT MINERALS

A dissertation submitted to the

Division of Graduate Studies
of the University of Cincinnati

in partial fulfillment of the
requirements for the degree of

DOCTOR OF PHILOSOPHY

in the Department of Geology
of the Graduate School of Arts and Sciences

1972

by

Larry E. Drafall

B.S., University of Illinois, 1967
M.S., University of Cincinnati, 1969

UNIVERSITY OF CINCINNATI

June 26 19 72

I hereby recommend that the thesis prepared under my supervision by Larry E. Drafall

entitled Differential Thermal Analysis and High Temperature X-Ray Diffraction of the Lead Sulfantimonides and other Selected Sulfosalt Minerals

be accepted as fulfilling this part of the requirements for the degree of Doctor of Philosophy

Approved by:

Frank L. Kourkey

Reuben G. Bullard

Form 668—Grad. School—1M—3-69

CONTENTS

Page

Abstract 1

Acknowledgements 4

Introduction 5

Structure 6

Methods and Procedures

- Differential Thermal Analysis 9
- Calibration of Temperature Recorder 11
- Mineral Synthesis 13
- X-ray Diffractometer 16
- Polished Sections 17
- X-ray Fluorescence 17
- Single Crystal Studies 20
- High Temperature X-ray Diffraction Camera 21
- Nonius Guinier - DeWolff Powder Diffraction Camera . . 23
- Computer Programming 25

Lead Sulfantimonides 26

- Zinckenite 27
- Plagionite 40
- Semseyite 50
- Boulangerite 56

Pb-Sb-S System 71

- Zinckenite 74
- Plagionite 76
- Semseyite 77
- Boulangerite 78
- Dadsonite and Heteromorphite 82

Minerals Without An Intermediate Transition 87

- Meneghinite 87
- Jamesonite 91
- Stannite 96

Page

Minerals With An Intermediate Transition 107

Enargite 107
Emplectite 121

Cu-Bi-S System 133

Conclusions 142

Geologic Applications 147

References Cited 150

Appendix 154

LIST OF TABLES

Number		Page
1	Localities of Natural Specimens	7
2	Transition Temperatures of Inorganic Substances	14
3	Minerals in the Pb-Sb-S System	26
4	Zinckenite Analyses and Cell Contents	28
5	Zinckenite X-ray Diffraction Data	30
6	Robinsonite X-ray Diffraction Data	31
7	Comparison of d-values for Robinsonite	36
8	Zinckenite Cell Refinement Data	39
9	Plagionite Analyses and Cell Contents	41
10	Plagionite X-ray Diffraction Data	43
11	Phase II Diffraction Data At Room and High Temperatures	46
12	Atomic Positions and Temperature Factors in Plagionite	48
13	Plagionite Cell Refinement Data	49
14	Semseyite Analyses and Cell Contents	51
15	Semseyite X-ray Diffraction Data	53
16	Semseyite Cell Refinement Data	55
17	Boulangerite Chemical Analyses	57
18	Boulangerite X-ray Diffraction Data	59
19	Comparison of d-values for Boulangerite at High Temperature	62
20	Comparison of d-values for Quenched Boulangerite	63
21	Atomic Parameters of Boulangerite	66
22	Boulangerite Cell Refinement Data at Room Temperature	67
23	Boulangerite Cell Refinement at Elevated Temperatures	69

LIST OF TABLES (Continued)

Number		Page
24	Pertinent Extracts for the Construction of Figures 20 and 21	73
25	X-ray Data for Phases Synthesized in the Pb-Sb-S System (from Craig, 1969)	80a
26	Dadsonite X-ray Diffraction Data	83
27	Heteromorphite X-ray Diffraction Data	85
28	Meneghinite X-ray Diffraction Data	89
29	Meneghinite Cell Refinement Data	91
30	Jamesonite X-ray Diffraction Data	93
31	Jamesonite Cell Refinement Data	94
32	Stannite X-ray Diffraction Data	98
33	Herzenbergite X-ray Diffraction Data	99
34	Atomic Parameters of Stannite	105
35	Enargite X-ray Diffraction Data	110
36	Tennantite X-ray Diffraction Data	111
37	Atomic Parameters for Enargite	117
38	Atomic Parameters for Tennantite	117
39	Enargite and Tennantite Cell Refinement Data	119
40	Emplectite X-ray Diffraction Data	124
41	Cuprobismutite X-ray Diffraction Data	125
42	Wittichenite X-ray Diffraction Data	126
43	Emplectite X-ray Diffraction Data at Elevated Temperatures	131
44	Wittichenite and Phase X Cell Refinement Data	138

LIST OF TABLES (Continued)

Number		Page
	Least Square Cell Refinement For:	
45	Zinckenite at Room Temperature from Pribram, Bohemia . .	156
46	Zinckenite at 527° C	158
47	Zinckenite at Room Temperature from Juliani, Peru . . .	159
48	Robinsonite at Room Temperature	161
49	Plagionite at Room Temperature from Wolfsberg, Germany .	163
50	Semseyite at Room Temperature from Kisbanya, Hungary . .	165
51	Galena at 657° C	167
52	Boulangerite at Room Temperature from St. Antonia, Calif.	168
53	Boulangerite at 593° C	170
54	Boulangerite at 593° C	171
55	Boulangerite at 593° C	172
56	Galena at 646° C	173
57	Meneghinite at Room Temperature from Bottino, Italy .. .	174
58	Jamesonite at Room Temperature from Huanuni, Bolivia . .	175
59	Stannite at Room Temperature from Mine LaFab, Bolivia .	177
60	Stannite at 490° C	178
61	Zincian Stannite at Room Temperature from Snowflake Mine, B.C.	179
62	Zincian Stannite at 607° C	180
63	Enargite at Room Temperature from Ouray Co., Colorado .	181
64	Tennantite at 590° C	182
65	Cubic Phase at 610° C	183

LIST OF TABLES (Continued)

Number		Page
66	Emplectite at Room Temperature from Johanngeargenstadt, Saxony	184
67	Cuprobismutite at 410° C	185
68	Cuprobismutite at 410° C	186
69	Cuprobismutite Quenched	187
70	Phase X at 480° C	188
71	Wittichenite at 480° C	189
72	Wittichenite Quenched	190
73	Phase X Quenched	191

LIST OF FIGURES

Figure		Page
1	Picture of DTA Apparatus	10
2	KNO_3 Thermograms	12
3	DTA Calibration Curves	15
4	Standard Curve for PbS	18
5	Standard Curve for Sb_2S_3	19
6	Picture of High Temperature Camera	22
7	Picture of Nonius Camera	24
8	Zinckenite Thermogram and Diffractogram	29
9	Zinckenite Powder Patterns	34
10	Robinsonite Powder Patterns	35
11	Structural Diagram for Zinckenite	38
12	Plagionite Thermogram and Diffractograms	42
13	Plagionite Powder Patterns	45
14	Structural Projection of Plagionite	47
15	Semseyite Thermogram and Diffractograms	52
16	Semseyite Powder Patterns	54
17	Boulangerite Thermogram and Diffractograms	58
18	Boulangerite Powder Patterns	61
19	Structural Diagram for Boulangerite	65
20	Equilibrium Diagram for the Pb-Sb-S System (Jaeger and Van Klooster)	72
21	Equilibrium Diagram for the Pb-Sb-S System (Iitsuka)	72
22	Equilibrium Diagram for the Pb-Sb-S System (Kitakaze)	79

LIST OF FIGURES (Continued)

Figure		Page
23	Equilibrium Diagram for the Pb-Sb-S System (Craig)	80
24	Equilibrium Diagram for the Pb-Sb-S System	81
25	Meneghinite Thermogram and Diffractograms	88
26	Jamesonite Thermogram and Diffractograms	92
27	Powder Patterns for Boulangerite, Jamesonite & Meneghinite	95
28	Stannite Thermogram and Diffractograms	97
29	Stannite Powder Patterns	101
30	Zincian Stannite Powder Patterns	102
31	Structural Diagram of Stannite	104
32	Enargite Thermogram and Diffractograms	109
33	Enargite Powder Patterns	113
34	Structural Diagram of Enargite	115
35	Structural Diagram and Tennantite	116
36	Emplectite Thermogram and Diffractogram	122
37	Emplectite Diffractograms	123
38	Emplectite Powder Patterns	129
39	Emplectite Powder Patterns at High Temperatures	130
40	Equilibrium Diagram for the Cu-Bi-S System (Gaudin & Dicke)	134
41	Equilibrium Diagram for the Cu-Bi-S System (Buhlman) . . .	135
42	Structural Diagram for Emplectite	139

ABSTRACT

This paper is a study of the thermal history of selected sulfosalts in regard to polymorphic and decompositional transitions. The invariant points were determined in an open system at one atmosphere of nitrogen pressure in the DTA apparatus and in a closed system at elevated temperatures in a high temperature powder camera.

The lead-antimony-sulfur system contains the minerals zinckenite, robinsonite, plagionite, semseyite and boulangerite.

Zinckenite ($PbS \cdot Sb_2S_3$) melts incongruently with the transformation ($540 \pm 5°$ C) into robinsonite.

Synthetic robinsonite ($7PbS \cdot 6Sb_2S_3$) melts incongruently ($575 \pm 5°$ C) into a liquid and phase II which is assigned the composition $5PbS \cdot 3Sb_2S_3$.

Plagionite ($5PbS \cdot 4Sb_2S_3$) melts incongruently ($575 \pm 5°$C) into phase II which in turn transforms ($595 \pm 5°$C) into boulangerite and liquid. At $643 \pm 5°$ C boulangerite reacts with the liquid to form another liquid and galena, some of which remains until 660° C.

Semseyite ($9PbS \cdot 4Sb_2S_3$) transforms ($575 \pm 5°$ C) in the solid state into boulangerite and phase II. At $595 \pm 5°$ C phase II melts and forms a liquid and boulangerite which then melts incongruently ($643 \pm 5°$ C) to galena and a liquid.

Boulangerite ($5PbS \cdot 2Sb_2S_3$) at high temperature probably is orthorhombic in symmetry and melts incongruently ($643 \pm 5°$ C) into galena and liquid.

Other low temperature hydrothermal sulfosalts studied by this method include enargite, emplectite and stannite.

Enargite [$3Cu_2S \cdot (As,Sb)_2S_5$], with the release of sulfur on heating, forms the high temperature mineral tennantite. With slow cooling in a closed system, tennantite resorbs most of the sulfur again to form enargite. Equilibrium of the transition depends on the partial pressure of sulfur. The transformation is not a function of melting and could occur at low temperatures with high sulfur pressure. If the temperature of crystallization of an ore deposit can be determined from other indicators, the enargite-tennantite transition could have a practical application in determining the partial sulfur pressure.

Emplectite ($Cu_2S \cdot Bi_2S_3$) transforms (390 $\pm$ 10° C) into the high temperature polymorph cuprobismutite which with continued heating (470 $\pm$ 5° C) transfers in the solid state to wittichenite and phase X. According to DTA data, wittichenite melts at 506° C, while phase X melts over the range 506-610° C. At 613 $\pm$ 5° C in a closed system, a phase formed which most likely has the composition $CuBi_2S_9$ as reported by Buhlman (1971). The experiments in this study with minerals and the work of Nuffield (1947) and Buhlman (1971) with synthetic mixtures, have found a phase X but no natural occurrence of the substance has yet been reported.

Stannite (Cu_2FeSnS_4) at room temperature produces an X-ray diffraction pattern distinctly tetragonal in symmetry while zincian stannite [$Cu_2(Zn,Fe)SnS_4$] gives a diffraction pattern much less tetragonal in appearance. Above 360 $\pm$ 5° C thermal expansion of the cell dimension happens to result in $2\,a_o = c_o$ producing a "cubic" resembling pattern.

The minerals jamesonite ($4PbS \cdot FeS \cdot 3Sb_2S_3$) and meneghinite ($Cu_2S \cdot 26PbS \cdot 7Sb_2S_3$) did not make an intermediate phase transition with heating.

With several of the sulfosalt minerals studied, the high temperature quenched modification had a more complex symmetry and often equal or greater density than the low temperature form. This is not expected if the true symmetry of the high temperature form was preserved, but might result from the "collapse" of a lower density, more symmetrical high temperature form. High temperature X-ray diffraction of boulangerite, robinsonite and cuprobismutite suggests that this is indeed the case.

ACKNOWLEDGEMENTS

I wish to thank Dr. Frank Koucky for his excellent advice and guidance during the research and for criticism of the paper. Additional thanks is given to Drs. Attila Kilinc and Reuben Bullard for criticism of the paper, to the University of Cincinnati, Department of Geology, for providing the mineral specimens used in the research, and to Wright-Patterson AFB in Dayton, Ohio for the loan of the Unicam high temperature camera.

INTRODUCTION

The purpose of this research was to study the thermal history of selected sulfosalts in regard to polymorphic and decompositional transitions by differential thermal analysis and high temperature X-ray diffraction.

Chatelier (1887) and Roberts-Austin (1889) first used differential thermal analysis and since then this type of analysis has become very valuable in the study of clay minerals, sulfates, zeolites and carbonates. Workers such as Kopp (1948), Hiller and Probathian (1955), Levy (1958), Asensio, Isidoro and Sabetier (1958), and Stone (1960) have experimented with sulfides, but DTA of sulfosalts has been rather neglected.

Until recently, sulfides have received little attention because of oxidation at low temperatures, destructive effects on thermocouples and sample holders, and recrystallization and vaporization of Sb_2S_3 at high temperatures. The use of special stainless steel alloys and inert gas atmosphere furnaces have alleviated many of the problems associated with the study of dry sulfides at elevated temperatures. Other difficulties encountered were the rare occurrence of most sulfosalts and their similarities in physical appearance. Many specimens in various collections were originally misidentified until X-ray diffraction was employed.

High temperature X-ray diffraction and differential thermal analysis at low pressure probably does not reflect conditions in many ore deposits, but are useful in outlining phase fields that could be studied later under greater pressure in hydrothermal systems.

The sulfosalts were selected to avoid minerals with a high percentage of arsenic and by the availability of pure samples which were obtained from the University of Cincinnati mineralogy collection and the U. S. National Museum in Washington, D. C. Table 1 gives a listing of the minerals studied and the locality where collected.

The structure of a particular mineral is discussed only if a transition occurred during heating or cooling. Unfortunately, the structure of sulfosalts has not been investigated very extensively and many questions remain to be answered concerning atomic positions, inter-atomic distances and several structural arrangements.

STRUCTURE

According to Berry (1965), sulfosalts can be thought of as "multiple" sulfides of the form AmBnXp in which A is one or more metals, B a semi-metal and X is sulfur or rarely Se. Lead and silver are the most common metals (A) in sulfosalts while copper and iron are less common with mercury, thallium, and manganese rare. The semi-metals are arsenic, antimony, bismuth, germanium, tin, vanadium, tellurium, and selenium.

Ross (1957) points out that many sulfosalts are commonly close packed in the cubic face-centered and hexagonal manner. The sulfur atoms are frequently in closest packing with the metal atoms generally in the interstices of the sulfur lattices. Slight deficiency or excess of atoms does not seem to alter the basic structure although substitution of a single metal in a basic structure may cause distortion or suppression of the symmetry. Ross indicates that there are about 12 basic structures

TABLE 1

LOCALITIES OF NATURAL SPECIMENS

Dana No.	Mineral	Museum No.	Location
388	Zinckenite	A1774	Pribram, Bohemia
"	"		Wolfsberg, Germany
"	"	J-1*	Julcani, Peru
"	"		Sacarambu, Romania
3742	Plagionite	A263	Wolfsberg, Germany
"	"		
3744	Semseyite	A860	Kisbańya, Hungary
"	"		Arnsberg, Germany
351	Boulangerite	A868	St. Antonia, Calif.
"	"		Rimini, Montana
"	"	A4337	Ouroro, Mexico
3311	Meneghinite	A888	Bottino, Tuscany, Italy
367	Jamesonite		Huanuni, Bolivia
2632	Stannite	A807	Mine La Fabulosa, Bolivia
	Zincian stannite	Ward's	Snowflake Mine, B.C.
3322	Enargite	A325	Ouray Co., Colorado
3592	Emplectite	A853	Johanngeorgenstadt, Saxony

A = University of Cincinnati collection number
NM = U.S. National Museum
* = Gift of Mr. Arenas (associated with Herminia Mine, Julcani District, Huancavelica, Peru.)

from which exist a large number of derivative forms because of atom substitution, additions, and defects like omissions and thermal disorder.

Strock (1936) recognized defect structures where a group of like-atoms could occupy singly or in common with other atoms, one set of equivalent positions, more than one set of the same coordination number, or positions of various coordination. Defect structures appear to be quite common due to the interstitial metal substitutions and thermal motion.

At elevated temperatures, Ross (1957) stated that chemically complex sulfides (and sulfosalts) may be transformed into simple structural types by thermal disorder. In a complex sulfide $MM'S_2$, the metal ions M and M' may become randomly distributed because of thermal agitation and interchange within a relatively stable sulfur network. As metal M' becomes indistinguishable from M, the structure becomes hybridized and higher crystal symmetry is imparted. The simple structure of phase (M,M')S is ultimately acquired. She concludes that basic high temperature forms of many complex sulfosalt minerals may be simple derivatives.

METHODS AND PROCEDURES

Differential Thermal Analysis

The Controlled Atmosphere Differential Thermal Analysis apparatus (Fig. 1), model KA-W, Serial #155 is manufactured by Robert Stone Co., Austin, Texas. The instrument has a Leeds and Northrup Speedomax H temperature recorder and a Speedomax W thermogram recorder.

An inert atmosphere of nitrogen at one atmosphere was flushed into the chamber after evacuation to keep the sulfosalts from oxidizing in the matched stainless steel alloy sample cups. Norton Alundum RR, the inert standard, was first placed in both cups to check the amount of base-line drift. The base-line or zero line represented the state where both the inert standard and the sample were heating at the same rate and were therefore at the same temperature. If the sample absorbed or released heat, the balance was destroyed and a peak was recorded on the chart representing the thermal differential between the inert standard and the sample.

The amount of baseline drift depends on how identical are the matched sample cups, the sensitivity, the heating rate, and the closeness in weight of the sample and the inert standard. In most runs, the drift was quite small and the base-line closely followed a vertical line on the recording chart.

The heating rate was 6° C/minute with a recording chart sensitivity of approximately 0.225 or 0.45 millivolts depending on the desired size of the peak. By not setting the sensitivity too high, the base-line was

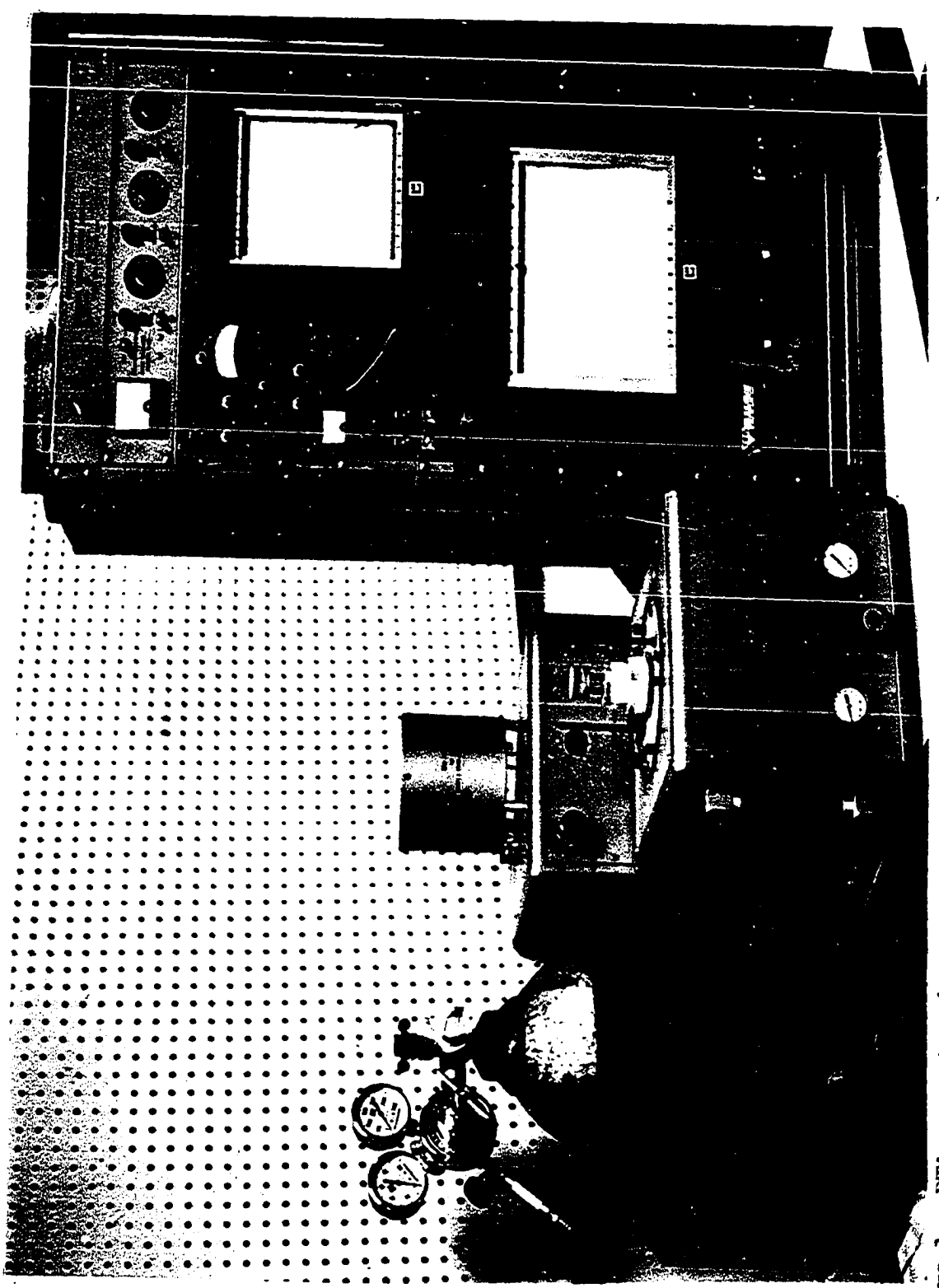

Figure 1. DTA apparatus (model KA-W, Serial #155), manufactured by Robert Stone Co., Austin, Texas

quite straight which allowed increased accuracy in reading the temperature where a peak departed from the base-line. By using the lower sensitivity, however, peak height and area also decreased. Figure 2 shows thermograms for the same substance (KNO_3) at different sensitivities. Note that with increased sensitivity, the base-line became more undulatory.

Alundum, placed in the cup, covered most of the terminal except the uppermost portion. The sample was placed in the cup so that direct contact was made with the top part of the terminal and the top part of the cup. When the mineral melted and cooled, the alundum kept the substance from hardening in the very bottom of the cup where it would have been impossible to remove. Direct contact remained between the terminal and sample at all times so that no lag occurred in recording temperature changes resulting from a transition or melting.

Sometimes several peaks occurred very close to the melting point which caused difficulty in determining where the transition involving recrystallization stopped, and melting began.

Calibration of Temperature Recorder

Several inorganic substances which gave sharp endothermic peaks, were used to calibrate the Leeds and Northrup Speedomax H temperature recorder on the DTA. At one hundred degree intervals, a pipping device made a one-half inch long mark on the thermogram. During heating of the furnace, the distance between successive marks at lower temperatures differed from the distance at high temperatures which indicated that the heating rate was not exactly linear. In order to check the recorder, substances were used which had inversions at various intervals ranging from 128° C to 652° C. Table 2 shows the results compared with the

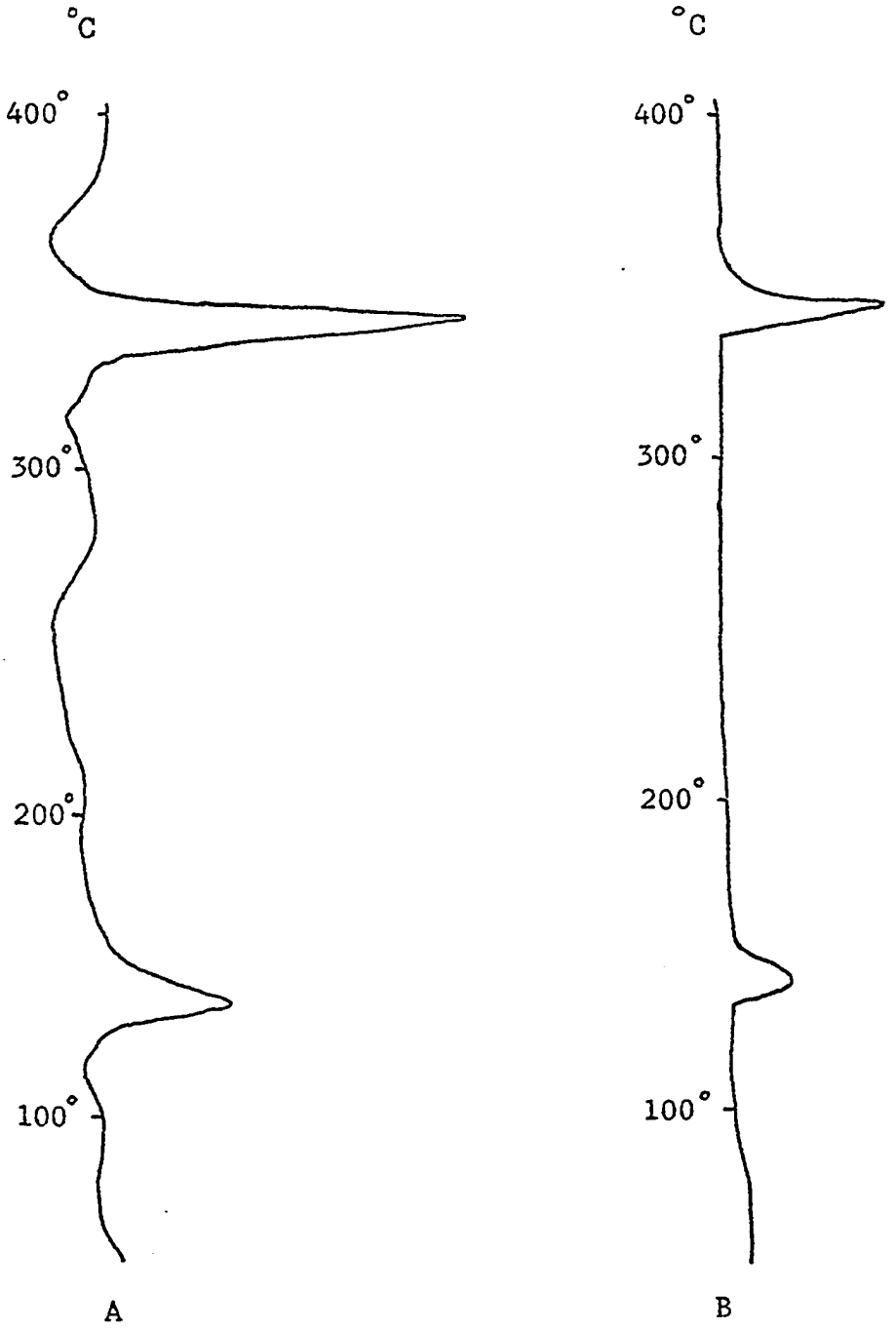

Figure 2 KNO_3 thermograms at two different sensitivities.
A) 0.225 millivolts B) 0.45 millivolts

accepted values taken from Barshad (1952) and the Handbook of Chemistry and Physics (1965-1966). In all cases, the temperatures record the initial departure from the base line and not maximum peak height temperatures. Transition temperatures for the minerals were adjusted to correspond with the temperature scale determined from the inorganic substances. Most of the minerals studied had transitions occurring between 500° C and 700° C where there was good agreement between the published and the recorded temperatures for the $\alpha \rightarrow \beta$ transition of quartz. Figure 3 shows the thermograms of the inorganic substances.

Mineral Synthesis

Synthetic minerals were stoichiometrically mixed (wt. %) which corresponded to jamesonite, zinckenite, semseyite, boulangerite, plagionite, and robinsonite. Dry reagent grade PbS, Sb_2S_3, Cu_2S, Fe and S were weighted on a Sartorius analytical balance accurate to .00001 g. to yield a final mixture of 5.0000 g. The mixture was then placed in a Spex mixer/mill for five minutes to homogenize the sample before being sealed in 3/8" vycor tubing. The vycor could be heated above 900° C without softening and more importantly the low coefficient of expansion of the silica glass, allowed for quenching in cold water without cracking.

A Kinney high vacuum pump (Model KC-2) evacuated the tubing and was kept running as the vycor was sealed with a gas-oxygen torch. The sealed tubes were heated in a Kanthal wire furnace with a Barber Colman temperature controller.

If elemental constituents were mixed for synthesis, high sulfur pressure could build up in the silica glass during heating, resulting in a possible explosion. In the case with jamesonite, where iron was

TABLE 2

Temperatures of transitions recorded on the DTA compared with the published values.

Substance	Type of reaction	DTA temp. ± 5°C.	Published temp.°C.
Ag_2SO_4	I	427	432 *
	M	645	652 *
quartz	I	574	573 #
KNO_3	I	129	129 #
	M	335	334 #
$AgNO_3$	I	160	160 *
	M	208	212 *
$NaNO_3$	M	304	306 #

I= inversion

M= melting

Taken from:

* Barshad, Am. Min., 1952

\# Handbook of Chemistry and Physics, 1965-66

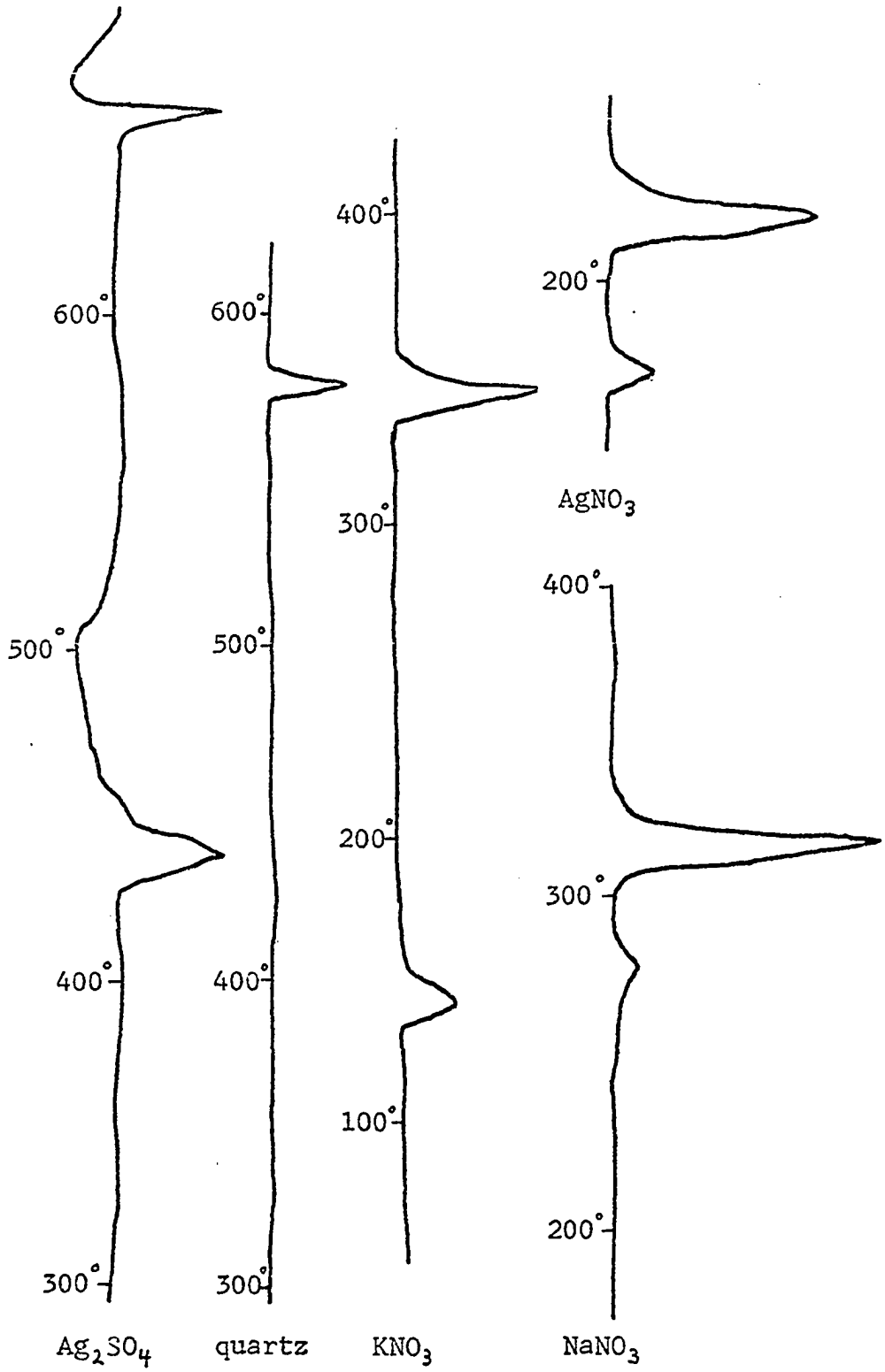

Figure 3 DTA Calibration Curves.

needed and no analytical grade FeS was available, elemental iron and sulfur were used, however the amount of sulfur was small and no problems resulted.

All the samples were melted in order to produce homogenization and lowered to experimental temperatures at furnace rate. If a high temperature phase was desired, the vycor tube was quenched by dropping it into cold water.

X-ray Diffractometer

An X-ray diffraction pattern was made of all minerals prior to heating in the DTA in order to verify the identification of the sample. A General Electric XRD-5 diffractometer was employed with nickel filtered copper radiation (CuK_α = 1.5405 Å) at 40 KV and 16 ma with a slit system of 3°/MR/0.1 (i.e., exit slit of 3° and detection slit of 0.1 with medium resolution sollar slits). A 2°/minute scan was used ranging from 16° two theta to around 50°.

The samples were ground in an agate mortar and a small amount of Duco cement, thinned with acetone, acted as the bonding agent in mounting the sample on glass slides. Peak intensities were estimated with the highest peak rated as 10 and the others scaled accordingly.

X-ray diffraction patterns indicated the heated samples were poorly crystallized because of the relatively rapid rates of cooling. In order to cool the minerals more slowly, the cooling water was turned off in the DTA furnace.

By holding the temperature at the point where a transition started, the atoms had a longer time to rearrange in the new structure and upon

cooling, the X-ray pattern showed much better crystallization than if the mineral was simply heated at the furnace rate above the transition temperature and then cooled.

Polished Sections

The samples used for the polished sections were placed in a 1-1/4" stainless steel sample holder and inserted in a Buehler hydraulic press using lucite thermoplastic as the mounting substance. The samples had to be heated to 140° C to melt the lucite and held at a pressure of 4200 psi. A Sampson-Patmore polisher was used to grind the sections for examination under a Leitz reflecting ore microscope.

The synthetic mixtures and natural minerals after heating above the melting point were usually porous and quite soft. These specimens generally produced poor polished sections and proved to be of limited value in this study.

X-ray Fluorescence

X-ray fluorescence was employed for major element analysis of lead and antimony. Various weight percentages of reagent grade PbS and Sb_2S_3 powder were mixed and pressed into discs to establish a standard calibration curve, however excess matrix absorption by the lead, resulted in a strongly nonlinear curve. By dilution of the desired 1 gram PbS-Sb_2S_3 mixture with .8000 grams silica and .2000 g lucite thermoplastic, the matrix absorption of the discs was greatly decreased and a useable standard curve could be attained. Discs were prepared by placing a 2.0000 g mixture (PbS,Sb_2S_3, silica, and lucite) in the bottom of the 1-1/4" stainless steel sample holder and two teaspoons of lucite deposited on

Figure 4

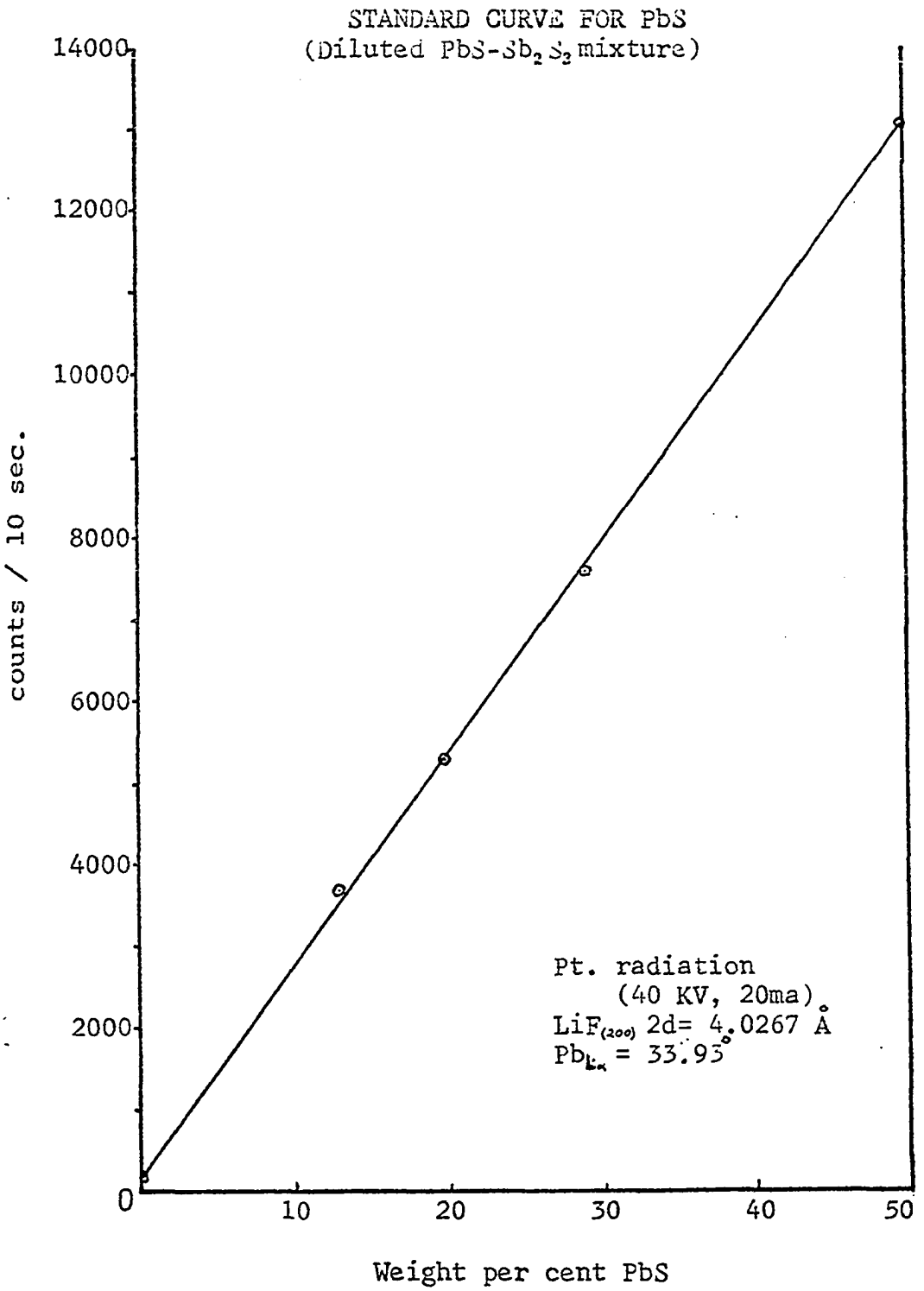

Figure 5

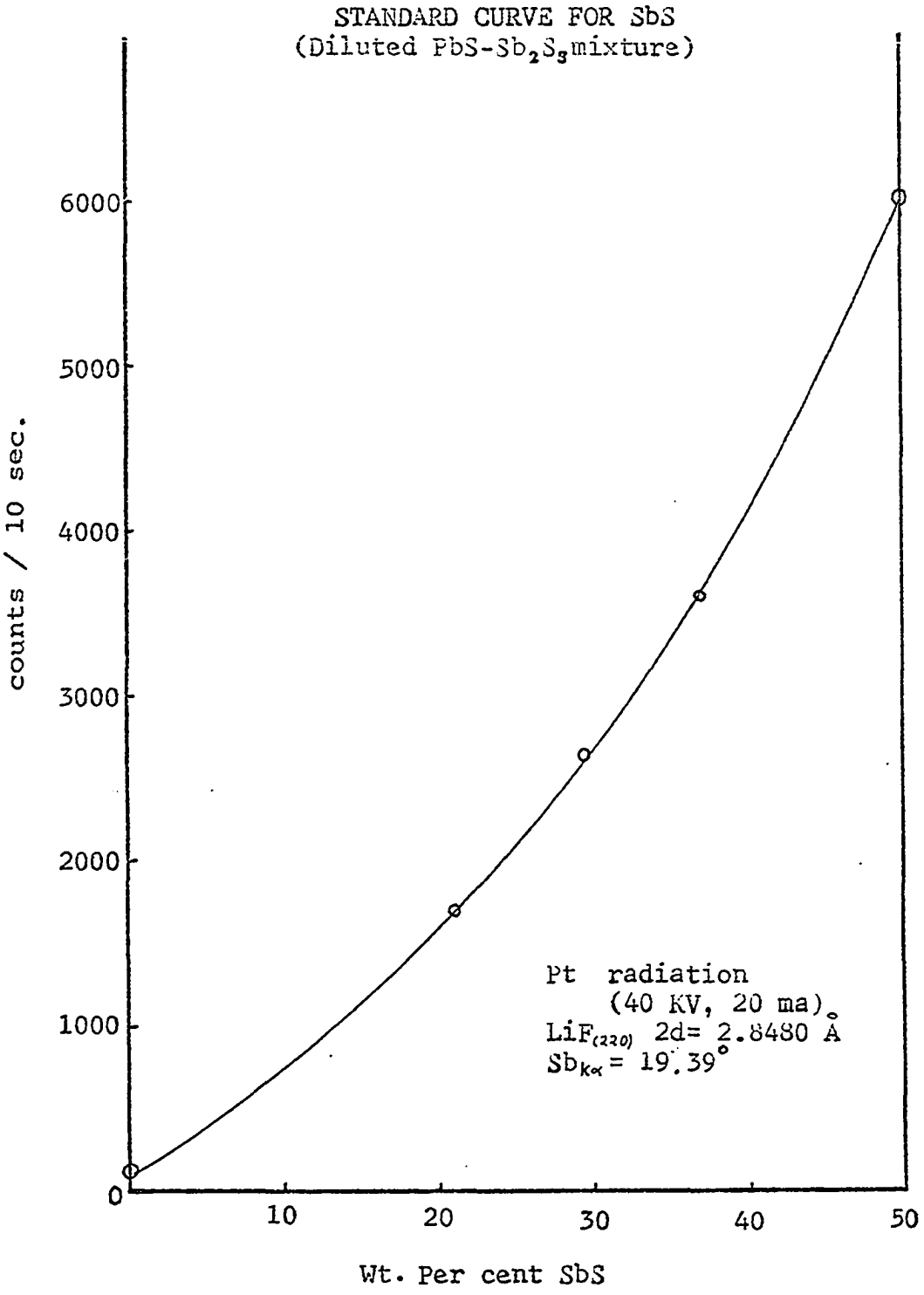

top. When melted and cooled the .2000 g of lucite in the sample acted as a binder and the resulting disc had a 1/2" clear lucite plastic layer with a 1/4" smooth coating of sample on one side.

A General Electric XSP-3 spectrometer was used with a platinum tube operating at 40 KV and 20 ma with a LiF analyzing crystal. For the standard lead curve, the LiF crystal, cut to give reflections off the (200) plane (2d = 4.0267 Å), was used and counts were taken on the PbLα peak at 33.93°. When establishing the standard curve for antimony, a new crystal of LiF cut to give reflections off the (220) plane (2d = 2.8480 Å), was used. The SbKα peak was at a small 2θ angle with the LiF (200) crystal and the roughness of the crystal gave a high background which interferred with the SbKα peak. (The LiF (200) enlarged the 2θ angle for SbKα from 13.46° out to 19.39° where more accurate peak to background counting could be made. Figures 4 and 5 show the standard calibration curves for lead and antimony, respectively.

All the mineral specimens of this study were analyzed by X-ray fluorescence to obtain a semi-quantitative range of composition of the elements. (Elements with an atomic weight lighter than potassium, including sulfur, were not studied since their energy was absorbed by air.)

Single Crystal Studies

Three minerals were studied by single crystal techniques using the Buerger precession and Weissenberg, X-ray cameras. A Stoe optical gnoniometer was employed for preliminary orientation before mounting on the precession camera for final alignment. In each case zero and one level photographs were obtained. Only very small crystals were available and

exposures with unfiltered FeKα = 1.9373 Å radiation at 35 KV and 16 ma ranged from 12-20 hours. The minerals studied will be discussed later in the text.

High Temperature X-ray Diffraction Camera

A Unicam S-150 High Temperature Powder Camera, manufactured by Unicam Instruments Ltd. of Cambridge, England, was used extensively in this study. Basically the camera furnace consists of two opposing hemispherical platinum shells with a 7.93 mm gap between shells for passage of the X-rays. Surrounding the furnace is a .002 inch thick aluminum foil X-ray window. The 19 cm diameter ring type film cassette encircles the window and records diffraction lines at Bragg angles from 5 to 85° on two film sections each 28.0 cm by 3.5 cm. The sample mounted on a three inch ceramic rod enters the camera from the top and is rotated by a small electric motor. A sheathed chromel-alumel thermocouple entering the camera from the bottom, was connected to a Leeds and Northrup millivolt potentiometer for temperature measurement.

A Welch Duo-Seal vacuum pump was operating continuously during a run and pulled a vacuum of about 25 microns (1×10^{-2} mm H_9) as measured by a thermocouple gauge.

The samples for the camera were sealed in tiny quartz tubes about .7 mm OD with a wall thickness of .01 mm. Quartz was used as a standard to calibrate the two faducia marks that appear on the film. Exposure times for high temperature patterns ranged from 3 to 5 hours using a copper tube (CuK_α = 1.5405) operating at 35 kilovolts and 12 milliamps with no filter. Intensities were estimated with the strongest line rating a 10 on a scale of 1/2 to ten.

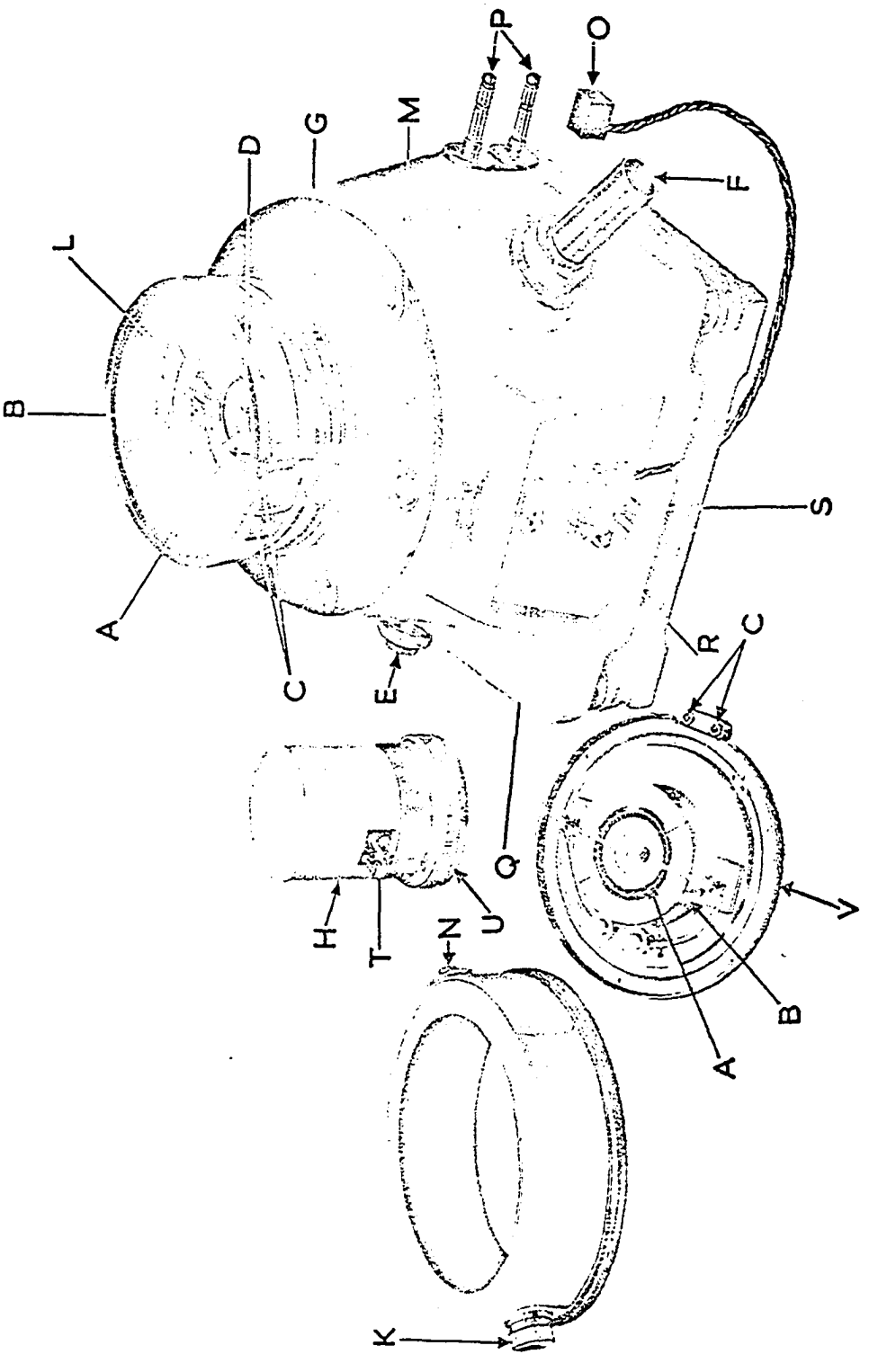

Figure 6. Unicam high temperature powder camera.

The quality of the high temperature patterns was not as good as the Nonius camera patterns because the quartz tubes and aluminum foil windows decreased intensities, most samples partially recrystallized, and absorption of X-rays by the sample.

Nonius Guinier - DeWolff Powder Diffraction Camera

The Nonius Guinier - DeWolff camera, manufactured in Delft, Holland was used extensively in this study for identifying minerals and quenched phases. The design of this camera is very unique in that the incident X-rays strike a monochromator (curved quartz crystal) and the K_α of $(10\bar{1}1)$ peak is diffracted off the crystal onto the sample which moves back and forth through the beam. Much of the radiation passes straight through the camera while only the K_α of each reflection is diffracted onto the film. Since no general radiation or K_β radiation reaches the film, the patterns have very little fogging and produce clear films even at very small theta angles.

Cobalt radiation (CoK_α = 1.7902 Å) was used which has a larger wave-length than copper radiation and spreads lines with small theta angles to larger angles allowing for better measurement of lines with large d-values. On conventional powder cameras, these lines would often be obscured by the general radiation fogging at low angles. (Note that many of the lines with very large d-values were recorded with the Nonius camera that had not been reported in the literature where regular powder cameras were used.)

The Nonius camera has a special holder which X-rays four samples at once; usually a standard such as quartz and three samples which are pressed on Scotch Magic Mending tape. The tape is transparent enough not

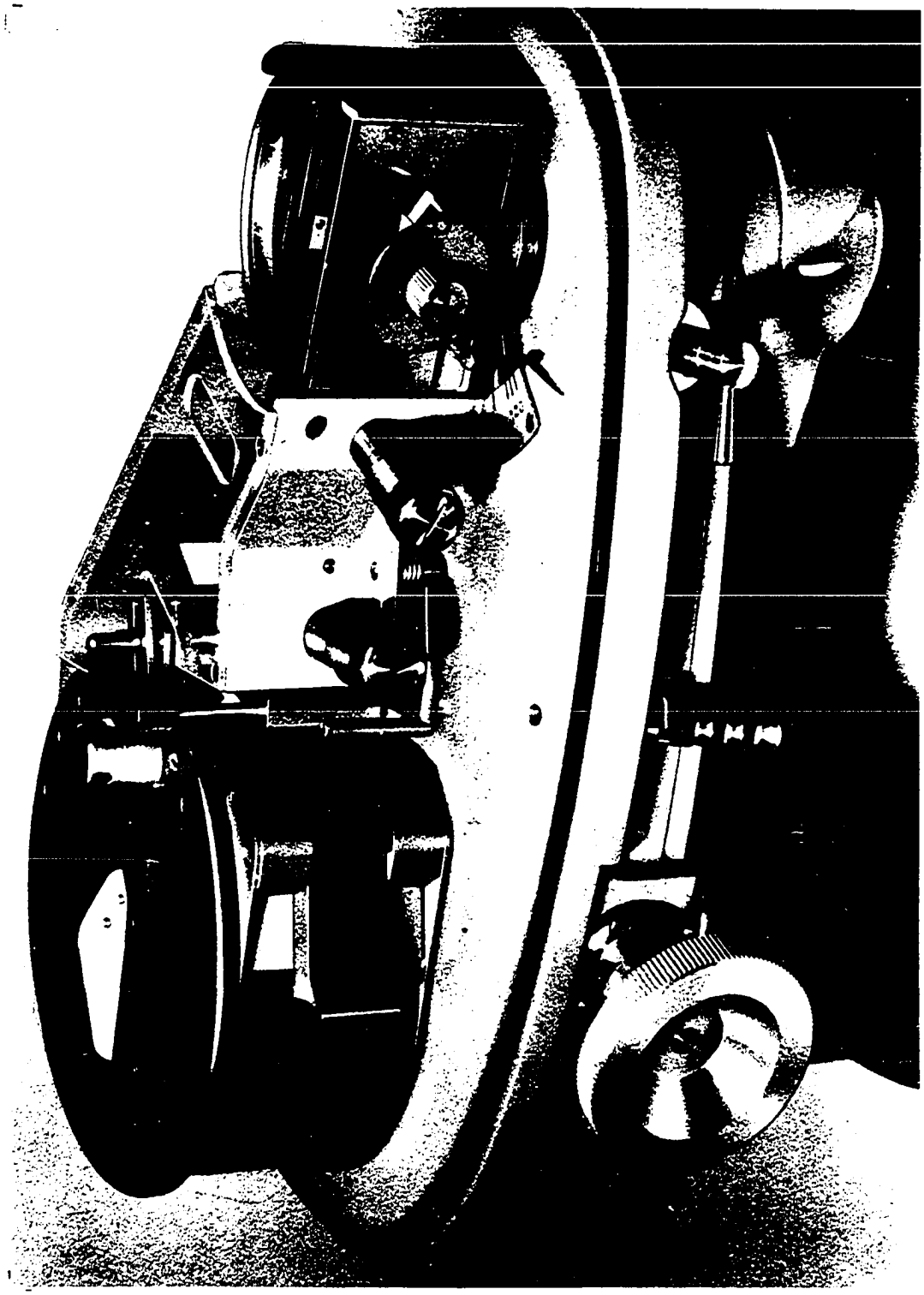

Figure 7. Nonius Guinier-DeWolff powder camera.

to impair intensities while also not producing any diffraction lines.

Calibration of the film is easily accomplished by measuring the quartz standard and applying the correction factor to the other samples. This comparison to a quartz standard allows very high accuracy ($\pm$ .002 Å) since film shrinkage is compensated for.

Another advantage of the Nonius camera is that very little sample is required to produce a good pattern. (Care must be taken to grind the sample to a fine powder to eliminate spotty lines.)

Normal exposure time was approximately 20 hours with a $Co_{K\alpha}$ X-ray tube operating at 35 kilovolts and 12 milliamps. Again intensities were estimated with the strongest line rated a 10 on a scale of 10.

Computer Programming

An IBM 360 computer was used for the least squares unit cell refinement. The Fortran IV program refined approximate starting values for unit cell lengths and unit cell interaxial angles, and also determined the appropriate (hkl) for the observed reflections.

All cell refinements at room temperature used data measured from the Nonius film and all elevated temperatures refinements used data from the Unicam camera.

LEAD SULFANTIMONIDES

The lead-antimony-sulfur system contains the minerals fülöppite, zinckenite, robinsonite, plagionite, semseyite, and boulangerite arranged in increasing Pb:S ratio. All of these minerals were studied except fülöppite, where no suitable sample was available.

TABLE 3

MINERALS IN THE Pb-Sb-S SYSTEM

Name	ratio of $PbS:Sb_2S_3$	Formula	Wt. % PbS	Wt. % Sb_2S_3	Synonym
fülöppite	3:4	$Pb_3Sb_8S_{15}$	34.5	65.5	
zinckenite*	1:1	$PbSb_2S_4$	41.0	59.0	keeleyite
robinsonite*	7:6	$Pb_7Sb_{12}S_{25}$	45.1	54.9	"mineral X"
plagionite	5:4	$Pb_5Sb_8S_{17}$	46.8	53.2	
semseyite	9:4	$Pb_9Sb_8S_{21}$	61.3	39.7	
boulangerite*	5:2	$Pb_5Sb_4S_{11}$	63.7	36.3	mullanite, yenerite, falkmanite, epiboulangerite

* Feather ores - needle like acicular crystals

ZINCKENITE

Zinckenite ($PbSb_2S_4$) was named after the mineralogist and mining geologist J. K. Zincken (1798-1862), and early work on this mineral was done by Rose (1826), Groth (1882), Eakins (1890) and Gordon (1922). Zinckenite forms thin striated [0001] prismatic crystals often found in fibrous aggregates associated with jamesonite, boulangerite, bournonite, stibnite and other sulfosalts.

Vaux and Bannister (1938) determined the unit cell as hexagonal although originally zinckenite was considered orthorhombic (pseudo-hexagonal) with twinning on (110). Nuffield (1945) confirmed the cell dimensions which are:

$$a = 44.15 \qquad c = 8.62 \qquad A = 80 \text{ or } 81 \qquad P6_3$$

A zero-level Weissenberg photograph about the needle axis [0001] of a zinckenite crystal from Pribram, Bohemia (A1774) was obtained which confirmed the hexagonal symmetry and was very similar to the zero-level photograph given by Nuffield (1945). (Table 4 gives the chemical analyses of zinckenite.)

DTA

A sample of zinckenite from Pribram, Bohemia was heated to 600° C, cooled, and X-rayed. The diffraction pattern indicated that the quenched high temperature phase was quite similar to robinsonite. The thermogram (Fig. 8) showed two endothermic peaks rather close to each other between 500° C and 600° C. By making a series of runs, the first endothermic peak was found to correspond to the transition of zinckenite into robinsonite. The second peak represented the melting of robinsonite but the start of melting was difficult to determine because of the

Table 4

Zinckenite: Analyses and Cell Contents*

M= 46,907

	1	2	3	4	5	6	A	B
Pb	31.84	30.80	34.33	29.33	34.58	34.58	35.79	32.60
Fe	...	...	0.06	0.08	0.05	0.14	...	...
Cu	0.42	...	0.70	...	...	...	...	...
Sb	44.39	46.18	42.15	46.17	42.30	42.30	42.06	44.70
	...	...	...	...	0.48	...	...	...
S	22.58	23.04	22.63	23.10	21.84	21.63	22.15	22.70
	99.23	100.02	99.87	99.62[1]	99.70	98.65	100.00	100.00
Pb	72.63	69.71	77.81	67.28	78.51	79.35	81 80	72
Fe	...	...	0.51	0.68	4.21	1.19	.. ..	..
Cu	3.12	...	5.17	...	...	...	.. ..	..
Sb	172.33	177.87	162.58	180.23	163.45	165.19	162 160	168
As	...	...	...	...	3.01	...	.. ..	..
S	332.94	337.03	331.53	342.50	320.50	320.80	324 320	324

1. Wolfsberg, Harz; anal. H. Rose (1826). 2. Kinzigthal, Baden; anal. Hilger (1877, in Dana, 1892). 3. Wolfsberg, Harz; anal. Guillemaine (1898). 4. Nagybanya, Romania; anal. de Finaly (in de Finaly & Koch, 1929). [1]Incl. insol. 0.94. 5. Bridge River district, British Columbia; anal. J. R. Williams & Son (in Warren & Thompson, 1944). 6. Anal. 5 after removal of As as FeAsS. A. Calculated for 81 or 80 $[PbS \cdot Sb_2S_3]$. B. Calculated for 12 $[6PbS \cdot 7Sb_2S_3]$.

*Taken from Nuffield, 1945.

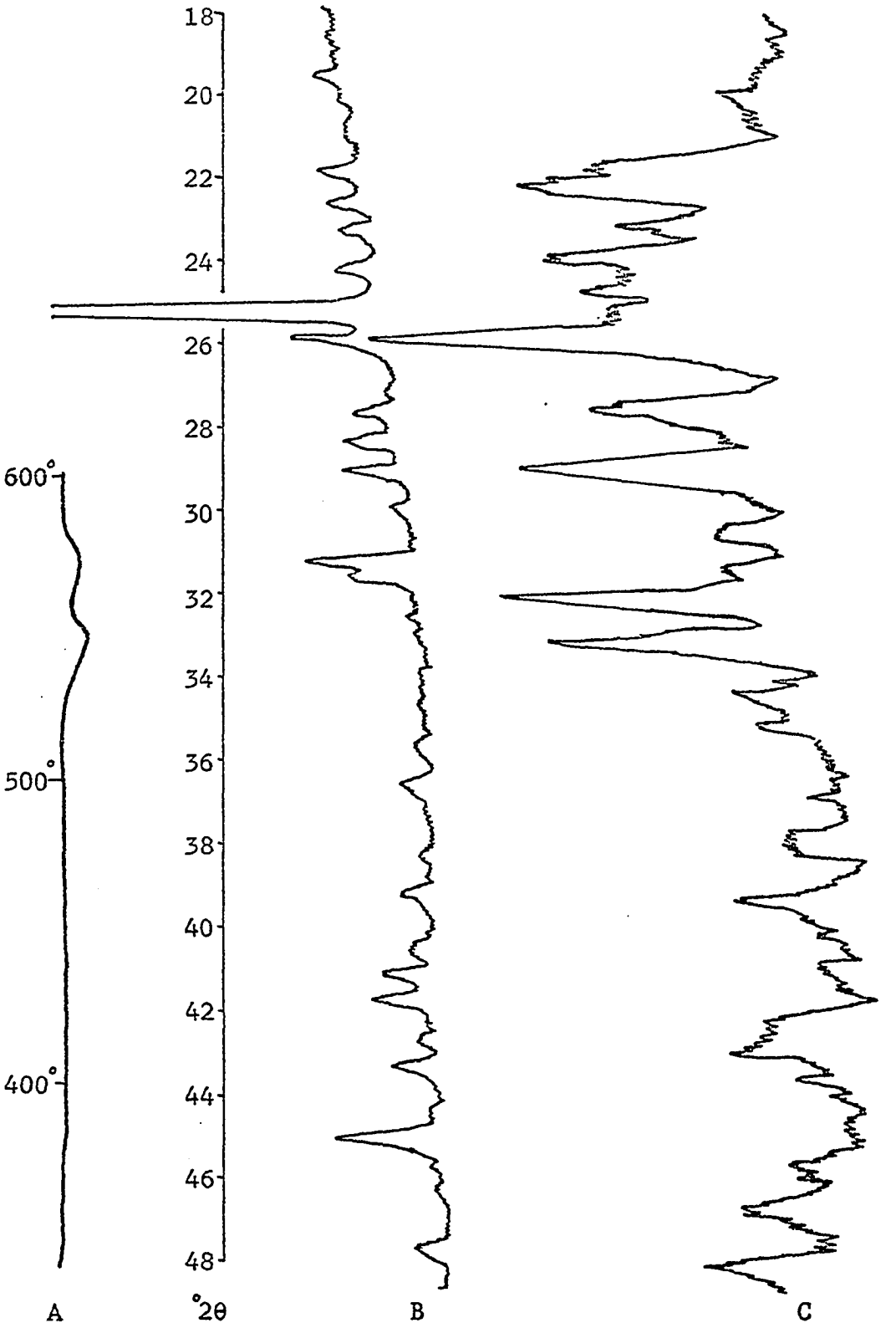

Figure 8 Zinckenite thermogram(A) and diffractograms of unheated(B) and heated(C-robinsonite) samples.

TABLE 5

ZINCKENITE - $PbS \cdot Sb_2S_3$

Hexagonal, C_6^6 - P6; a= 44.15, c= 8.62;
Z= 81 or 80.

Taken from Berry and Thompson, (1962).

NR= not recorded

I	d(meas.)	hkil	d(calc.)	I	d(unheated)*
½	5.50	$44\bar{8}0$	5.52	1	5.64
½	4.80	$08\bar{8}0$	4.78		NR
½	4.42	$4\cdot6\cdot\bar{10}\cdot0$	4.39	1	4.45
1	3.95	$04\bar{4}2$	3.93	1	3.90
1	3.56	$06\bar{6}2$	3.57	1	3.59
10	3.45	$2\cdot10\cdot\bar{12}\cdot0$	3.43	10	3.45
1	3.36	$44\bar{8}2$	3.40	1	3.39
1	3.08	$4\cdot6\cdot\bar{10}\cdot2$ $4\cdot10\cdot\bar{14}\cdot0$	3.07 3.06	1	3.08
2	3.02	$2\cdot8\cdot\bar{10}\cdot2$	3.00	1	3.01
½	2.91	$2\cdot12\cdot\bar{14}\cdot0$	2.91	½	2.91
4	2.81	$6\cdot6\cdot\bar{12}\cdot2$	2.80	3	2.79
½	2.70	$2\cdot10\cdot\bar{12}\cdot2$	2.68	½	2.67
½	2.54	$0\cdot12\cdot\bar{12}\cdot2$ $6\cdot8\cdot\bar{14}\cdot2$ $2\cdot14\cdot\bar{16}\cdot0$	2.56 2.54 2.53		NR
1	2.42	$2\cdot12\cdot\bar{14}\cdot2$ $6\cdot12\cdot\bar{18}\cdot0$	2.41 2.41	1	2.42
½	2.30	$0\cdot14\cdot\bar{14}\cdot2$ $6\cdot10\cdot\bar{16}\cdot2$	2.31 2.31		NR
1	2.25	$4\cdot12\cdot\bar{16}\cdot2$ $2\cdot16\cdot\bar{18}\cdot0$	2.26 2.24	1	2.24
1	2.16	0004 $6\cdot14\cdot\bar{20}\cdot0$	2.15 2.15	1	2.15
2	2.13	$8\cdot10\cdot\bar{18}\cdot2$ $0\cdot18\cdot\bar{18}\cdot0$	2.13 2.12	1	2.12
2	2.06	$4\cdot16\cdot\bar{20}\cdot0$ $4\cdot14\cdot\bar{18}\cdot2$	2.09 2.05	1	2.05
3	1.99	$2\cdot16\cdot\bar{18}\cdot2$ $8\cdot14\cdot\bar{22}\cdot0$	1.99 1.98	2	1.97

* See robinsonite table for d-values obtained from heating zinckenite to 520°C.

TABLE 6

ROBINSONITE - $7PbS \cdot 6Sb_2S_3$

Triclinic, $C_i^1 - P\bar{1}$, a= 16.51, b= 17.62, c= 3.97; $\alpha = 96°04'$, $\beta = 96°22'$, $\gamma = 91°12'$; Z= 1

Taken from Berry and Thompson, (1962).

NR= not recorded
NS= not scanned
b= broad peak

I	d(meas.)	hkl	d(calc.)	I	d(heated)*
½	7.4	$2\bar{1}0$	7.52		NS
		210	7.33		
½	6.0	$2\bar{2}0$	6.08		NS
		220	5.88		
½	5.44	300	5.47		NR
		130	5.44		
½	5.16	310	5.16		NR
½	4.35	040	4.38	½	4.40
8	4.04	400	4.10	5	4.06
		$3\bar{3}0$	4.05		
8	3.92	410	3.96	6	3.97b
		330	3.92		
		$1\bar{2}0$	3.92		
6	3.79	240	3.81	8	3.81
6	3.66	$\bar{2}01$	3.71	6	3.67
		$\bar{2}\bar{1}1$	3.69		
		420	3.67		
5	3.47	050	3.50		NR
		$3\bar{4}0$	3.47		
		$1\bar{5}0$	3.45		
10	3.39	$4\bar{3}0$	3.41	10	3.40
		150	3.40		
		$2\bar{1}1$	3.40		
		201	3.39		
		301	3.37		
½	3.28	$\bar{1}31$	3.31		NR
		121	3.29		
		211	3.26		
		$\bar{2}\bar{3}1$	3.26		
		$2\bar{5}0$	3.26		
6	3.18	510	3.20	5	3.19
		250	3.18		

ROBINSONITE (cont.)

I	d(meas.)	hkl	d(calc.)	I	d(heated)*
		221	3.05		
		4$\bar{4}$0	3.04		
8	3.03	520	3.04	7	3.05
		301	3.03		
		3$\bar{3}$1	3.02		
1	2.96	-	-		NR
2	2.88	-	-	1	2.89b
2	2.81	-	-	1	2.80b
8	2.75	-	-	7	2.76
8	2.67	-	-	6	2.67
1	2.59	-	-	2	2.58
½	2.53	-	-	2	2.54
2	2.33	-	-	1	2.33b
2	2.27	-	-	3	2.27
1	2.18	-	-	½	2.18
1	2.13	-	-		NR
4	2.11	-	-	3	2.12b
2	2.05	-	-	½	2.05b
½	2.01	-	-		NR
3	1.97	-	-	2	1.95
6	1.86	-	-	3	1.88

* Formed from heating zinckenite to 520°C.

small temperature intervals between peaks. The following table compares the composition and X-ray crystallography of the two minerals:

	Zinckenite	Robinsonite
Composition	$PbS \cdot Sb_2S_3$	$7PbS \cdot 6Sb_2S_3$
Symmetry Class	hexagonal	triclinic
Space group	$P6_3$	P1
Cell dimension	$a_o = 44.15$ $c_o = 8.62$	a = 16.51 b = 17.62 c = 3.97 $\alpha = 96°04'$ $\beta = 96°22'$ $\gamma = 91°12'$

High Temperature X-ray Diffraction

Zinckenite from the same locality as used in the DTA apparatus, was heated in the high temperature X-ray camera to 562 ± 5° C, producing a diffraction pattern (Table 46) similar to robinsonite. Unfortunately, the sample invariably recrystallized into rather coarse needle-like crystals partially oriented with their long dimension parallel to the quartz tube. This recrystallization resulted in poor quality diffraction patterns and made their interpretation more difficult.

The pattern indicated that the high temperature robinsonite was orthorhombic and "collapsed" to triclinic symmetry after cooling. Such a symmetry change would be expected where zinckenite (hexagonal) transformed into modified robinsonite (orthorhombic-high temperature) and not robinsonite (triclinic). The temperature of the transformation in the closed system occurred in the interval 527-562 ± 5° C which was in agreement with Craig's (1969) temperature of 545 ± 5° C. The vapor pressure in the closed tubes apparently raised the transformation

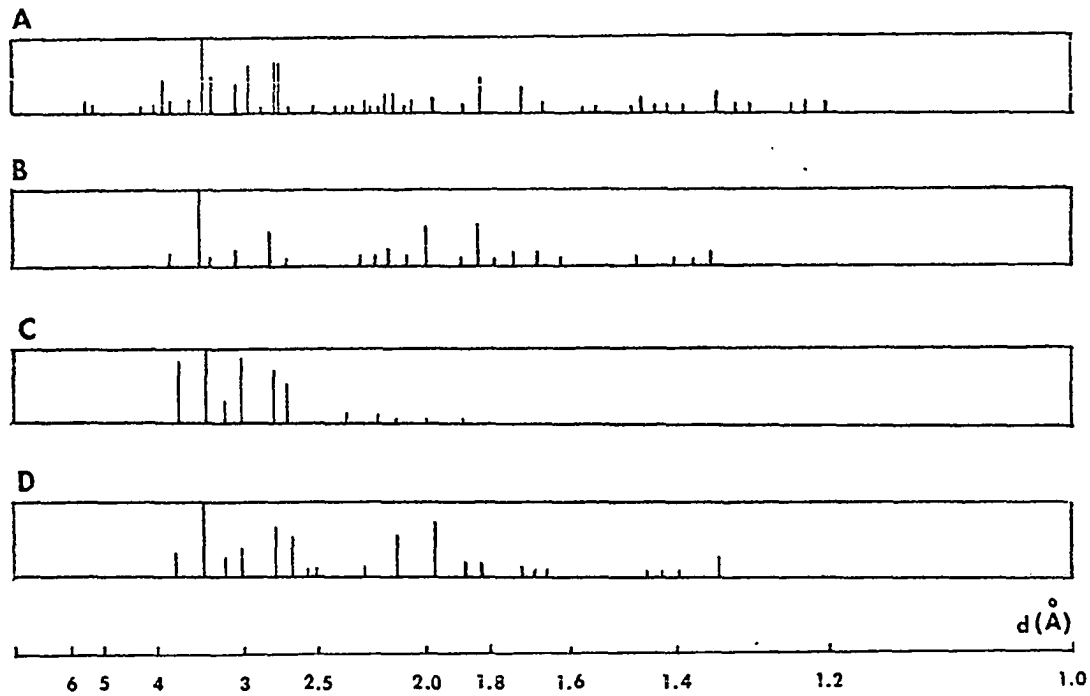

Figure 9 Zinckenite A) unheated B) at 544°C. C) robinsonite at 562°C., formed from heating zinckenite above 540°C. D) robinsonite quenched to room temperature.

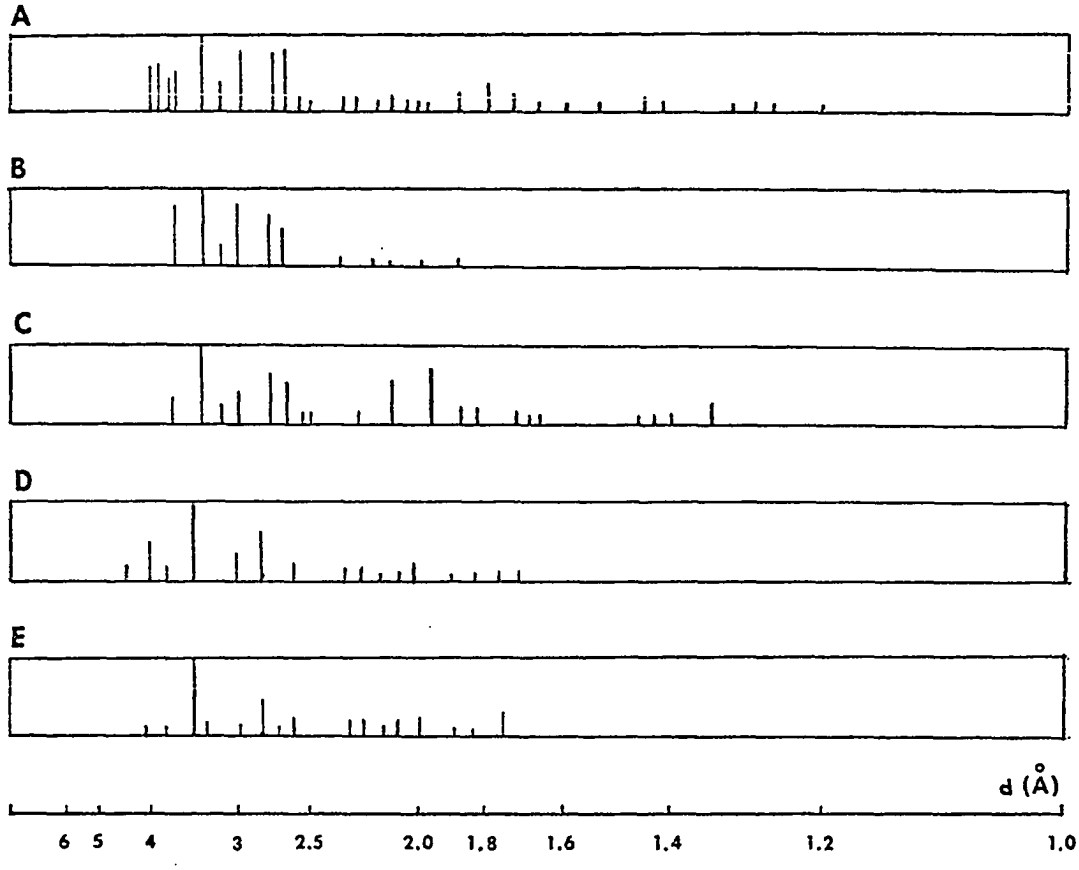

Figure 10 Robinsonite A) synthetic robinsonite at room temperature B) robinsonite at 562°C., formed by heating zinckenite above 540°C. C) robinsonite quenched to room temperature D) phase II at 580°C., formed by heating robinsonite above 575°C. E) phase II at 590°C., formed by heating plagionite above 575°C.

TABLE 7

COMPARISON OF d-VALUES FOR ROBINSONITE

A) robinsonite at room temperature
B) synthetic robinsonite at room temperature
C) robinsonite formed from heating zinckenite to 562° C
D) robinsonite quenched and X-rayed at room temperature

A		B		C		D	
I	d	I	d	I	d	I	d
1/2	7.4						
1/2	6.0						
1/2	5.44						
1/2	5.16						
1/2	4.35					1	4.34
8	4.04	1	4.04				
8	3.92	1	3.93			1	3.93
6	3.79	1	3.80	9	3.74	1	3.78
6	3.66						
5	3.47						
10	3.39	10	3.39	10	3.40	10	3.42
1/2	3.28						
6	3.18	3	3.19	3	3.23	3	3.23
8	3.03	8	3.03	9	3.07	3	3.03
1	2.96						
2	2.88						
2	2.81						
8	2.75	8	2.76	7	2.79	6	2.78
8	2.67	8	2.67	5	2.69	5	2.67
1	2.59	1/2	2.58			1/2	2.59
1/2	2.53	1/2	2.52			1/2	2.52
2	2.33	1	2.34	1/2	2.36		
1	2.27	1	2.27			1	2.27
1	2.18	1/2	2.18	1	2.21	1/2	2.19
1	2.13						
4	2.11	1	2.11	1/2	2.13	5	2.12
2	2.05	1/2	2.05			1/2	2.06
1/2	2.01	1/2	2.03				
3	1.97	1	1.98	1/2	2.01	7	1.98
6	1.86	2	1.88	1/2	1.89	2	1.88
4	1.79	3	1.80			2	1.83
2	1.72	2	1.72			1	1.72
1/2	1.66	1/2	1.66			1	1.66
2	1.34	1/2	1.34			3	1.35
1	1.31	1/2	1.31				
1	1.28	1/2	1.29				

temperature of zinckenite into robinsonite compared to the temperature obtained from the DTA where the Sb_2S_3 vapor was allowed to escape.

Structure

The structure of zinckenite (Fig. 11) was proposed by Bokii and Romanova (1962) but the structure of robinsonite is not yet known so the structural nature of the reaction is indeterminable. The zinckenite structure becomes unstable due to atomic agitation and transforms into robinsonite which has a more open structure and can accommodate the increased thermal motion of the atoms. With rapid cooling the robinsonite "collapses" into the low symmetry triclinic form. With slow cooling a reaction probably occurs with stibnite, resulting in a stable low temperature mineral like zinckenite or perhaps fülöppite. (The very limited occurrence of robinsonite tends to substantiate the probability that robinsonite is a quenched metastable high temperature form.)

Least Squares Cell Refinement

Four samples of zinckenite from Pribram, Bohemia; Julcani, Peru; Wolfsberg, Germany; and Sacarambu, Romania were refined using the least squares method (Table 8). Note that the a_o unit cell size has a considerably greater variation than the c_o dimension. The high temperature Pribram, Bohemia sample shows significent expansion of the a_o direction and practically none in the c_o length. X-ray fluorescence showed that the Julcani, Peru sample contained around 1% silver which probably accounted for the large a_o length compared to the other localities.

The Nonius powder patterns show several lines that have not been reported in the literature. These lines occur on all four patterns and

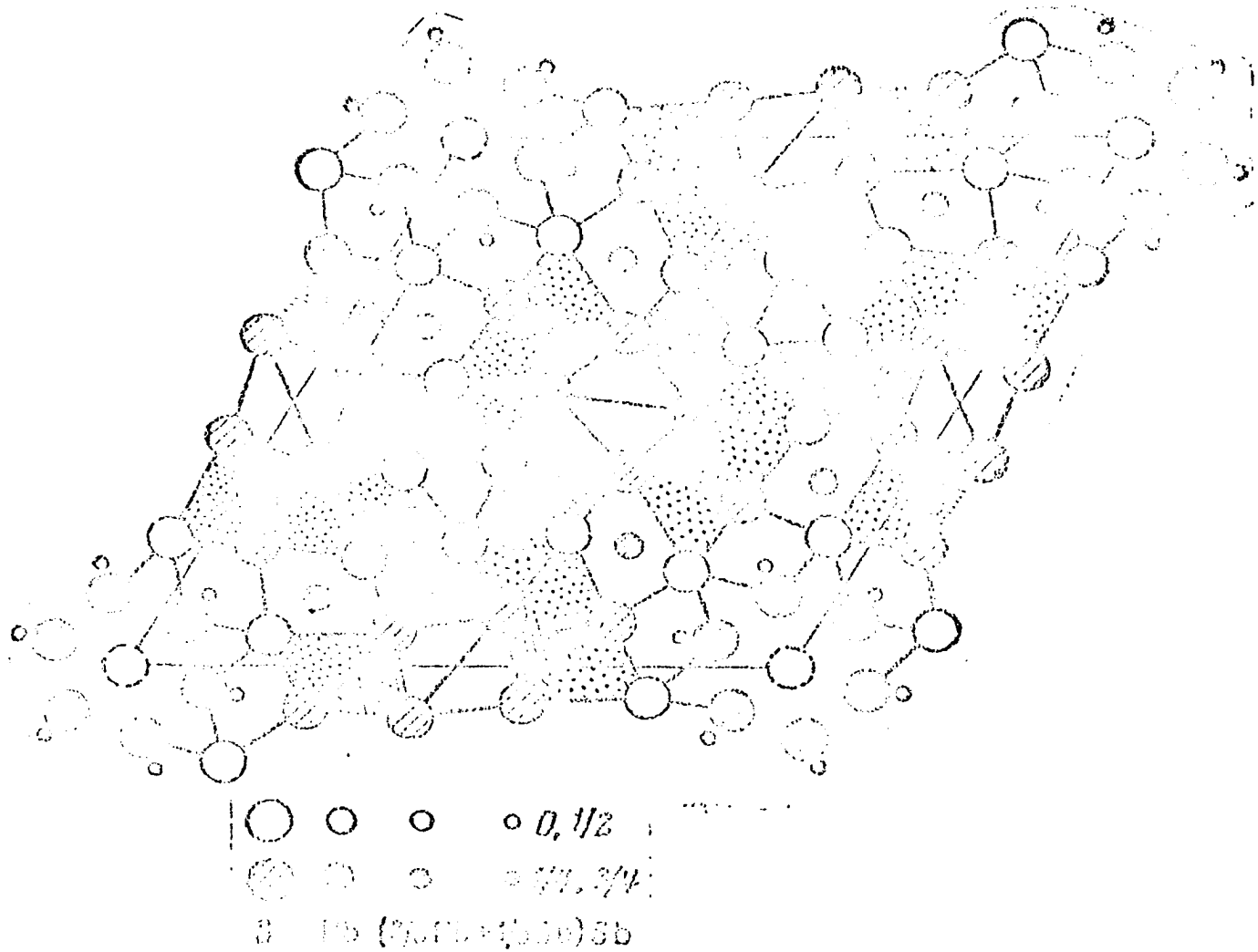

Figure 11. Projection on XY of the proposed structure of zinckenite $PbSb_2S_4$(Pb_3/m, Z = 20, a = 22.10, c = 8.688). From Bokii and Romanona, 1962.

are very close to a theoretical reflection as determined by the computer program.

TABLE 8

ZINCKENITE

Wolfsberg, Germany*	Pribram Bolivia	Julcani, Peru	Wolfsberg, Germany	Sacarambu, Romania
a_o = 44.15	44.116	44.221	44.103	44.163
c_o = 8.62	8.622	8.624	8.636	8.632
$\alpha = \beta$ = 90°	90°	90°	90°	90°
γ = 120°	120°	120°	120°	120°

	Pribram (at 544° C)
a_o =	44.337
c_o =	8.626
$\alpha = \beta$ =	90°
γ =	120°

*Vaux and Bannister (1938) confirmed by Nuffield (1945).

(Note that the standard errors of the direct cell parameters for all the minerals are given in the Appendix and are omitted from the tables in the text.)

PLAGIONITE

Plagionite ($Pb_5Sb_8S_{17}$) is a rare mineral originally studied by Zincken (1831), and Rose (1833). Zincken (1831), Spencer (1897), and Zambonini (1912) made specific gravity measurements while Schneiderhöhn and Ramdohr (1931) and Short (1940) determined its nature microchemically. Plagionite forms thick tabular [001] or short prismatic crystals with striations [110] and is associated with cassiterite, franckerite, and other lead sulfosalts. Table 8 gives chemical analyses for plagionite.

DTA

Plagionite from Wolfsberg, Germany was heated above its melting point, cooled and X-rayed. The thermogram (Fig. 12) showed a series of endothermic peaks ranging from 524° to 650 ± 5° C. Two more samples were heated, one to 548° and the other to 587° C. In both cases boulangerite was present and therefore the first peak starting at 526 ± 5° C represented the transition of plagionite to boulangerite. With an increase of temperature, plagionite became unstable and formed boulangerite which melted incongruently as indicated by the broad endothermic peak on the thermogram. In order to check the reversibility of the above reaction, identical samples of plagionite were sealed and heated in vycor tubing above the transition temperature of 526° C. One of the samples was quenched and X-rayed which verified the reaction occurred. The other tube was cooled slowly over a period of two days, and the diffractogram again showed boulangerite. Small stibnite crystals were found on the sides of the vycor which indicated that much of the Sb_2S_3 had not been absorbed to form plagionite. The possibility

Table 9

Plagionite: Analyses and Cell Contents*

M= 10,166

	1	2	3	4	5	6	A	B
Cu	...	...	...	1.27	...	...	...	...
Ag	...	...	...	...	...	0.18	...	...
Pb	40.52	40.62	40.98	39.36	41.24	40.28	40.50	40.55
Sb	37.94	37.49	37.53	37.84	37.35	38.30	37.86	38.12
S	21.53	21.89	21.49	21.10	21.10	21.43	21.42	21.33
	99.99	100.00	100.00	99.57	99.69	100.19	99.78	100.00
Cu	...	...	...	2.04	...	...	...	...
Ag	...	...	...	...	...	0.17	...	...
Pb	19.88	19.93	20.11	19.39	20.30	19.72	19.89	20
Sb	31.68	31.30	31.34	31.73	31.28	31.92	31.54	32
S	68.28	69.42	68.15	67.20	67.12	67.83	68.00	68

1, 2. Wolfsberg, Harz; anal. H. Rose (1833, in Hintze, 1904, p. 1019). 3. Wolfsberg, Harz; anal. Kudernatsch (1836, in Hintze, 1904). 4. Wolfsberg, Harz; anal. Schultz (1860, in Hintze, 1904). 5. Wolfsberg, Harz; anal. Prior (in Spencer, 1899). 6. Oruro, Bolivia; anal. Zambonini (1912). A. Average composition and cell content. B. Calculated for $5PbS \cdot 4Sb_2S_3$.

* Taken from Nuffield and Peacock, 1944.

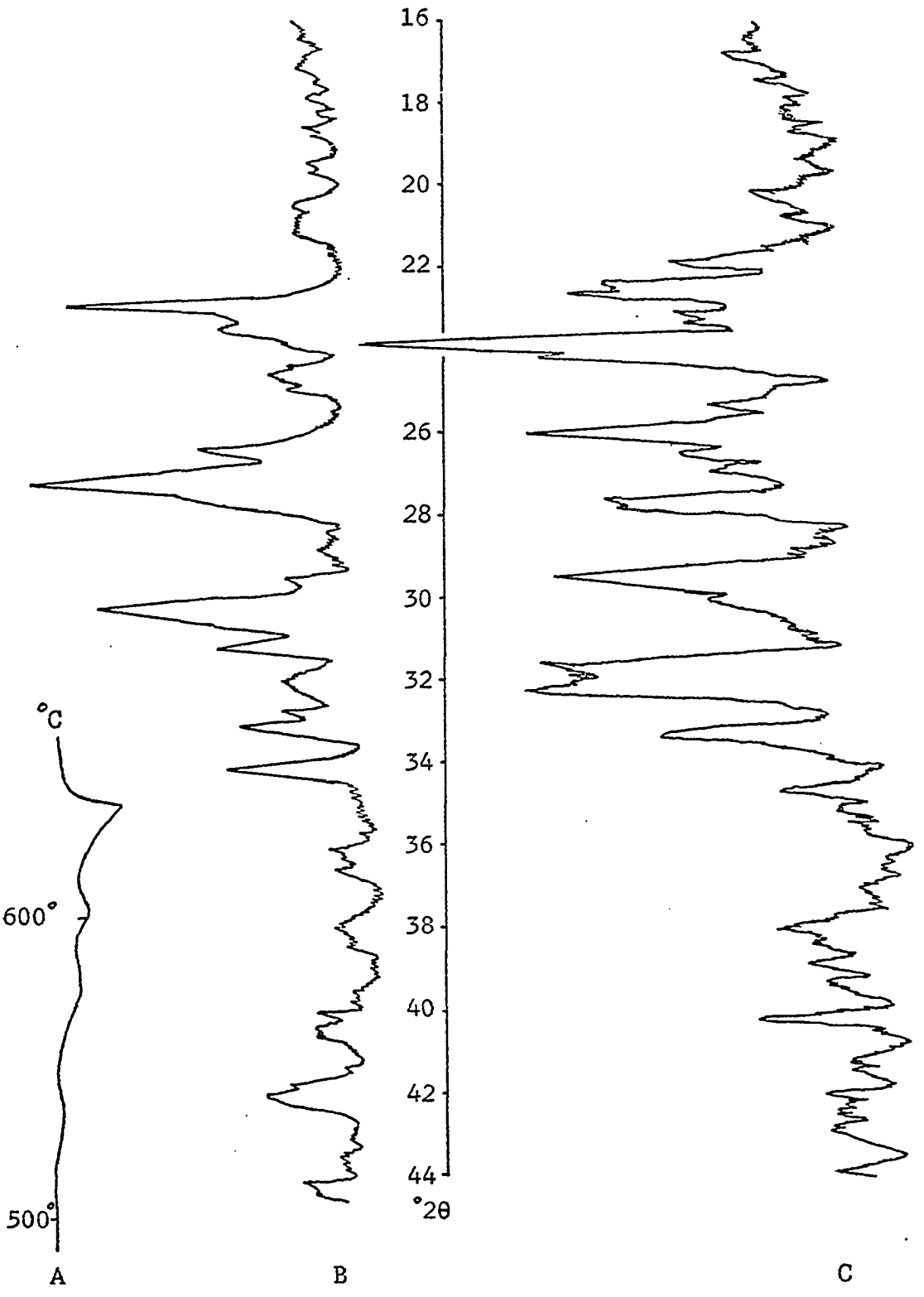

Figure 12 Plagionite thermogram (A) and diffractograms of unheated(B) and heated(C) samples. The heated specimen is boulangerite which formed from plagionite.

TABLE 10

PLAGIONITE - $5PbS \cdot 4Sb_2S_3$

Monoclinic, C_{2h}^6 - $C2/c$; a= 13.48, b= 11.83, c= 19.98, β = 107°11'; Z= 4

Taken from Berry and Thompson, (1962).

NS= not scanned
NR= not recorded

I	d(meas.)	hkl	d(calc.)	I	d(unheated)
2	5.87	112	5.88		NS
6	3.85	114	3.87	6	3.87
		$\bar{1}15$	3,79		
½	3.79	130	3.77	1	3.78
		$\bar{1}31$	3.76		
		131	3.64		
1	3.63	$\bar{3}14$	3.61	1	3.62
		$\bar{1}32$	3.61		
		132	3.41		
		312	3.39		
½	3.38	204	3.38	2	3.37
		$\bar{1}33$	3.37		
		$\bar{4}02$	3.37		
	3.39	223	3.30		
10	3.23	400	3.22	10	3.26
		$\bar{4}22$	2.93		
		$\bar{3}16$	2.92		
9	2.92	041	2.92	9	2.94
		$\bar{4}21$	2.91		
		402	2.81		
3	2.79	026	2.80	1	2.79
		331	2.79		
		043	2.68		
½	2.67	$\bar{2}42$	2.67	1	2.70
		$\bar{3}32$	2.63		
		225	2.62		
8	2.63	$\bar{4}25$	2.62	3	2.63
		241	2.62		
2	2.49	$\bar{2}44$	2.48	1	2.49
1	2.38	008	2.39	1	2.37
		243	2.37		
		$\bar{4}23$	2.37		
		404	2.36		
1	2.36	$\bar{3}18$	2.36		NR
		226	2.35		
		$\bar{2}44$	2.23		
1	2.22	$\bar{1}53$	2.22	1	2.22
		$\bar{4}42$	2.22		
		$\bar{4}44$	2.15		
		153	2.15		
6	2.14	600	2.15	4	2.15
		$\bar{1}54$	2.14		

still remained however, that the cooling was too rapid to attain equilibrium and the transition is reversible.

At a temperature of about 610° C another rather large peak started which represented a transformation of boulangerite into galena. (Consult the section on boulangerite for more information concerning this transition.)

High Temperature X-Ray Diffraction

A sample from Wolfsberg, Germany was heated in the X-ray camera to a temperature of 587 ± 5° C. The powder pattern (Table 11) indicated that the plagionite transformed into a new phase which was orthorhombic in symmetry. Craig (personal communication) also reported a phase ($5PbS \cdot 3Sb_2S_3$ - called Phase II) in that temperature range. However, his data from a quenched sample did not correspond very closely with the high temperature pattern. The composition of this phase was not determined by the author. Therefore, Craig's data will tentatively be used.

At a temperature of 595 ± 5° C phase II changed in boulangerite at which temperature it was probably orthorhombic in symmetry. (See the least squares section on boulangerite for a more detailed discussion of the high temperature symmetry.) With further heating (643° C) boulangerite changed into galena (Fig. 13-E) which was present at least up to 660° C.

Structure

Cho and Wuensch (1969) determined the structure of plagionite as follows: An asymmetric unit contains 3 Pb, 4 Sb, and 9 S where two of the Pb atoms have octahedral coordination and together form a

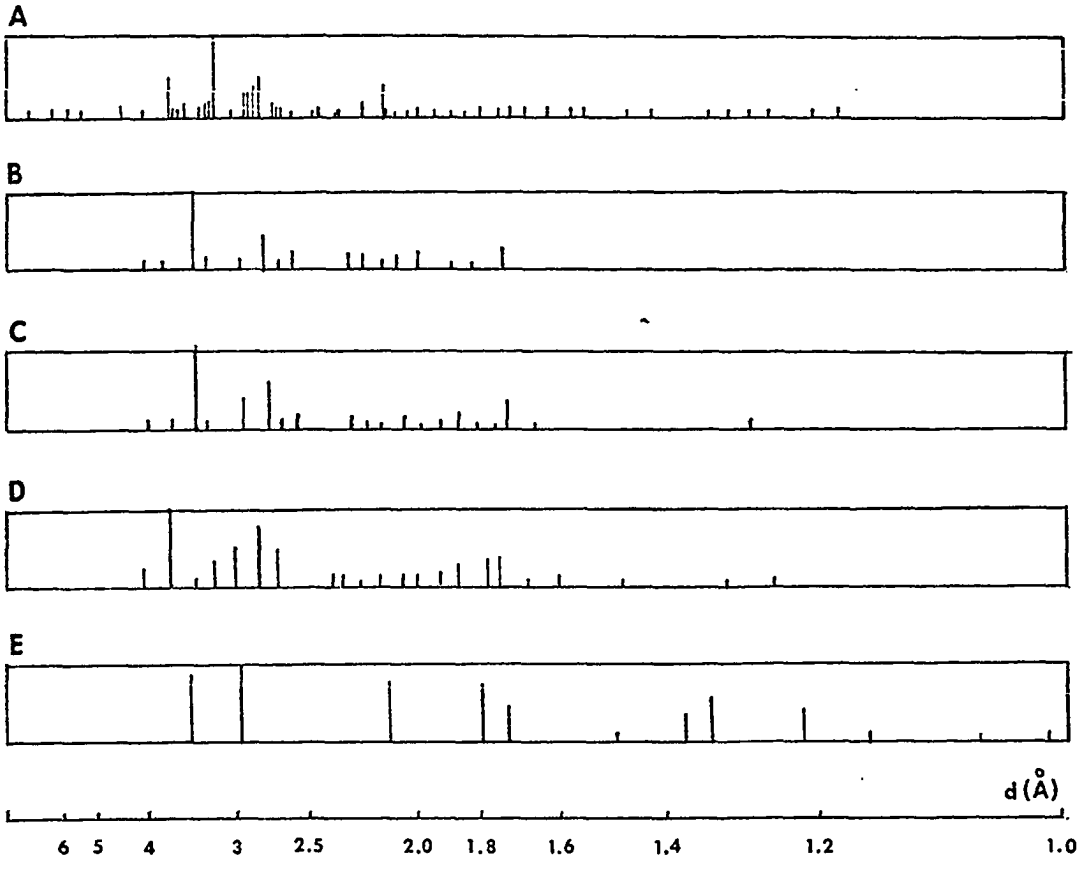

Figure 13 Plagionite A) unheated B) phase II at 590°C., formed by heating plagionite above 575°C. C) phase II quenched to room temperature D) boulangerite at 613°C., formed by heating plagionite above 597°C. E) galena at 646 C., formed by heating plagionite above 642°C.

TABLE 11

PHASE II FORMED FROM HEATING PLAGIONITE TO 590° C

Phase II (room temperature)		Phase II (590° C)	
I	d	I	d
1	4.07	1/2	4.08
1	3.76	1/2	3.82
10	3.42	10	3.46
1	3.28	1	3.32
4	2.97	1	3.02
6	2.78	4	2.81
1	2.69	1	2.72
2	2.59	2	2.62
1	2.29	2	2.30
1	2.22	2	2.24
		1/2	2.15
2	2.07	1	2.10
4	2.00	2	2.03
1	1.94		
2	1.88	1/2	1.90
		1/2	1.84
3	1.74	3	1.75
1/2	1.52		
1/2	1.29		

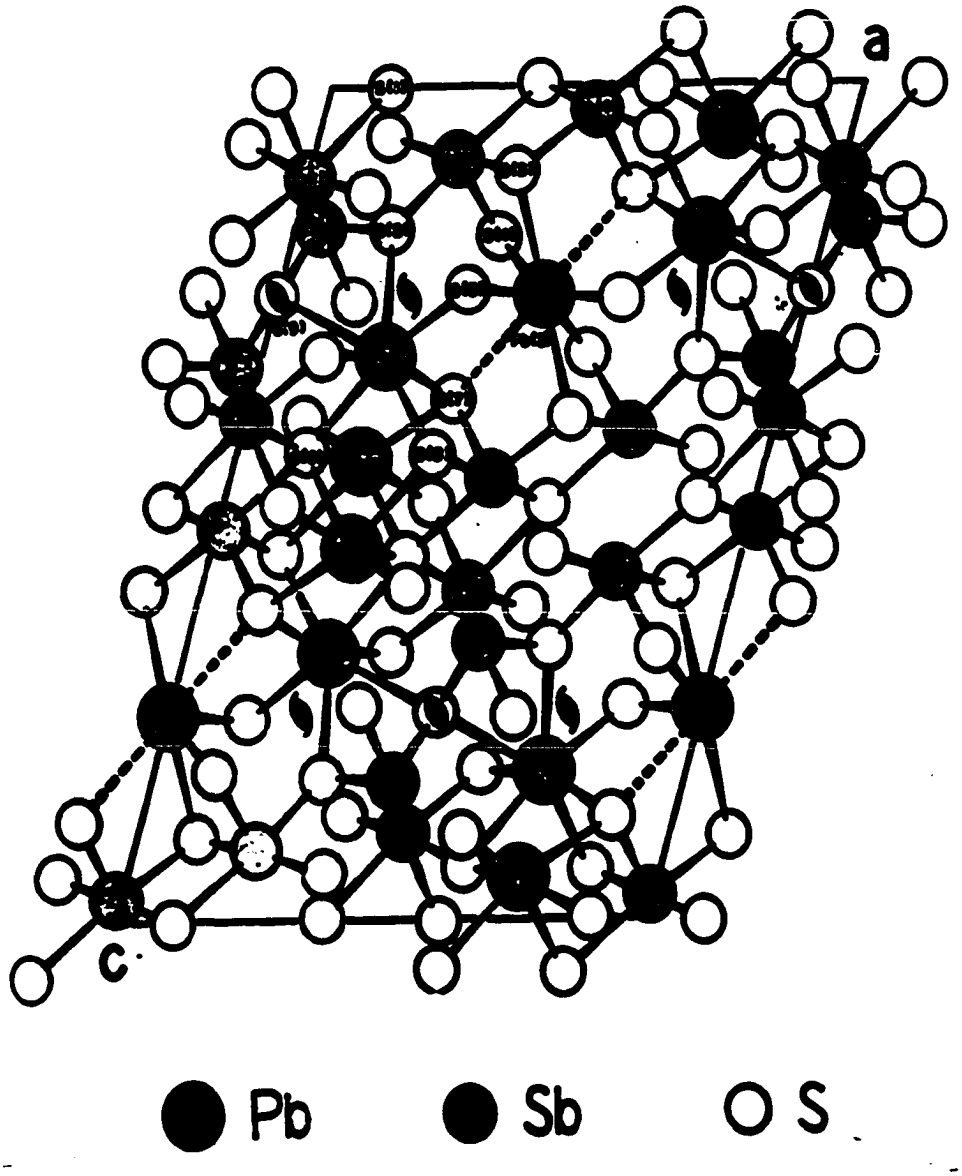

Figure 14 Projection along b of the coordination polyhedra contained between y=0 and y=$\frac{1}{2}$ in plagionite. The C lattice provides an equivalent layer shifted $\frac{1}{2}\frac{1}{2}0$ above the depicted polyhedra. (from Cho and Wuensch 1970)

PbS - like chain of 4 octahedra parallel to c. The third Pb has a distorted square antiprism coordination and links the octahedral clusters into infinite chains running parallel to [10$\bar{1}$]. The chains are flanked on either side by a stibnite-like slab of Sb square pyramids of finite extent. The vertices of the pyramids are directed toward the Pb chain while the bases of the Sb pyramids on neighboring chains are opposed to one another and parallel to (112). Table 12 lists the atomic positions for plagionite with the standard deviations in parentheses.

TABLE 12

ATOMIC POSITIONS AND TEMPERATURE FACTORS IN PLAGIONITE

Atom	x	y	z	B ($Å^2$)
Pb (1)	0.2366 (3)	0.0862 (3)	0.4484 (2)	2.67 (5)
Pb (2)	0.2310 (2)	0.3741 (2)	0.3220 (2)	2.18 (4)
Pb (3)	0.0	0.8199 (4)	0.25	2.68 (7)
Sb (1)	0.0018 (4)	0.4816 (4)	0.1053 (3)	2.54 (8)
Sb (2)	0.2710 (4)	0.1903 (4)	0.0857 (2)	1.83 (6)
Sb (3)	0.0461 (3)	0.1250 (4)	0.1671 (2)	1.80 (6)
Sb (4)	0.5094 (3)	0.3047 (3)	0.0285 (2)	1.77 (6)
S (1)	0.1087(12)	0.4160(13)	0.0009 (9)	1.72(21)
S (2)	0.1812(14)	0.2662(14)	0.1709 (9)	2.14(25)
S (3)	0.3887(10)	0.3613(11)	0.1017 (7)	1.49(21)
S (4)	0.3865(11)	0.0766(11)	0.1790 (8)	1.70(21)
S (5)	0.3532(14)	0.4954(14)	0.2438(10)	1.98(24)
S (6)	0.1314(12)	0.3104(12)	0.4367 (8)	1.59(21)
S (7)	0.3812(12)	0.1926(13)	0.3759 (8)	2.18(25)
S (8)	0.3699(14)	0.4742(14)	0.4417 (9)	1.92(23)
S (9)	0.0	0.2569(23)	0.25	2.36(38)

Least Squares Cell Refinement

Two samples of plagionite were refined with the results tabulated below. Note that the published parameters are very similar to the refined values as all samples came from Wolfsberg, Germany.

TABLE 13

PLAGIONITE

Muffield & Peacock (1945) (Wolfsberg, Germany)	Wolfsberg	Wolfsberg
a_o = 13.48	13.490	13.472
b_o = 11.83	11.836	11.832
c_o = 19.98	19.979	20.010
β = 107°11'	107°18'	107°10'

SEMSEYITE

Semseyite was named after a Hungarian nobleman, Andor von Semsey (? - 1923). Krenner (1884) first studied the mineral, however the data was inaccurate due to poor samples found at Felsöbanya, Hungary. Semseyite is quite similar to plagionite in appearance and occurs as tabular or prismatic crystals which are often twisted or composed of subparallel individuals. The crystals used in this study were globular aggregates with a core of galena from Kisbánya, Hungary. (The galena could not be entirely separated as one can see from the diffractogram.)

Smith (1919) obtained good measurements on crystals from Dumfriesshire, Scotland and derived the accepted formula $9PbS \cdot 4Sb_2S_3$. In 1944, Nuffield and Peacock measured single crystal photographs on material from Kisbánya, Romania obtaining the cell dimensions which are given in Table 15 along with the X-ray powder data. (Chemical analyses are given in Table 14.)

DTA

The thermogram for semseyite showed a smooth melting curve starting at 611 ± 5° C with no intermediate peaks. The X-ray diffraction pattern (Fig. 15) indicated that semseyite again crystallized from the melt and the galena impurity appeared unchanged.

High Temperature X-ray Diffraction

A sample from Kisbánya, Hungary transformed at 575 ± 5° C into boulangerite which was very similar to the one formed from heating plagionite. With further heating (643° C) the boulangerite formed galena which remained at least until 657° C.

Table 14

Semseyite: Analyses and Cell Contents

M= 14,078

	1	2	3	4	5	6	A	B
Ag	...	...	1.6	...	0.25	...	...	...
Fe	0.10	...	...	0.67	...	...	...	...
Pb	53.16	51.84	52.9	52.37	54.27	53.21	52.77	53.10
Sb	26.90	28.62	24.8	25.49	26.17	26.95	26.81	27.73
S	19.42	19.42	18.7	18.81	18.99	19.90	19.24	19.17
	99.58	99.88	98.0	99.81[5]	99.69[8]	100.14[9]	99.52	100.00
Ag	...	...	2.13	...	0.33	...	...	...
Fe	0.25	...	...	0.69	...	...	...	...
Pb	36.27	35.26	36.67	36.55	36.99	36.13	36.13	36
Sb	31.23	33.13	29.26	30.28	30.36	31.14	31.23	32
S	85.64	85.38	83.79	84.86	83.66	87.33	85.12	84

1. Felsöbánya, Romania; anal. Sipöcz (1886). 2. Wolfsberg, Harz; anal. Prior (in Spencer, 1899). 3. Oruro, Bolivia; anal. Prior (in Spencer, 1907). 4. Glendinning, Dumfriesshire; anal. Prior (in Smith, 1919). [5]Incl. Zn trace, $MgCO_3$ trace, $CaCO_3$ 1.66, insol. 0.81. 5. Kisbánya, Romania; anal. Finaly, in Koch, 1932 (Min. Abs. 5-190). [8]Incl. insol. 0.01. 6. O-Radna, Romania; anal. Endrédy, in Koch, 1932 (Min. Abs. 5-190). [9]Incl. insol. 0.08. A. Average composition and cell content. B. Calculated for $4[9PbS \cdot 4Sb_2S_3]$.

*Taken from Nuffield and Peacock, 1945.

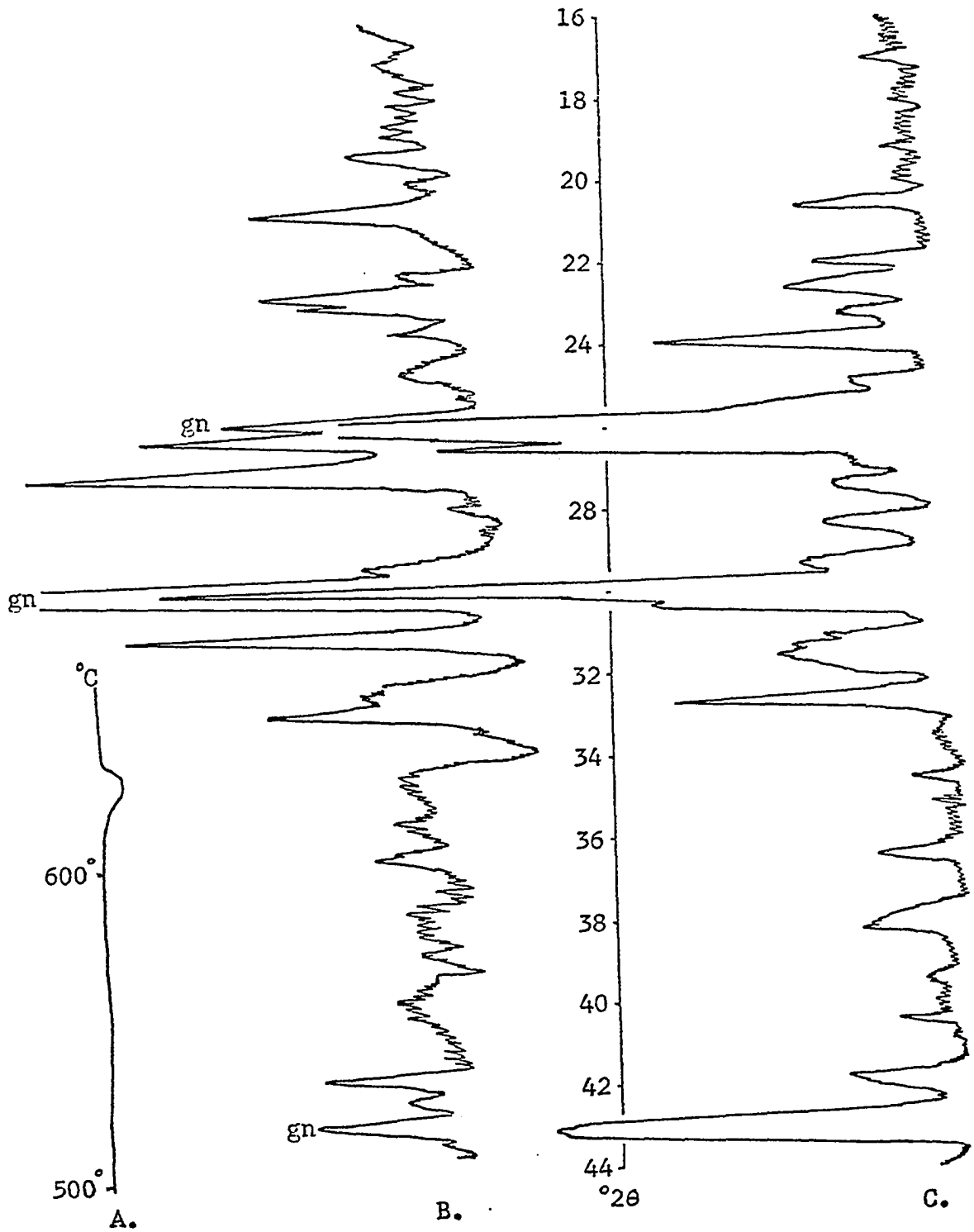

Figure 15 Semseyite thermogram (A) showing melting peak and diffractograms of unheated (B) and heated (C) samples. (Note galena impurity.)

TABLE 15

SEMSEYITE - $9PbS \cdot 4Sb_2S_3$

Monoclinic, C_{2h}^6-C2/c; a= 13.64, b= 12.01, c= 24.57, β = 105°49; Z= 4

Taken from Berry and Thompson, (1962).

I	d(meas.)	hkl	d(calc.)
½	6.61	200	6.56
½	5.47	113	5.41
½	4.58	114	4.54
		$\bar{1}$15	4.53
½	4.21	221	4.22
		024	4.21
		$\bar{2}$23	4.21
5	3.85	$\bar{3}$14	3.87
		130	3.83
½	3.75	131	3.73
		$\bar{1}$32	3.73
2	3.59	315	3.59
		$\bar{2}$25	3.58
8	3.38	116	3.38
		$\bar{1}$17	3.37
10	3.27	400	3.28
		$\bar{2}$26	3.26
		$\bar{4}$04	3.24
9	2.98	041	2.98
		117	2.98
		$\bar{1}$18	2.97
		225	2.97
		$\bar{2}$27	2.96
		008	2.95
		420	2.88
4	2.87	$\bar{4}$24	2.87
		331	2.87
		135	2.86
1	2.78	421	2.78
		$\bar{4}$25	2.77
4	2.71	226	2.71
		$\bar{2}$28	2.70
1	2.49	243	2.49
		227	2.47
½	2.38	-	-
3	2.25	-	-
3	2.16	-	-

gn= galena
NR= not recorded
* heated to 650°C.

I	d(unheated)	I	d(heated)*
½	6.58		NR
1	5.48		NR
1	4.58	½	4.60
4	4.26	1	4.29
6	3.89	2	3.93
1	3.75	4	3.72
1	3.58	1	3.59
	3.45(gn)		3.45(gn)
8	3.38	10	3.37
10	3.28	2	3.26
	(semseyite & galena)		
9	2.86	3	2.84
	NR		NR
5	2.71	4	2.74
1	2.45	2	2.47
	NR	2	2.35
½	2.24	1	2.23
2	2.15	2	2.16
	2.10(gn)		2.10(gn)

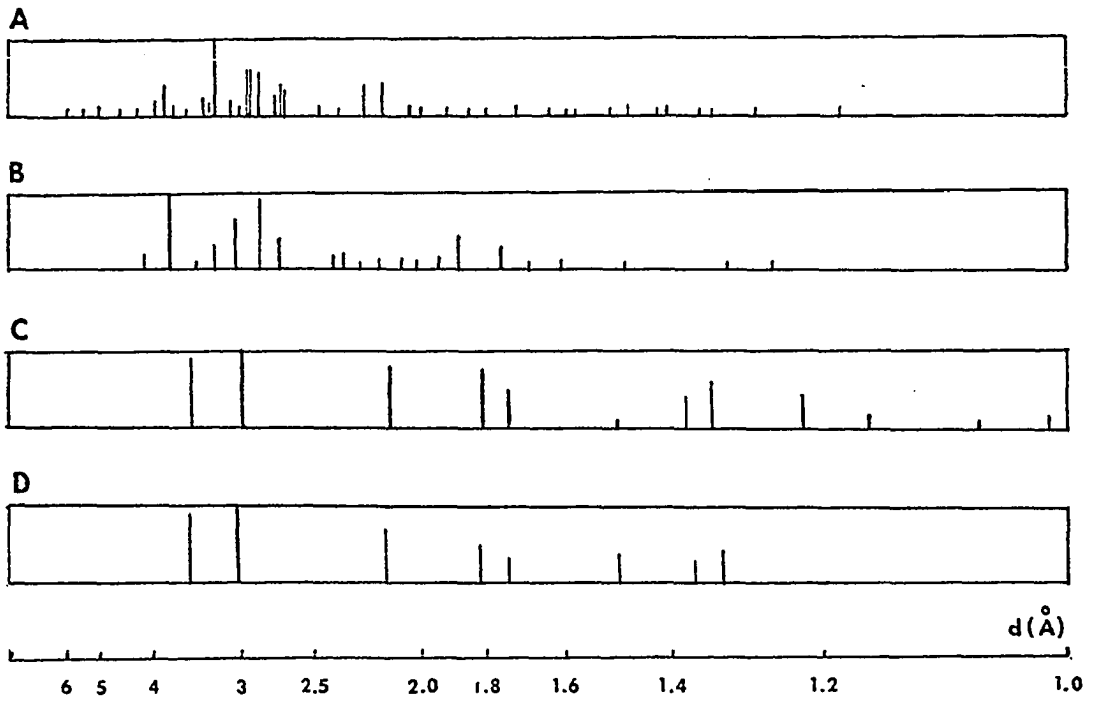

Figure 16 Semseyite A) unheated B) boulangerite at 588°C., formed by heating semseyite above 575°C. C) galena at 646°C., formed by heating semseyite above 647°C. D) galena quenched to room temperature.

Structure

The structure of semseyite has not yet been determined so that the nature of the transition of semseyite into boulangerite is unknown.

Least Square Cell Refinement

Two samples of semseyite were refined and compared below with the published values. Very little variation of cell parameters existed among the samples.

TABLE 16

SEMSEYITE

	Kisbańya, Hungary Berry (1940)	Kisbańya, Hungary	Arnsberg, Germany
a_o =	13.64	13.644	13.644
b_o =	12.01	12.004	12.024
c_o =	24.57	24.560	24.558
β =	105°49'	105°49'	105"54'

(See the section on boulangerite for the cell refinement of the semseyite → boulangerite and boulangerite → galena transformation.)

BOULANGERITE

The mineral was named after a French mining engineer C. L. Boulanger (1810-1849). Early work was done by Boulanger (1835), Thaulow (1837), Hausmann (1839), Rammelsberg (1839, 1846, 1875) and Sjogren (1897) who derived the formula $5PbS \cdot 2Sb_2S_3$ on material from Sala, Sweden.

Boulangerite occurs as long prismatic to acicular needles, which are deeply striated parallel to [001] fibrous masses and as plumose aggregates associated with galena, stibnite, sphalerite, pyrite, arseno-pyrite, quartz and other lead sulfosalts in hydrothermal veins formed at low or moderate temperatures.

DTA

A sample of boulangerite from St. Antonia, California was heated to 700° C. The thermogram (Fig. 17) showed an endothermic peak starting at 570 $\pm$ 5° C which represented the incongruent melting of boulangerite. The peak leveled off slightly at 600° C and then formed a second higher peak which represented the change of boulangerite into galena. The thermogram for plagionite (Fig. 12) which formed boulangerite also shows a secondary peak starting at 610° C. Since boulangerite melted incongruently around 570° C the peak should be fairly smooth and gradually taper off as the last crystals melted. With this thermogram however, the second sharp peak indicated that another change occurred before all the crystals of boulangerite melted. This change would be the formation of galena (Table 54).

TABLE 17

BOULANGERITE: CHEMICAL ANALYSES*

	1	2	3	4
Ag	...	...	0.06	...
Pb	55.42	55.35	55.45	54.7
Sb	25.50	24.95	25.40	30.4
Fe	0.25	0.51	.13	
As	0.24	0.71	0.36	
S	18.50	18.40	18.45	15.1
	99.89	99.92	99.85	100.2

1. Randall Creek, B.C., anal. Williams (in H. V. Warren and R. M. Thompson, 1945: Univ. Toronto Stud., Geol. Ser., 49, p. 80.

2. Sullivan Mine, near Kimberly, B.C., anal. Williams (in H. V. Warren and R. M. Thompson, 1945: Univ. Toronto Stud., Geol. Ser., 49, p. 79).

3. Lamarr Mine, Omineca Mining Division, B.C. analysis and reference is the same as #2 above.

4. Montpay Township, B. C. anal. Gould (in J. E. Hawley, 1941: Univ. Toronto Stud., Geol. Ser., 46, p. 25).

*Taken from Geological Survey of Canada, Department of Energy, Mines and Resources. Paper 69-45, p. 97-101, 1970.

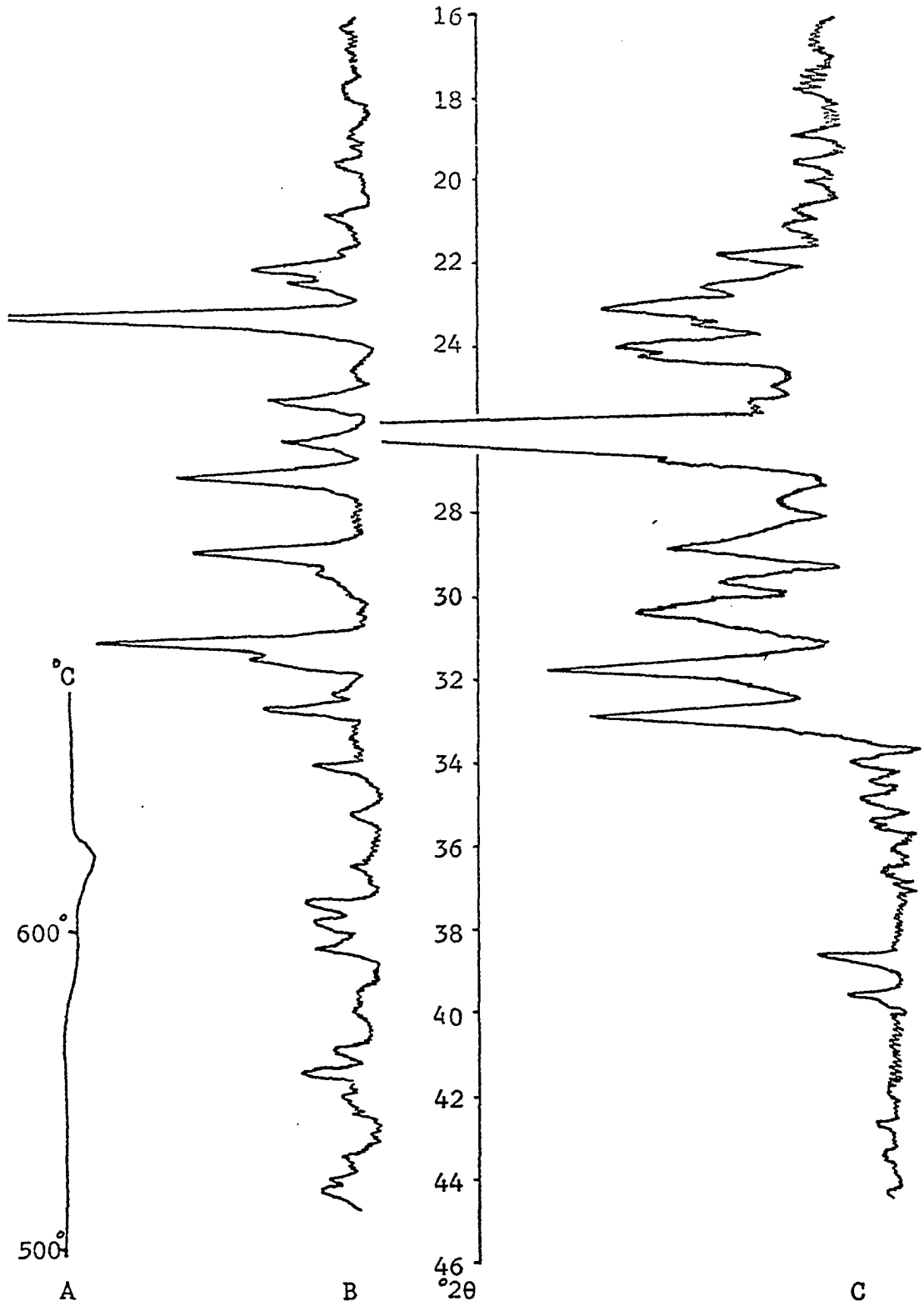

Figure 17 Boulangerite thermogram(A) and diffractograms of unheated(B) and heated(C) samples.

TABLE 18

BOULANGERITE - $5PbS \cdot 2Sb_2S_3$

Monoclinic, C_{2h}^5 - $P2_1/a$; a= 21.56, b= 23.51, c= 8.09, β = 100°48'; Z= 8

Taken from Berry and Thompson, (1962).

NR= not recorded
NS= not scanned

I	d(meas.)	hkl	d(calc.)	I	d(unheated)	I	d(heated)*
		012	3.92			2	4.07
2	3.93	$\bar{2}12$	3.92	1	3.94	3	3.93
		350	3.91				
		112	3.73			2	3.86
10	3.72	$\bar{3}12$	3.73	10	3.74	10	3.73
		530	3.73				
1	3.44	540	3.44	1	3.44	7	3.42
2	3.30	170	3.32	1	3.31	1	3.31
		630	3.22				
4	3.21	132	3.20	5	3.22	6	3.23
		$\bar{3}32$	3.20				
		052	3.03				
		$\bar{2}52$	3.03				
4	3.01	242	3.01	4	3.01	6	3.03
		$\bar{4}42$	3.01				
						2	2.98
		342	2.82				
		$\bar{5}42$	2.82				
9	2.81	$\bar{1}62$	2.81	7	2.80	7	2.83
		062	2.80				
		$\bar{2}62$	2.80			7	2.77
		352	2.65				
3	2.68	$\bar{5}52$	2.65	1	2.67	4	2.69
$\frac{1}{2}$	2.59	-	-	$\frac{1}{2}$	2.57	1	2.59
		532	2.52				
$\frac{1}{2}$	2.51	$\bar{7}32$	2.52	$\frac{1}{2}$	2.50		NR
2	2.33	490	2.34	1	2.35	1	2.37
3	2.14	4100	2.15	1	2.15	1	2.14
1	2.05	5100	2.05	1	2.04	1	2.05
		024	1.96				
1	1.96	$\bar{4}24$	1.96	1	1.94		
3	1.91	-	-	2	1.89		
						2	2.25

* Formed from heating plagionite to 610°C and are listed here to compare with the published d-values for boulangerite.

High Temperature X-Ray Diffraction

Boulangerite was heated in the camera and at 643 ± 5° C transformed into galena which remained at least until 660°. The temperature of the transition recorded on the DTA apparatus was lower because the sample was heated in an open system where the vapor pressure could not build up.

Structure

Reliable cell dimensions were determined by Berry (1940) from single-crystal photographs on material from Gold Hunter Mine, Mullan, Idaho.

Monoclinic C_{2h}^5-$P2_1/a$

a = 21.56, b = 23.51, c = 8.09, = 100°48', Z = 8

Born and Hellner (1960) re-examined a sample of boulangerite from Pribram, Bohemia and compared their results with Berry's. Weissenberg photographs of the 0 and 2nd level were in agreement with Berry's with respect to the subcell, but a weak first level showed orthorhombic and not monoclinic symmetry. Nevertheless, the difference in the intensities of related reflections in Berry's photographs are slight and Born and Hellner used the large unit cell of orthorhombic symmetry with a_o = 42.28, b_o = 23.46 and c_o = 8.07 Å; space group $Bb2_1m$. The basis for their structural determination was the formula $Pb_{20}Sb_{16}S_{44}$ for the subcell. The first layer and the very weak reflections of the 0 and 2nd layers were neglected in the first approximation of the structure because of large anisotropic influence of the absorption factor and in addition the weak reflections were influenced by the superstructure.

Born and Hellner (1960) proposed the boulangerite structure where 3 positions are occupied by Pb and 3 by Sb with a statistical distribution of Pb and Sb in positions 4–6 of the subcell. (Positions indicated in

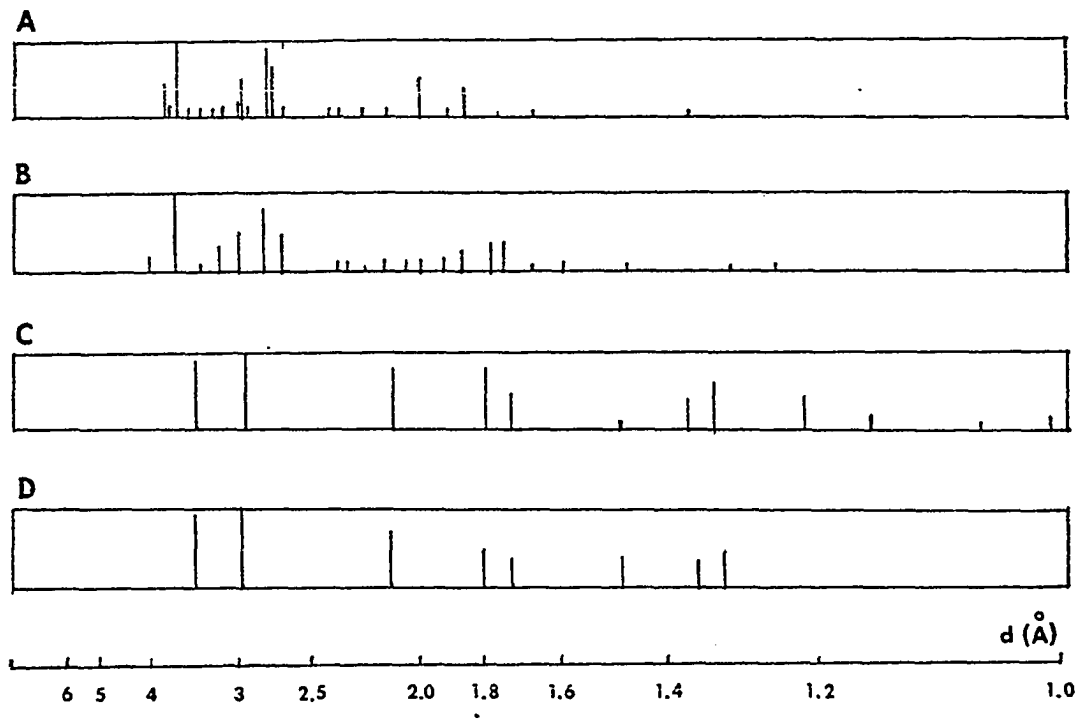

Figure 18 Boulangerite A) unheated B) at 593°C. C) galena at 646°C., formed by heating boulangerite above 643°C. D) galena quenched to room temperature.

TABLE 19

COMPARISON OF d-VALUES FOR BOULANGERITE AT HIGH TEMPERATURES

A. Boulangerite at 593° C

B. Boulangerite formed from heating plagionite to 613° C

C. Boulangerite formed from heating semseyite to 588° C

A		B		C	
I	d	I	d	I	d
2	4.12	1/2	4.13	2	4.15
10	3.73	10	3.75	10	3.74
1/2	3.45	1/2	3.46	1/2	3.46
		2	3.35		
3	3.23	3	3.26	3	3.23
5	3.03	6	3.04	7	3.04
8	2.83	6	2.84	9	2.83
5	2.71	4	2.72	4	2.72
1/2	2.38			1	2.39
1/2	2.33			1	2.34
1/2	2.26			1/2	2.27
2	2.16	3	2.17	1	2.16
2	2.07	2	2.08	1	2.07
2	2.02	2	2.03	1	2.02
2	1.94	2	1.94	1	1.04
2	1.87	7	1.88	4	1.88
1	1.84				
1	1.79			1	1.79

Lattice Parameters (Å)

a_o =	21.638	21.697	21.670
b_o =	23.605	23.469	23.532
c_o =	8.067	8.115	8.087
β =	100°21'	100°43'	100°29'

TABLE 20

COMPARISON OF d-VALUES FROM QUENCHED BOULANGERITES

A) regular boulangerite
B) formed from heating plagionite
C) formed from heating semseyite

A		B		C	
I	d	I	d	I	d
1/2	6.08	1/2	6.09	1/2	6.07
		1/2	4.57	1/2	4.58
1/2	4.40	1/2	4.40	1/2	4.39
1/ 2	4.10	1/2	4.07	1/2	4.07
				1/2	4.00
				1/2	3.94
2	3.90	3	3.91	4	3.90
1	3.85	1/2	3.85	1	3.83
10	3.73	10	3.72	10	3.72
2	3.67	1	3.66	3	3.66
1/2	3.59	1/2	3.58	1/2	3.59
1/2	3.47	1/2	3.51	1	3.49
2	3.44	1/2	3.45	1	3.44
		1/2	3.41	1	3.41
1/2	3.35	1/2	3.35	1	3.34
1	3.31	1	3.31	2	3.30
				1/2	3.27
2	3.23	2	3.22	3	3.21
1	3.19	1	3.19	2	3.18
1/2	3.16				
1/2	3.09				
1/2	3.07				
2	3.03	3	3.03	2	3.02
4	3.00	4	3.00	6	2.99
1	2.96	1	2.96	3	2.96
1/2	2.94	1/2	2.93	1	2.93
1/2	2.91				
7	2.83	6	2.83	2	2.82
7	2.81	6	2.80	8	2.80
6	2.78	7	2.77	8	2.77
1/2	2.73				
1/2	2.72	1/2	2.71	1/2	2.71
1/2	2.70	1/2	2.69	1	2.69
1/2	2.65	1/2	2.65	1	2.64
1/2	2.59	1/2	2.59	1	2.59
		1/2	2.54		
1/2	2.52	1/2	2.51	1	2.51
		1/2	2.48	1/2	2.44

A		B		C	
I	d	I	d	I	d
1	2.42	1	2.42	1	2.42
2	2.37	1	2.37	1/2	2.36
1/2	2.34	1/2	2.34	1	2.34
1	2.31	1/2	2.31	1	2.31
		1/2	2.28		
2	2.25	2	2.25	1	2.24
		1/2	2.23		
		1/2	2.20		
1/2	2.18	1/2	2.18	1	2.17
		1/2	2.15	1	2.14
1/2	2.12	1/2	2.12	1/2	2.13
1/2	2.07	1/2	2.09	1/2	2.09
1/2	2.05	1/2	2.05	1/2	2.05
1/2	2.04	1/2	2.03	1/2	2.03
4	2.01	3	2.01	6	2.01
		1/2	1.98	1	1.99
				1/2	1.97
1	1.93	1/2	1.92	1/2	1.92
		1/2	1.89	1/2	1.89
3	1.86	4	1.86	5	1.86

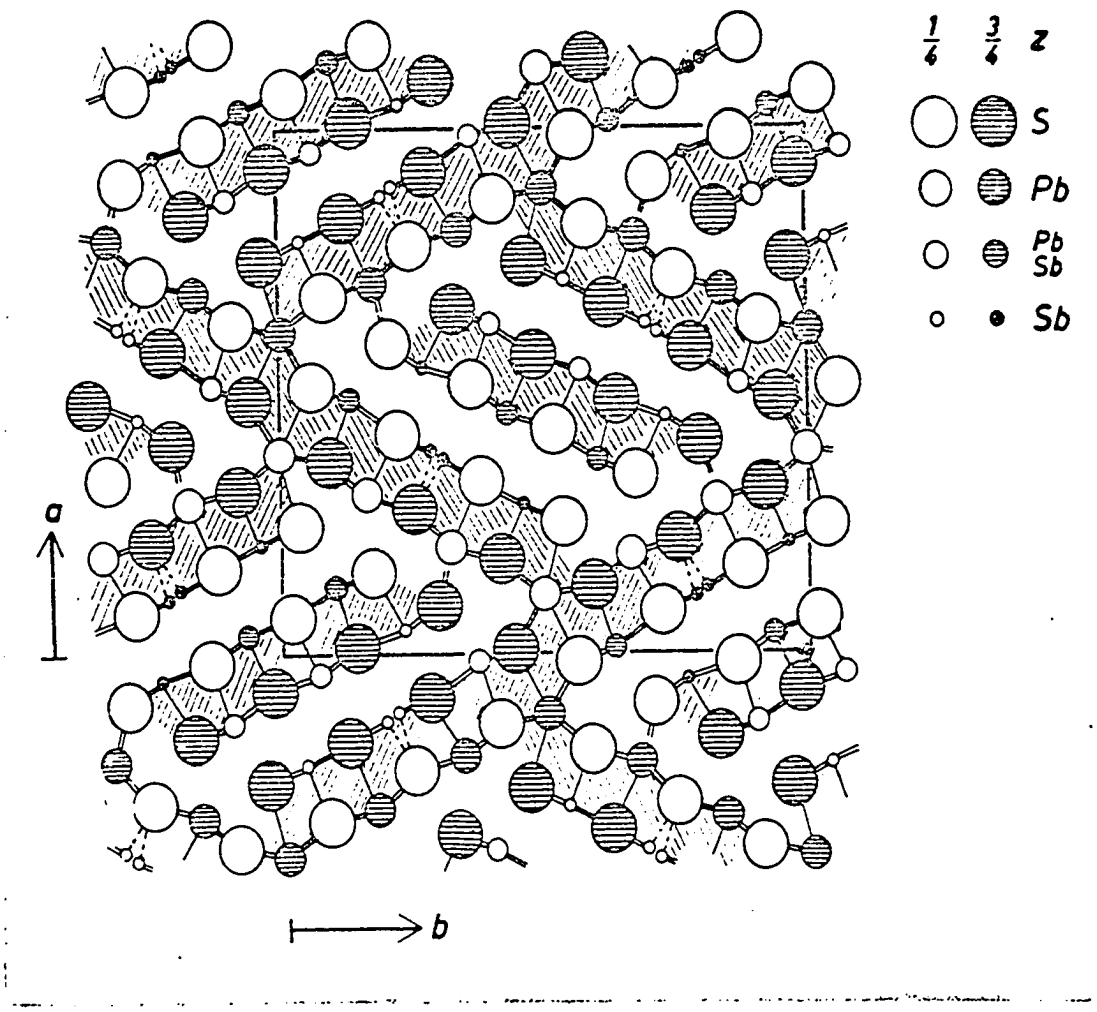

Figure 19 The structure of boulangerite for the sub-cell, projected on (001); the hatched parts indicate the chains in the c-direction. (Born and Hellner, 1960).

TABLE 21

Atomic Parameters of Boulangerite*

No. of atom	Symbol	Parameter x	y	z
1	Pb	0.307	0.160	0.250
2	Pb	117	498	250
3	Pb	206	323	250
4	Pb, Sb	458	433	750
5	Pb, Sb	132	098	750
6	Pb, Sb	486	129	750
7	Sb	287	462	750
8	Sb	046	232	250
9a	Sb/2	388	283	750
9b	Sb/2	372	307	750
10	S	069	017	250
11	S	247	028	250
12	S	156	175	250
13	S	420	219	250
14	S	330	375	250
15	S	372	088	750
16	S	014	138	750
17	S	278	251	750
18	S	096	295	750
19	S	186	415	750
20	S	013	441	750

* Taken from Born and Hellner, 1960.

Table 21.) The atomic form factor was $(f_{Pb} + f_{Sb})/2$ which is reasonable for the superstructure and indicates that Pb and Sb alternate in the c direction. Two antimony atoms were in position 9 and therefore the atomic form factor for 9a and 9b has the value of f Sb/2. Table 21 gives the atomic parameters of boulangerite and Figure 19 shows the structural projection on the (001) plane.

Least Squares Cell Refinement

Two samples of boulangerite were refined and the results are compared below with the published values by Berry (1940) on material from Idaho.

TABLE 22

St. Antonia, California	Rimini, Montana	Gold Hunter Mine Mullan, Idaho
a_o = 21.558	21.558	21.56
b_o = 23.490	23.502	23.51
c_o = 8.074	8.080	8.09
β = 100°40'	100°31'	100°48'

The two Nonius patterns had several extra lines that were not recorded by Berry. These lines appeared on both films and could be matched with a theoretical reflection from the cell refinement. Simple crystal photographs of the Rimini, Montana sample indicated a very strong zero (hk0) and number two level (hk2) while the one level (hkl) was very weak. If a moderate or strong line had two possible hkl indices and one choice was (hk0) or (hk2) and the other choice (hkl) or (hk3), the former would be expected because of the large number of strong reflections on the zero and two levels. A line with very weak intensity could be a one or three level reflection.

A high temperature pattern (593° C) of the St. Antonia sample gave the following results:

$a_o = 21.512$

$b_o = 23.707$

$c_o = 8.103$

$\beta = 99°45'$

With higher temperatures the a_o dimension decreased slightly and the c_o direction increased. A rather large expansion occurred in the b_o parameter and the beta angle became slightly smaller. At high temperatures the writer believes boulangerite has orthorhombic symmetry and in order to substantiate this, the lattice parameters for a orthorhombic cell (from Born and Hellner, 1960) were used for the cell refinement. With such a large unit cell, the theoretical number of reflections was quite large so that both refinements (i.e., monoclinic and orthorhombic cell) have about the same number of accepted lines with about the same theta tolerance. A very large cell the size of 42 Å is not likely since disordering of the metal atoms usually occurs at high temperatures. The h indice of the hkl's in the orthorhombic cell is an even number and therefore the a_o direction can be divided by two. The cell refinement using the new a_o dimension accepted more lines than the other two refinements but the tolerance was also higher. No definite conclusion can be reached as to the symmetry of boulangerite at high temperatures, but the smaller orthorhombic cell appears to be the best and most probable choice. (See Tables 53, 54, and 55 for comparison of the cell refinements.)

Transition of Phase II into Boulangerite

Refinement of boulangerite formed from phase II is in Table 23.

TABLE 23

BOULANGERITE

Room Temperature St. Antonia, Calif.	593° St. Antonia	Boulangerite from phase II (613° C)	Boulangerite from semseyite (587° C)
a_o = 21.558	21.512	21.577	21.535
b_o = 23.490	23.707	23.671	23.701
c_o = 8.074	8.103	8.146	8.100
β = 100°40'	99°45'	100°13'	99°53'
	Quenched Sample of the Above		
	a_o = 21.627	21.608	21.557
	b_o = 23.441	23.471	23.428
	c_o = 8.075	8.041	8.055
	β = 100°27'	100°36'	100°37'

Transition of Semseyite into Boulangerite

The refinement of boulangerite formed from semseyite (Table 23) also showed high temperature expansion of the cell parameters especially in the b_o direction. The boulangerite probably has some solid solution at high temperatures which accounted for the range of cell dimensions between boulangerite which formed from phase II and semseyite.

All three high temperature boulangerites have strikingly similar cell dimensions and the b_o direction showed considerable expansion compared to the room temperature sample. Table 23 compares the high temperature dimensions with the dimensions from the corresponding quenched sample.

With quenching of the high temperature samples, the b_o length decreased significantly while the c_o direction in each case decreased

slightly. The a_o length actually increased slightly with cooling which was rather surprising. Normally one expects all three lattice parameters to expand with heating and contract again with quenching. In boulangerite, the a_o and c_o lengths showed relatively small expansions and contractions however, b_o changed very significantly. The beta angle in each case decreased slightly with heating and increased with quenching.

Apparently the atomic bonds in the b_o direction are not as strong as in the a_o and c_o directions and were able to expand somewhat in response to the increased thermal energy produced by heating.

Transition of Boulangerite → Galena

The cell refinement of the boulangerite to galena transformation showed that the galena at high temperatures had a unit cell length of 6.014 Å compared to a_o = 5.969 at room temperature.

Transition of Semseyite → Boulangerite → Galena

The galena formed from the above transformation had a high temperature unit cell length of a_o = 6.010 Å which was very similar to the 6.014 of the previous refinement.

Transition of Plagionite → Phase II → Boulangerite → Galena

The high temperature diffraction pattern identified galena but was quite poor with only a few of the most intense lines visible. A least squares cell refinement did not seem very meaningful with such a small number of diffuse lines.

Pb-Sb-S SYSTEM

Previous investigations of the Pb-Sb-S system were done by Sommerlad (1898), Jaeger and Van Klooster (1912), Iitsuka (1919), and Schank (1939). X-ray determination of the minerals was lacking in these studies and the visual identification of the phases obtained, is therefore questionable. Figure 20 is an equilibrium diagram for the PbS-Sb_2S_3 system redrawn by Robinson (1948) from thermal data of Jaeger and Van Klooster. For fusions containing more than 60 wt. percent PbS, Jaeger and Van Klooster found the reactions were so sluggish that changes in slope of the cooling curves were beyond their limit of interpretation. Iitsuka's determination (Fig. 21) of the melting temperatures of PbS (1050° C) and Sb_2S_3 (516° C) are too low and should read 1120° C and 550° C which means the temperatures throughout the system are correspondingly low. Both diagrams were constructed from data obtained by direct fusion of PbS and Sb_2S_3. Robinson employed deposition from aqueous solutions at 425° C and 2000 bars pressure as well as direct fusion. (Table 24 presents some of the data for constructing the diagrams.) Both equilibrium diagrams have an eutectic point at 15 wt. % PbS and a number of peritectic points.

More recent work was done by A. Kitakawa (unpublished Master's thesis, Yamagachi Univ., 1968, Fig.22). James Craig (personal communication, 1969) who worked concurrently with this study, constructed the diagram in Figure 23 which is basically similar to the writer's.

All previous work studied quenched phases where the true high temperature could have "collapsed" with cooling into a modified structure. Some transitions are unquenchable and would therefore be unobserved at

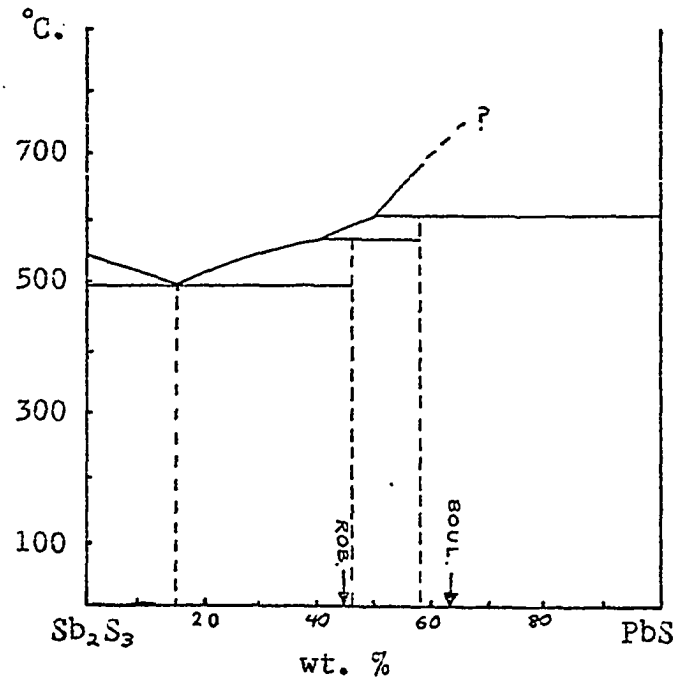

Figure 20 Equilibrium diagram for the PbS-Sb_2S_3 system. Redrawn by Robinson from thermal data of Jaeger and Van Klooster (1912).

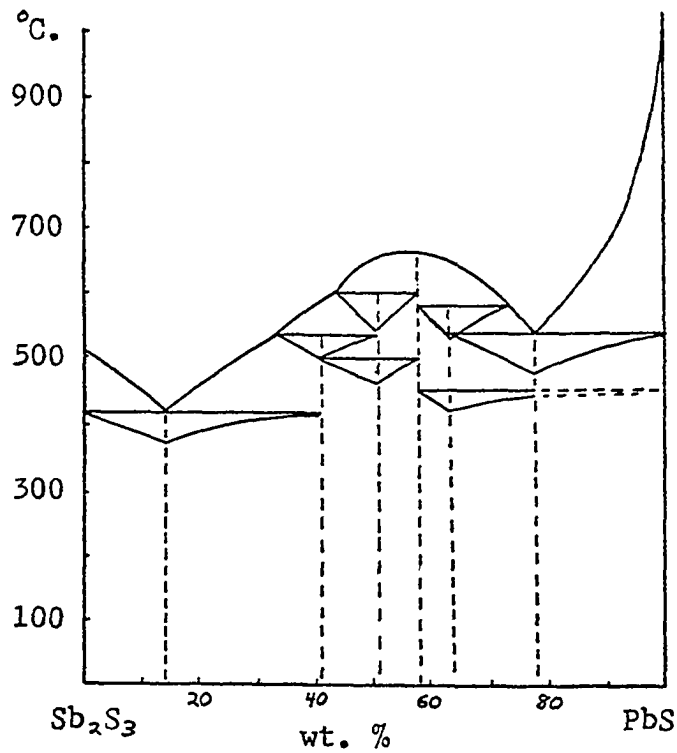

Figure 21 Equilibrium diagram for the PbS-Sb_2S_3 system, after Iitsuka (1919).

TABLE 24 *

Pertinent extracts from the thermal data on which the equilibrium diagrams (fig.20 & 21) are based.

Wt. % PbS	Mineral	°C Primary crystallization	Transition		Eutectic
100 (J&V.K.)	Galena PbS	1120	-	-	-
100 (I)	Galena PbS	1051	-	-	-
78 (I)	Eutectic	557	-	-	-
63 (I)	Boulangerite ($5PbS \cdot 2Sb_2S_3$)	590	596.8	468	-
58 (J&V.K.)	Jamesonite ($2PbS \cdot Sb_2S_3$)	609	-	-	-
51 (I)	Warrenite ($3PbS \cdot 2Sb_2S_3$)	660	610	513	-
46.7(J&V.K.)	Plagionite ($5PbS \cdot 4Sb_2S_3$)	590	565	522	391
58 (I)	Jamesonite ($2PbS \cdot Sb_2S_3$)	672	-	-	-
41 (I)	Zinkenite ($PbS \cdot Sb_2S_3$)	594.6	546	-	-
20 (J&V.K.)	Eutectic	495	-	-	-
14 (I)	Eutectic	428	-	-	-
0 (J&V.K.)	Stibnite (Sb_2S_3)	546	-	-	-
0 (I)	Stibnite (")	516.3	-	-	-

(J&V.K. = Jaeger and Van Klooster; I= Iitsuka)

* Taken from Robinson, 1948.

room temperature. The following however, is an interpretation of predominantly high temperature X-ray diffraction data for construction of a phase equilibrium diagram of the lead sulfantimonides. (Mineral synthesis and differential thermal analysis is also used where applicable.)

ZINCKENITE ($PbS \cdot Sb_2S_3$)

The high temperature powder pattern indicated that with heating, zinckenite's unit cell dimensions expanded and at a temperature near 540° C transformed into robinsonite and a liquid. With continued heating, robinsonite started to melt with the liquid changing composition along the liquidus. Finally all the robinsonite melted (~575°) and only liquid remained which of course gave no diffraction pattern. The DTA thermogram showed two endothermic peaks where the zinckenite transformed into robinsonite and where the robinsonite melted incongruently (Fig. 8). The following equations represent the reactions.

$$7PbS \cdot 7Sb_2S_3 \xrightarrow{540°} 7PbS \cdot 6Sb_2S_3 + L$$

(zinckenite) (robinsonite)

$$7PbS \cdot 6Sb_2S_3 \xrightarrow{\sim 575°} L$$

(robinsonite)

When heated in the DTA apparatus, the zinckenite transformed into robinsonite and much of the antimony and sulfur probably was vaporized and removed from the immediate vicinity of the sample. (The alumina in the DTA sample cup had a slight red-orange coating which could be from sublimated Sb and S.) In order to study the behavior of Sb and S, a zinckenite sample was sealed in an evacuated vycor tube and heated to 600° C. After slow cooling, tiny stibnite crystals were formed at the opposite end of the vycor tube which indicated the Sb_2S_3 was vaporized

during heating. [Robinson (1948) also noted that invariably, heating of a sample involved loss of Sb_2S_3 by sublimation.]

Synthetic minerals of varying compositions were studied and compared with natural minerals. Substances with a PbS to Sb_2S_3 ratio of 3:4 (#23), 6:7 and 1:1 were mixed in hopes of synthesizing zinckenite (1:1), however in each case, a material close to robinsonite in composition, crystallized. The diffractograms for robinsonite were essentially the same except the 3:4 mixture had an extra 3.60 Å peak due to slight mixture with stibnite. The initial ratio of $PbS \cdot Sb_2S_3$ does not appear too critical for the formation of robinsonite because apparently the excess Sb_2S_3 is vaporized until the composition is at least close to the ideal robinsonite ratio of 7:6. If the synthetic mixture was stibnite deficient (or PbS rich) with respect to robinsonite (such as the 4:3 mixture), boulangerite crystallized instead. At the high temperature of formation, robinsonite could have a limited amount of solid solution.

A polished section of sample #23 (i.e. 3:4) showed only the presence of robinsonite and no stibnite. The stibnite peak on the diffraction pattern of sample 23 was probably caused by sublimation of the excess Sb_2S_3 on the surface of the sample with cooling. Stibnite therefore did not show up in the polished section.

A single crystal from #23 was mounted on the Weissenberg rotation camera for 0 and 1 level photographs. The results showed that the crystal was robinsonite and the indexed spots could be matched with the (hkl) values given by Berry and Thompson (1962). (Very few artificial crystals of robinsonite have ever been grown.)

For the high temperature camera, zinckenite was sealed in tiny quartz

tubes (.7 mm OD) where only a very small air space was present. Any sulfur and antimony vaporized during heating could not escape and was kept in close contact with the sample. After the zinckenite to robinsonite transition, the tube was cooled very slowly in order to check the reversibility of the reaction. When the sample reached room temperature the diffraction pattern only showed robinsonite. In all probability however, the reaction is reversible and cooling was too rapid.

Synthetic robinsonite was heated in the high temperature camera and at 575° C produced a rather weak pattern very similar to phase II which formed from heating plagionite. The composition of phase II was not determined and was plotted according to Craig's data. The equation for the reaction is as follows:

$$7PbS \cdot 6Sb_2S_3 \xrightarrow{575^\circ} 5PbS \cdot 3Sb_2S_3 + L$$

(robinsonite) (phase II)

Most of the synthetic robinsonite samples sealed in quartz tubes leaked at high temperatures. Apparently the mixture had a slight excess of Sb_2S_3 which vaporized increasing the pressure to the point of failure of the quartz tubes.

PLAGIONITE ($5PbS \cdot 4Sb_2S_3$)

Plagionite heated to 580° changed into phase II which in turn transformed into boulangerite (595°) and finally galena at 643° C. Following the composition of plagionite on the T-X diagram showed that the plagionite transformed into phase II ($5PbS \cdot 3Sb_2S_3$) and liquid I. At 597° C phase II changed into crystals of boulangerite and a liquid which changed composition along the liquidus until at 642° C the boulangerite

formed crystals of galena and a liquid. The following equations represent the reactions:

$$5PbS \cdot 4Sb_2S_3 \xrightarrow{575^\circ} 5PbS \cdot 3Sb_2S_3 + L_I$$

(plagionite) (phase II)

$$L_I + 5PbS \cdot 3Sb_2S_3 \xrightarrow{595^\circ} 5\ PbS \cdot 2Sb_2S_3 + L_{II}$$

(phase II) (boulangerite)

$$L_{II} + 5PbS \cdot 2Sb_2S_3 \xrightarrow{643^\circ} PbS + L_{III}$$

(boulangerite) (galena)

$$L_{III} + PbS \longrightarrow L_{IV}$$

Craig reported a small field of robinsonite and phase II at a temperature of 576 $\pm$ 5° to 582 $\pm$ 3° C. Plagionite had the appropriate composition to intersect this field with heating, but only phase II was identified.

The exact temperature at which all the galena melted could not be determined because of the poor quality diffraction patterns at this temperature and composition. [Galena was present at least up to 660° C.]

SEMSEYITE ($9PbS \cdot 4Sb_2S_3$)

Semseyite transformed into boulangerite which in turn changed into galena. According to the equilibrium diagram (Fig. 24), boulangerite and phase II should form, however only boulangerite was identified. Since semseyite has a composition much closer to boulangerite than to phase II, the lever principle indicates considerable more crystals of boulangerite (73%) form compared to phase II (27%). The small amount of phase II therefore went undetected. At 595° C phase II melted and a liquid and boulangerite remained. Continued heating caused boulangerite crystals to melt with the liquid changing composition along the liquidus. Boulangerite at

643° C reacted with the liquid to form galena. The following equations show the reactions:

$$5(9PbS \cdot 4Sb_2S_3) \xrightarrow{575°} 7(5PbS \cdot 2Sb_2S_3) + 2(5PbS \cdot 3Sb_2S_3)$$

(semseyite) (boulangerite) (phase II)

$$\text{boulangerite} + 5PbS \cdot 3Sb_2S_3 \xrightarrow{595°} L_I + \text{boulangerite}$$

(phase II)

$$5PbS \cdot 2Sb_2S_3 + L_I \xrightarrow{643°} PbS + L_{II}$$

(boulangerite) (galena)

$$PbS + L_{II} \xrightarrow{?} L_{III}$$

BOULANGERITE ($5PbS \cdot 2Sb_2S_3$)

With heating, boulangerite transformed at 643° C into galena and a liquid. The galena was present at least to a temperature of 660° C. Because of the very high melting point of galena (1120° C), the exact temperature where all the galena melted to a liquid was not determined.

Craig (1969) reported a change of boulangerite into a phase I but no such reaction was detected with the high temperature camera. The stability field of the phase is very small which makes identification difficult.

Robinsonite, plagionite, and semseyite are rare in nature and associations are not well described. Most reported cases of semseyite are as growths on galena and could represent a vapor-galena type of reaction. Plagionite and robinsonite may also result from a vapor reaction on pre-existing minerals.

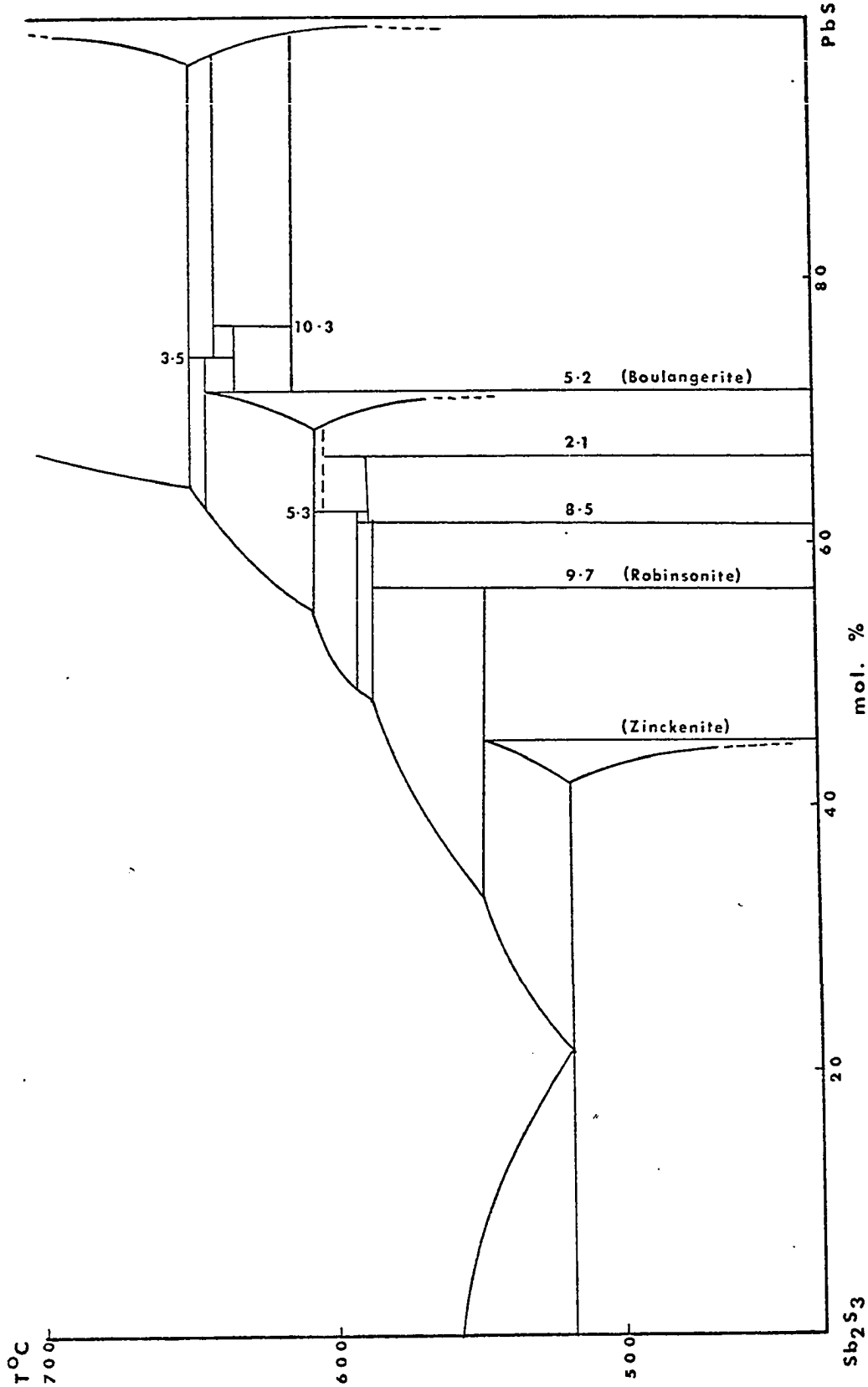

Figure 22. T-X equilibrium diagram for the Pb-Sb-S system (after Kitakawa, 1968).

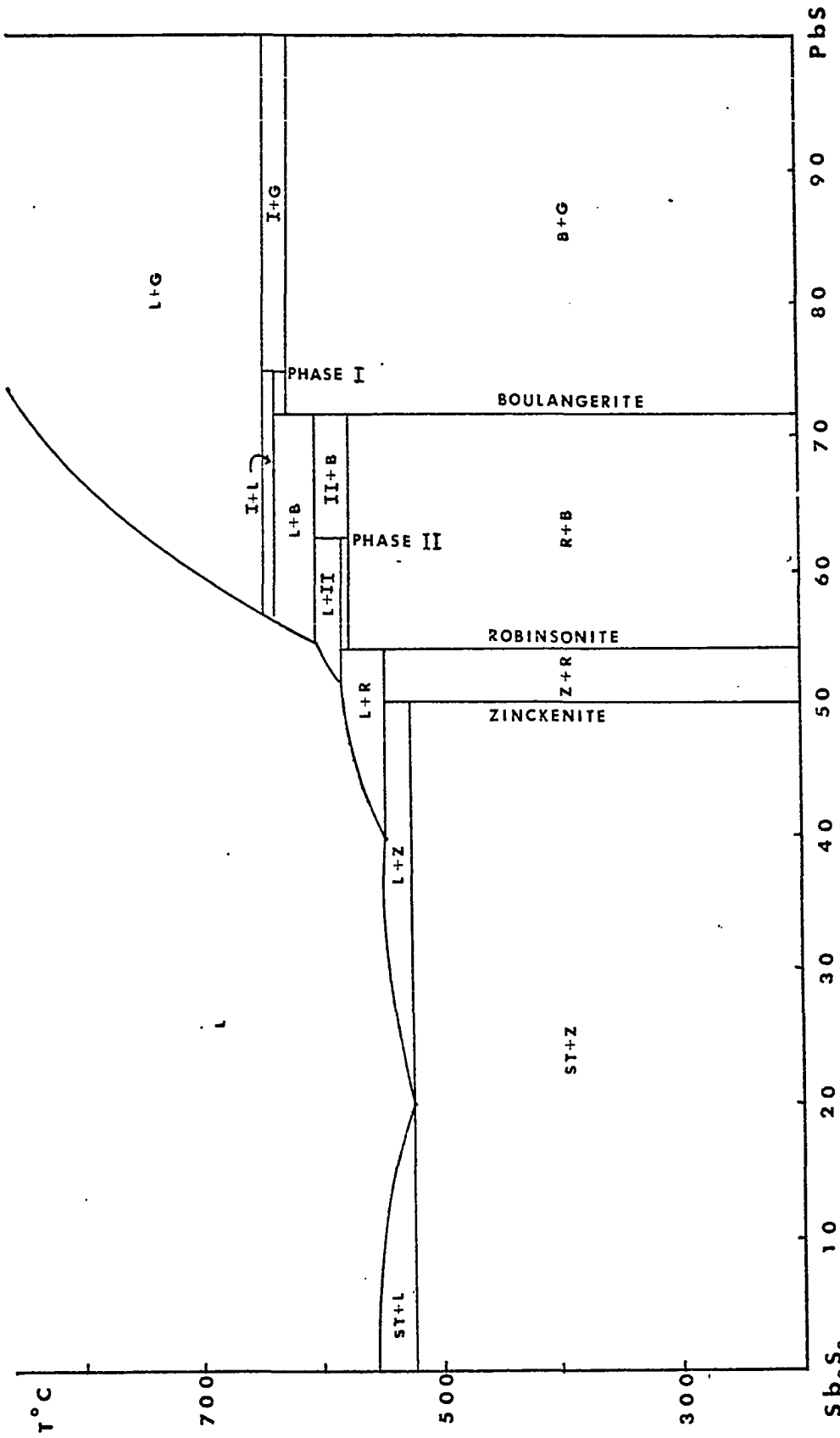

Figure 23. T-X diagram for the Pb-Sb-S system. (Craig, personal communication, 1969).

TABLE 25

X-RAY DATA FOR PHASES SYNTHESIZED IN THE Pb-Sb-S SYSTEM
(from Craig, 1969)

$3PbS \cdot Sb_2S_3$		zinckenite		robinsonite		Phase II $5PbS \cdot 3Sb_2S_3$		boulangerite	
d (Å)	I	d (Å)	I	d (Å)	I	d (Å)	I	d (Å)	I
4.62	1	5.54	1/2	4.40	1	5.69	1	4.37	1
4.23	1	5.28	1/2	4.04	5	5.46	1/2	3.90	3
4.11	2	4.37	1/2	3.98	7	4.93	1	3.83	2
4.08	1/2	3.92	1	3.92	2	4.30	2	3.72	10
3.87	1	3.56	1/2	3.80	4	3.72	10	3.66	3
3.80	1	3.43	10	3.71	4	3.54	1	3.43	1
3.74	3	3.20	1	3.66	4	3.40	1/2	3.30	3
3.69	8	3.14	2	3.58	2	3.29	3	3.22	5
3.41	4	3.08	1	3.51	2	3.28	1	3.19	2
3.32	4	3.03	2	3.45	2	3.27	4	3.01 3.00	5
3.27	8	3.00	2	3.40	10	3.24	4	2.96	1
3.24	2	2.91	1	3.30	2	3.16	6	2.93	1
3.06	6	2.80	3	3.20	1	2.94	1	2.82 2.81	9
2.96	5								
2.92	3	2.77	3	3.03	6	2.85	4	2.77	7
2.82	1	2.67	2	3.01	1	2.80	1/2	2.74	1
2.77	6	2.54	1	2.89	1	2.73	1	2.72	2
2.39	1/2	2.41	1	2.81	2	2.52	1	2.69	3
2.31	1/2	2.30	1	2.76	5	2.31	1/2	2.64	1
2.13	3	2.26	1	2.67	5	2.26	1	2.59	1
2.09	3	2.16	1	2.58	3	2.19	1/2	2.51	1/2
2.06	2	2.13	3	2.35	1	2.15	1	2.42	2
2.05	2	2.07	2	2.27	2	2.11	1	2.37	3
1.98	1	1.98	4	2.13	1/2	2.06	1	2.33	2
1.89	1/2	1.88	1	2.06	2	1.976	1	2.31	1
1.85	1/2	1.83	2	1.98	1	1.966	2	2.24	2
1.80	1	1.78	1	1.91	1	1.896	2	2.17	2
1.77	2	1.72	2	1.88	1	1.867	1	2.15	2
1.76	1	1.66	1	1.87	1	1.824	1	2.04	1
1.74	1			1.80	2	1.774	1	2.01	4
1.71	1/2			1.73	1	1.753	1	1.92	2
						1.718	1	1.86	7
								1.76	2

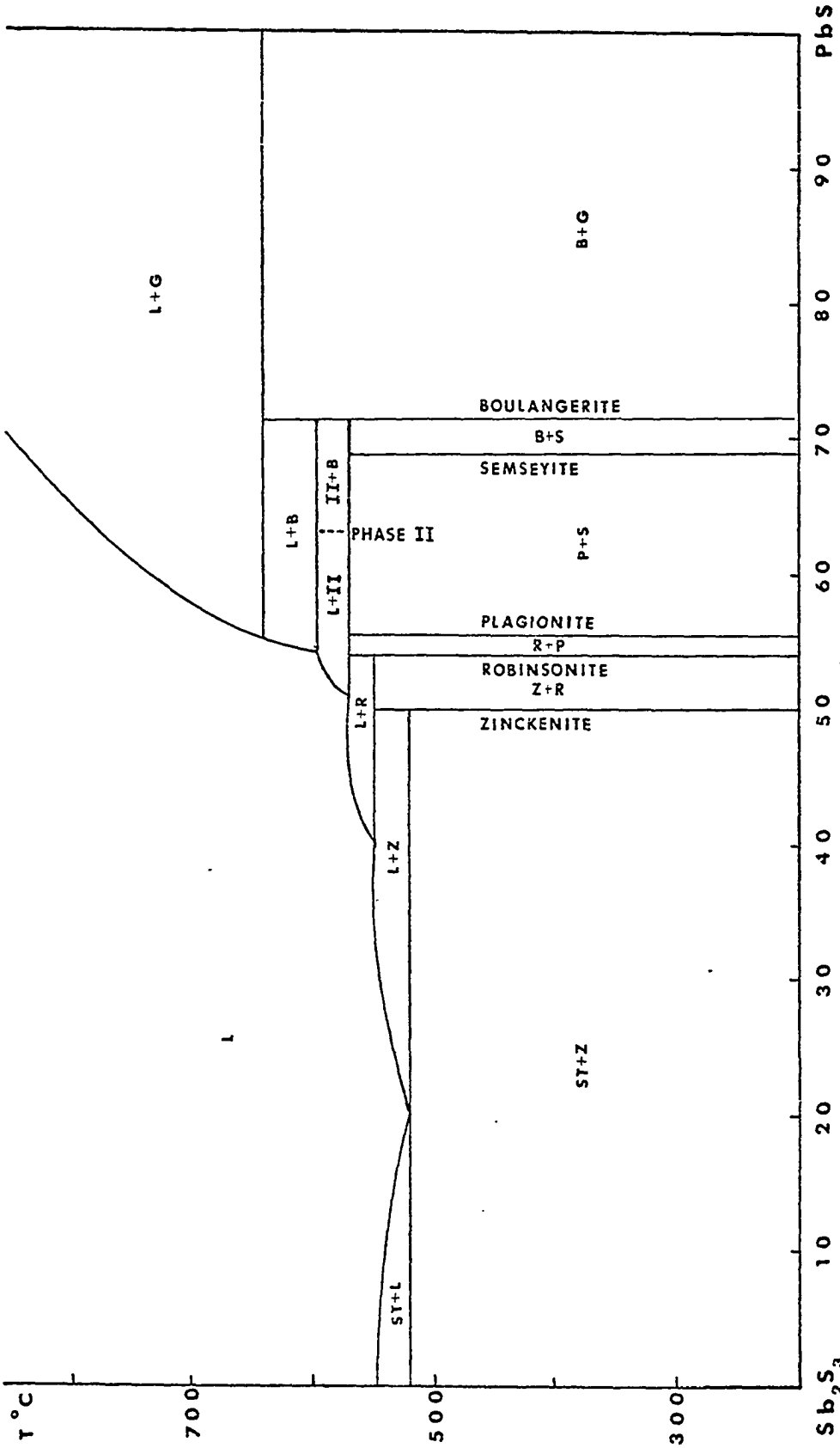

Figure 24 T-X diagram for the Pb-Sb-S system. (ST = stibnite, Z = zinckenite, R = robinsonite, P = plagionite, S= semseyite, B = boulangerite, G = galena, L = liquid.)

DADSONITE AND HETEROMORPHITE

The following two new minerals have recently been discovered and their compositions are not plotted on the Pb-Sb-S equilibrium diagram (Fig. 24). These minerals are quite rare and previously some doubt existed as to their validity.

Jambor (1969a) reported the occurrence of a new mineral which has the composition $11PbS \cdot 6Sb_2S_3$. This composition would be quite similar to phase II ($5PbS \cdot 3Sb_2S_3$) and could be the natural occurring equivalent of phase II. Table 26 compares the X-ray diffraction pattern for dadsonite with phase II and one can see similarities in the patterns.

Jambor (1969b) also concluded that three members of the plagionite groups, fuloppite, plagionite, and semseyite show linear correlations of the cell volume and density versus $PbS \cdot Sb_2S_3$ mol. ratios. He also demonstrates how this relationship can be used better to define the nature of the fourth member of the group, heteromorphite $7PbS \cdot 4Sb_2S_3$. (Table 27 gives the diffraction pattern for heteromorphite.)

TABLE 26

*DADSONITE - $11PbS \cdot 6Sb_2S_3$

Monoclinic: a = 19.05, b = 4.11, c = 17.33, β = 96°20'
*Taken from J. L. Jambor (1969a)

Dadsonite				phase II (at room temp.)	
I	d (meas.)	hkl	d (calc.)	I	d (meas.)
1	8.64	002	8.61		
3	8.18	$\bar{1}02$	8.19		
1	7.53	102	7.53		
1/2	6.75	$\bar{2}02$	6.75		
1/2	6.04	202	6.05		
1	5.69	$\bar{1}03$	5.67		
<1/2	5.36	103	5.38		
<1/2	4.70	$\bar{4}01$	4.70		
2	4.31	$\bar{1}04$	4.30		
4	4.10	010	4.11	1	4.07
3	4.03	303	4.03		
2	3.96	402	3.97		
1/2	3.87	$\bar{4}03$	3.87		
7	3.78	$\bar{5}01$	3.79	1	3.76
		500	3.79		
<1/2	3.73	$\bar{2}11$	3.72		
1/2	3.70	012	3.70		
6	3.62	$\bar{5}02$	3.62		
1/2	3.46	403	3.46		
10B	3.38	304	3.39	10	3.42
		$\bar{4}04$	3.38		
<1/2	3.34	502	3.33		
<1/2	3.25	113	3.26	1	3.28
<1/2	3.23	$\bar{2}13$	3.22		
2	3.158	600	3.156		
2	3.122	312	3.133		
1/2	3.071	$\bar{6}02$	3.075		
2	3.022	404	3.024		
1	2.994	$\bar{4}12$	2.989	4	2.97
2	2.888	305	2.893		
7	2.840	$\bar{4}12$	2.855		
		$\bar{2}06$	2.835		
6	2.794	$\bar{5}11$	2.785	6	2.78
3	2.726	$\bar{3}06$	2.729		
		$\bar{5}12$	2.715	1	2.69
		511	2.715		
3	2.648	405	2.650		
1	2.634				

TABLE 26 - Continued

Dadsonite				phase II (at room temp.)	
I	d (meas.)	hkl	d (calc.)	I	d (meas.)
<1/2	2.559			2	2.59
1	2.510				
<1/2	2.478				
1/2	2.454				
1	2.385				
1	2.360				
1/2	2.323				
<1/2	2.290			1	2.29
2	2.256				
4	2.218			1	2.22
<1/2	2.180				
1/2	2.159				
1/2	2.134				
1/2	2.115				
<1/2	2.093				
4	2.065			2	2.07
				4	2.00
2	1.934			1	1.93
1/2	1.921				
1/2	1.895				
4	1.886			2	1.88
<1/2	1.872				
<1/2	1.864				
1/2	1.846				
<1/2	1.830				
2	1.812				

TABLE 27

HETEROMORPHITE - $7PbS \cdot 4Sb_2S_3$

Monoclinic: C2/c, a = 13.60, b = 11.93, c = 21.22, β = 90°50'
Taken from J. L. Jambor (1969b)

I	d (meas.)	hkl	d (calc.)
1	10.59	002	10.61
1	6.89	$\bar{1}12$	6.88
2	5.58	$\bar{1}13$	5.58
1/2	4.58	$\bar{1}14$	4.58
<1/2	4.41	$\bar{2}21$	4.40
1	4.23	310	4.24
<1/2	3.96	024	3.96
1/2	3.92	312	3.92
6	3.85	$\bar{1}15$	3.85
4	3.82	130	3.82
7	3.75	131	3.75
1	3.59	132	3.59
1/2	3.44	$\bar{2}24$	3.44
8	3.40	400	3.40
10	3.30	$\bar{1}16$	3.30
8	3.25	$\bar{4}02$	3.25
<1/2	3.15	$\bar{2}06$	3.16
7	3.097	$\bar{2}25$	3.097
3	3.068	225	3.068
7B	2.970	$\bar{3}31$	2.964
7	2.884	$\bar{3}32$	2.885
2	2.838	422	2.836
4	2.794	$\bar{2}26$	2.790
3	2.763	$\bar{3}33$	2.764
1/2	2.722	240	2.731
5	2.710	$\bar{2}41$	2.711
		241	2.707
1	2.523	$\bar{2}27$	2.522
<1/2	2.499	227	2.500
3	2.460	208	2.459
2	2.281		
3	2.234		
6	2.135		
<1/2	2.127		
<1/2	2.098		
2	2.074		
1	2.065		
2B	2.020		
2B	1.975		

TABLE 27 - Continued

I	d (meas.)
1/2	1.911
1	1.892
3	1.884
1/2	1.859
1/2	1.847
<1/2	1.817
<1/2	1.795
1	1.767
1/2	1.753
1	1.725
<1/2	1.705
1/2	1.685

MINERALS WITHOUT AN INTERMEDIATE TRANSITION

The following section discusses the minerals which did not make an intermediate transition with heating.

MENEGHINITE

The mineral was named after Professor Meneghini (1811-1889) of Pisa, who first observed the species. Bechi (1852) described meneghinite from Bottino Mine near Tuscany, Italy where it occurs as slender prismatic [001], striated [001] crystals associated with galena, chalcopyrite, sphalerite, boulangerite, jamesonite, and albite.

Berry and Moddel (1941) determined the cell dimensions:

D_{2h}^{16}-Pbnm, a = 11.38, b = 24.09, c = 4.14, Z = 1

and the cell content as $Pb_{26}Cu_2Sb_{14}S_{48}$ while two copper free formulas were proposed by von Rath (1867) $Pb_4Sb_2S_7$ and by Palache, et al. (1938) $Pb_{13}Sb_7S_{23}$. Recently Fredrikson (1964) analyzed two crystals of meneghinite from Bottino with an Applied Research Laboratories electron microprobe X-ray analyzer and discovered that Pb, Sb, and Cu were homogeneously distributed in the mineral along with minute exsolved particles of galena. The probe analysis agreed fairly well with the formula $Pb_{26}Cu_2Sb_{14}S_{48}$ and that Cu does belong in the structure.

DTA

A sample from Bottino, Tuscany, Italy was heated to 650° C, cooled and X-rayed. From the diffraction pattern (Fig. 25), meneghinite could be identified along with intense galena peaks. The thermogram showed however, only the melting point at 613 ± 5° C and no intermediate peaks of decomposition. Upon closer examination of the diffractogram of the

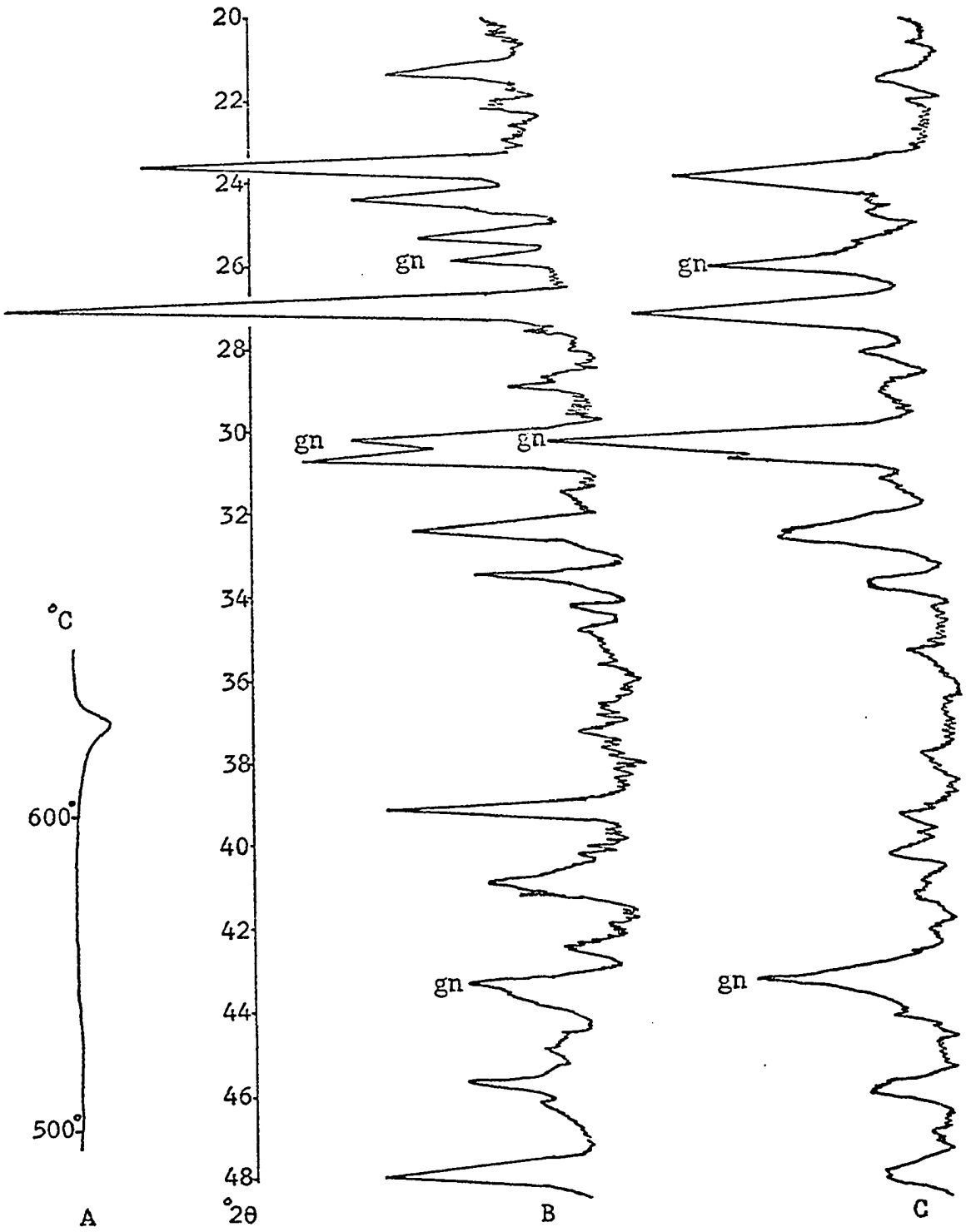

Figure 25 Meneghinite thermogram(A) and diffractograms of unheated(B) and heated(C) samples. (Note the larger amount of galena(gn) in the heated sample.)

TABLE 28

MENEGHINITE - $Cu_2S \cdot 26PbS \cdot 7Sb_2S_3$

Orthorhombic, D_{2h}^{16} - Pbnm; a= 11.38, b= 24.09, c= 4.14, Z=1

Taken from Berry and Thompson, (1962).

gn= galena
NR= not recorded
* heated to 650°C.

I	d(meas.)	hkl	d(calc.)	I	d(unheated)	I	d(heated)*
3	4.11	240	4.14	2	4.17	1	4.13
9	3.71	121	3.70	8	3.72	8	3.74
1	3.53	131	3.50		NR		NR
		211	3.32		3.44(gn)		3.44(gn)
10	3.30	170	3.29	10	3.32	10	3.28
		260	3.28				
1	3.08	231	3.09	1	3.08	½	3.08
		270	2.94		2.96(gn)		2.96(gn)
8	2.92	241	2.93	5	2.92	8	2.92
		180	2.91				
		360	2.76				
4	2.75	251	2.75	3	2.76	5	2.76
3	2.65	280	2.66	3	2.65	2	2.67
		081	2.43				
1	2.42	351	2.42	1	2.39	½	2.39
		0100	2.41				
1	2.31	421	2.30	2	2.31	½	2.29
3	2.24	431	2.25	2	2.22	1	2.25
		281	2.24				
3	2.19	470	2.19	2	2.20	1	2.19
		441	2.18				
1	2.12	540	2.13	1	2.13	½	2.14
		451	2.11				
		0101	2.08				
5	2.08	004	2.07		(men.&gn)		(men.&gn)
		480	2.07				
		461	2.02				
½	2.02	0120	2.01		NR		NR
4	1.97	560	1.98	3	1.97	2	1.98
		490	1.95				
		471	1.94				
1	1.94	531	1.94	½	1.94	½	1.94
		391	1.93				
		541	1.89				
4	1.88	232	1.89	3	1.89	3	1.90

unheated specimen, weak galena peaks were superimposed on the meneghinite pattern (Fig. 25), as would be anticipated from Fredrickson's observations. When the meneghinite was heated above the melting point, antimony and sulfur were vaporized leaving excess PbS which crystallized as galena and resulted in more intense galena peaks on the diffractogram of the heated sample.

At a high temperature during original crystallization from ore solutions, meneghinite probably had an expanded structure so that an excess of PbS could fit in the crystal lattice. Upon further cooling, the mineral could no longer hold this excess in a stable structure and the PbS was exsolved as tiny inclusions about 1 micron in size.

Structure

Euler and Hellner (1960) proposed the true cell dimensions as:

a = 11.363, b - 24.057, c - 24 x 4.128, space group C_{2v}^{7}-$Pn2_1m$ and derived atomic parameters from the subcell. (See this reference for greater detail.)

High Temperature Camera

Meneghinite from Italy did not make any intermediate transitions and showed only a slight lattice expansion with heating.

Least Squares Cell Refinement

The following table compares the room temperature and heated cell dimensions.

TABLE 29

Meneghinite (Berry and Moddle, 1941)	Room temperature Bottino, Italy	Heated to 570° C
a_o = 11.38	11.379	11.321
b_o = 24.09	24.097	24.150
c_o = 4.14	4.144	4.152

The b_o direction expanded considerably with heating while c_o remained about the same. The length of a_o actually decreased with heating which was highly unusual.

JAMESONITE

The mineral was named after the mineralogist Robert Jameson (1774-1854) for his early work in 1820 and 1821. Jamesonite occurs as acicular to fibrous [001] crystals, striated parallel to [001]. It is found associated with pyrite, galena, stibnite, sphalerite, tetrahedrite and other lead sulfosalts in hydrothermal veins of low to moderate temperatures.

Originally the composition of jamesonite was thought to be $Pb_2Sb_2S_5$, however later analyses showed the presence of iron $Pb_4FeSb_6S_{14}$.

DTA

A sample from Noche Buena, Zacatecas, Mexico was heated to a temperature of 660° C, cooled, and X-rayed. The diffraction pattern of the heated sample was quite similar to the unheated sample (Fig. 26, Table 30). The thermogram showed only an endothermic peak starting at 580 ± 5° C which is the melting point. (Due to the preferred orientation of the very acicular crystals during mounting of the sample, the intensi-

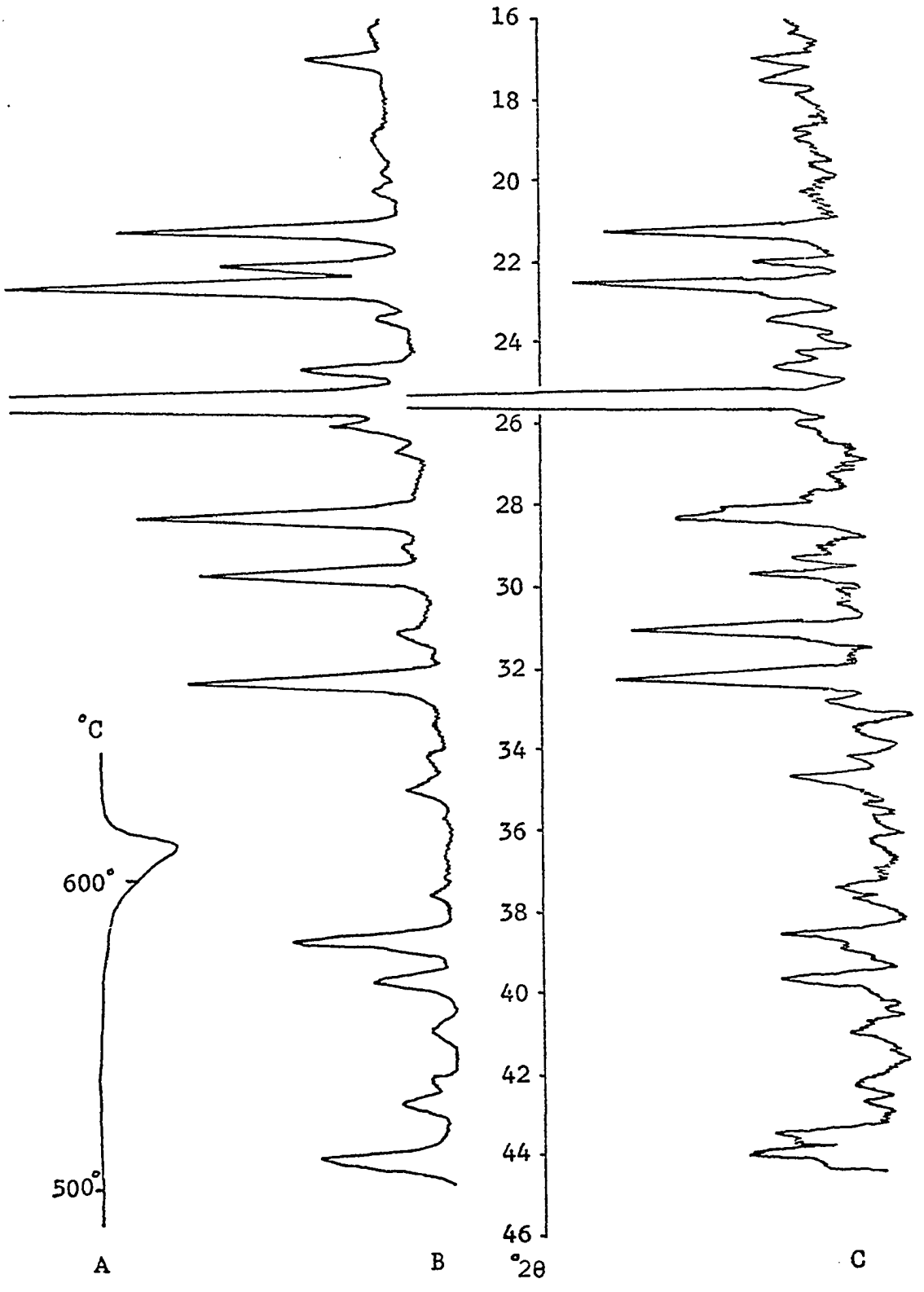

Figure 26 Jamesonite thermogram(A) and diffractograms of unheated(B) and heated(C) samples.

TABLE 30

JAMESONITE - $4PbS \cdot FeS \cdot 3Sb_2S_3$

Monoclinic, C_{2h}^5-P2/a; a= 15.71, b= 19.05, c= 4.04, β= 91°48'; Z= 2

Taken from Berry and Thompson (1962).

NS= not scanned
NR= not recorded
* heated to 635°C.

I	d(meas.)	hkl	d(calc.)	I	d(unheated)	I	d(heated)*
½	6.03	220	6.03		NS		NS
½	5.10	310	5.05	1	5.10		NR
3	4.10	240	4.07	3	4.16	3	4.16
4	3.87	400	3.92	4	3.91	4	3.92
2	3.72	021	3.72	1	3.74	1	3.74
		150	3.70				
3	3.59	121	3.59	2	3.57	1	3.57
10	3.44	250	3.43	10	3.46	10	3.46
1	3.34	430	3.34	1	3.39	½	3.39
		131	3.31				
5	3.18	060	3.17	3	3.18	3	3.17
5	3.09	510	3.10	3	3.13	3	3.12
		231	3.10				
		350	3.08				
		321	3.07				
2	2.95	260	2.93		NR		NR
9	2.84	411	2.83	1	2.84	4	2.84
		331	2.82				
8	2.75	411	2.74	3	2.74	4	2.75
		450	2.73				
1	2.63	341	2.63	1	2.56	2	2.59
		540	2.62				
1	2.36	521	2.36	½	2.38	1	2.38
		261	2.36				
		180	2.35				
3	2.30	640	2.29	2	2.33	2	2.33
4	2.24	171	2.24	1	2.25	2	2.25
		470	2.24				
		560	2.23				
		171	2.23				
1	2.16	380	2.17	1	2.18	1	2.18
		271	2.16				
½	2.11	730	2.11	1	2.11	1	2.11
5	2.06	371	2.06		NR	2	2.07
		570	2.06				
		081	2.05				
4	2.02	740	2.02	2	2.05	3	2.04
		660	2.02				

ties from the diffraction pattern differ slightly from those reported by Berry and Thompson, 1962.)

Structure

Nüzeki and Buerger (1957) have determined the structure and the atomic parameters, but no discussion will be given here since jamesonite melted without an intermediate transition involving structural change.

High Temperature Camera

Jamesonite from Huanuni, Bolivia was heated to its melting point of 595 ± 10° C without undergoing any intermediate phase transition. The patterns do show a slight lattice expansion with heating.

Least Squares Cell Refinement

The following table presents the cell refinement for jamesonite at room temperature.

TABLE 31

	Jamesonite Oruruo, Bolivia (Berry, 1940)	Jamesonite at room temperature Huanuni, Bolivia
a_o =	15.71	15.716
b_o =	19.05	19.177
c_o =	4.04	4.037
β =	91°48'	91°45'

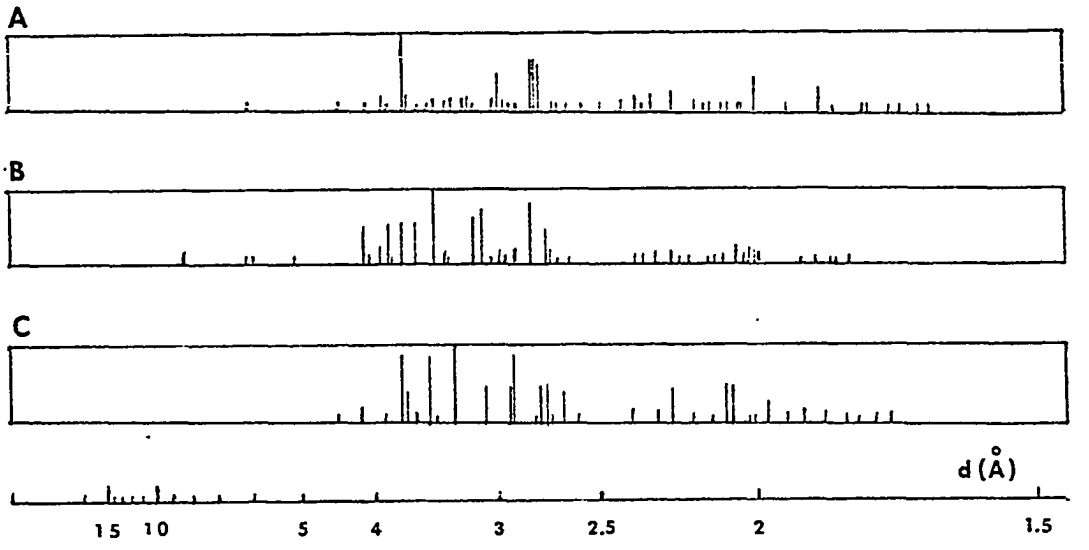

Figure 27 Nonius patterns A) boulangerite heated to 608°C. and quenched to room temperature B) unheated jamesonite C) unheated meneghinite.

STANNITE

Stannite (Cu_2FeSnS_4) was named after the Latin word for tin. Early workers with the mineral were Kloproth (1787), Werner (1789), Kirman (1796), Bendant (1832) and Dana (1868).

Crystals are rare and twinning produces a pseudododecahedral habit. Stannite is associated with sphalerite, chalcopyrite, tetrahedrite, pyrite, wolframite, cassiterite, and quartz.

Springer (1968) noted that generally stannite corresponds in composition to the formula Cu_2FeSnS_4, however noticeable deviations in the ratio of the metals can occur and considerable zinc may be present. Quantitative electron probe analyses by Springer indicate that zinc often substitutes for iron. The atomic ratio Cu:(Fe+Zn):Sn was not always 2:1:1 although the metal:sulfur ratio remained 1:1.

DTA

A sample from Mina LaFabulosa, Bolivia was used in the DTA studies because it appeared uniform in polished section (no Zn for Fe substitution) and was distinctly tetragonal. [Koucky (1959) stated the Zn-rich "isostannites" described are actually tetragonal with $2a_o=c_o$.]

The sample was heated to a temperature of 850° C (above the MP) and cooled at the furance rate. The X-ray diffraction pattern (Fig. 28) for the heated sample showed the presence of SnS and stannite. The author therefore believes that as the melt cools, the stannite forms a rather open "SnS type: structure where Cu^{+}, Fe^{++}, and Sn^{+4} are distributed randomly in the metal sites. As the mineral gradually cooled, the metal ions slowly migrated into the correct positions for the forming of the "orderly" structure of stannite. If the sample was cooled too quickly,

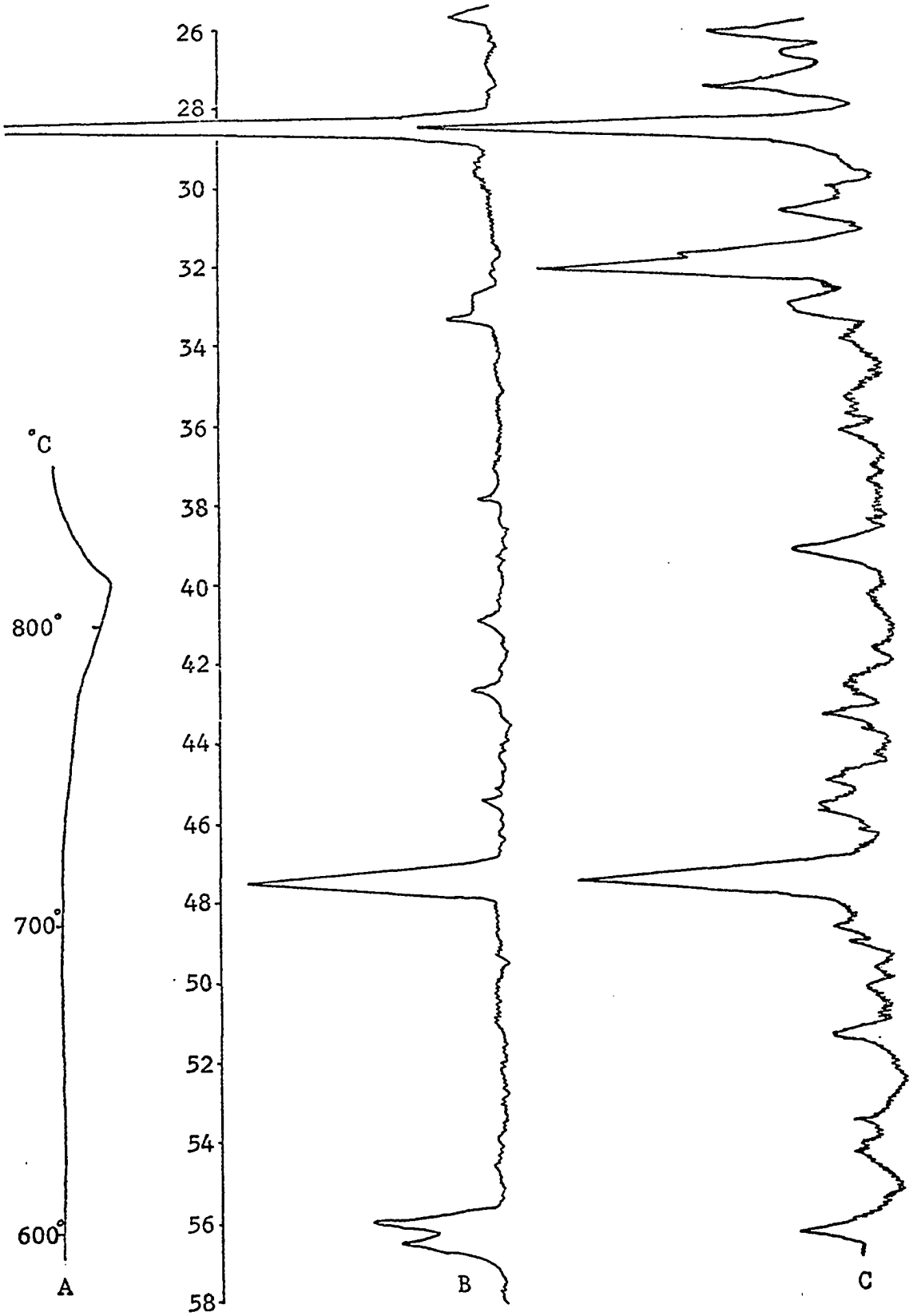

Figure 28 Stannite thermogram(A) and diffractograms of unheated(B) and heated(C) samples.

TABLE 32

STANNITE - Cu_2FeSnS_4

Tetragonal, D_{2d}^{11} - $I\bar{4}2m$; a= 5.47, c= 10.746; Z= 2

Taken from Berry and Thompson, (1962).				NR= not recorded NS= not scanned b= broad peak			
I	d(meas.)	hkl	d(calc.)	I	d(unheated)	I	d(heated)*
½	5.37	002	5.37		NR		NR
½	4.85	011	4.88	½	4.85	½	4.80
10	3.12	112	3.14	10	3.14	10	3.14
3	2.71	020	2,74	1b	2.71	2	2.74
		004	2.69				
½	2.46	022	2.44		NR		NR
½	2.38	121	2.39	½	2.38		NR
½	2.21	114	2.21	½	2.21		NR
7	1.92	024	1.92	5	1.92	8	1.93
4	1.64	132	1.65	4	1.65	2	1.64
3	1.63	033	1.63	3	1.63		NS
		116	1.63				
1	1.57	224	1.57	½	1.57		NS

* The heated diffractogram also showed the presence of a SnS-type structure which has the d-values listed in table 33.

TABLE 33

HERZENBERGITE - SnS*

Orthorhombic, D_{2h}^{16}-Pmcn; a= 3.99, b= 4.34, c= 11.20; Z= 4

Taken from Berry and Thompson, (1962).

NS= not scanned
NR= not recorded

I	d(meas.)	hkl	d(calc.)	I	d(heated)*
3	4.04	011	4.04	1	4.05
6	3.41	012	3.43	4	3.42
2	3.24	102	3.25	4	3.26
2	2.93	110	2.94	2	2.94
10	2.81	013	2.83	10	2.81
		004	2.80		
4	2.31	104	2.29	2	2.29
2	2.13	021	2.13	½	2.13
4	2.03	114	2.03	½	2.03
		022	2.02		
4	1.99	200	2.00	1	1.99
		015	1.99		
5	1.88	121	1.88	½	1.88
		202	1.88		
		023	1.88		
3	1.78	211	1.79	2	1.78
		115	1.78		
4	1.71	016	1.72	½	1.72
		024	1.72		
3	1.70	123	1.70	½	1.69

* Formed from cooling of a stannite melt.

the ions would not have sufficient time to occupy the ordered positions and some of the "SnS type: structure would be quenched in. (Refer to thermal disorder discussion in the Introduction.)

Generally a higher symmetry is expected at elevated temperatures compared to low temperatures. Stannite at room temperatures is tetragonal while SnS (herzenbergite) is orthorhombic, however at high temperatures the SnS probably is cubic and "collapses" into orthorhombic symmetry at low temperatures as indicated in the X-ray pattern.

The thermogram showed an endothermic peak starting at 740° C and continuing to 810° C (see Fig. 28). Such a long range is unusual for simple melting and instead could indicate that the stannite gradually absorbed heat as the structure was "expanding" to approach a high temperature cubic phase until thermal agitation was so large that the mineral melted (in the vicinity of the maximum peak height at 810° C).

High Temperature Camera

The stannite from Bolivia gave a distinct tetragonal pattern at room temperature. With heating the cell expanded where the doublet lines moved closer and closer together. (See the section on the cell refinement for more information.)

The stannite from Snowflake mine, British Columbia was Zn-rich and produced a pattern which was tetragonal but not as distinct as the other stannite. (The Zn substituted for some of the iron.) With heating the cell expansion produced a pattern which appeared to have cubic symmetry.

With rapid cooling both stannites "collapsed" to give a tetragonal cell which was still slightly larger than the original room temperature

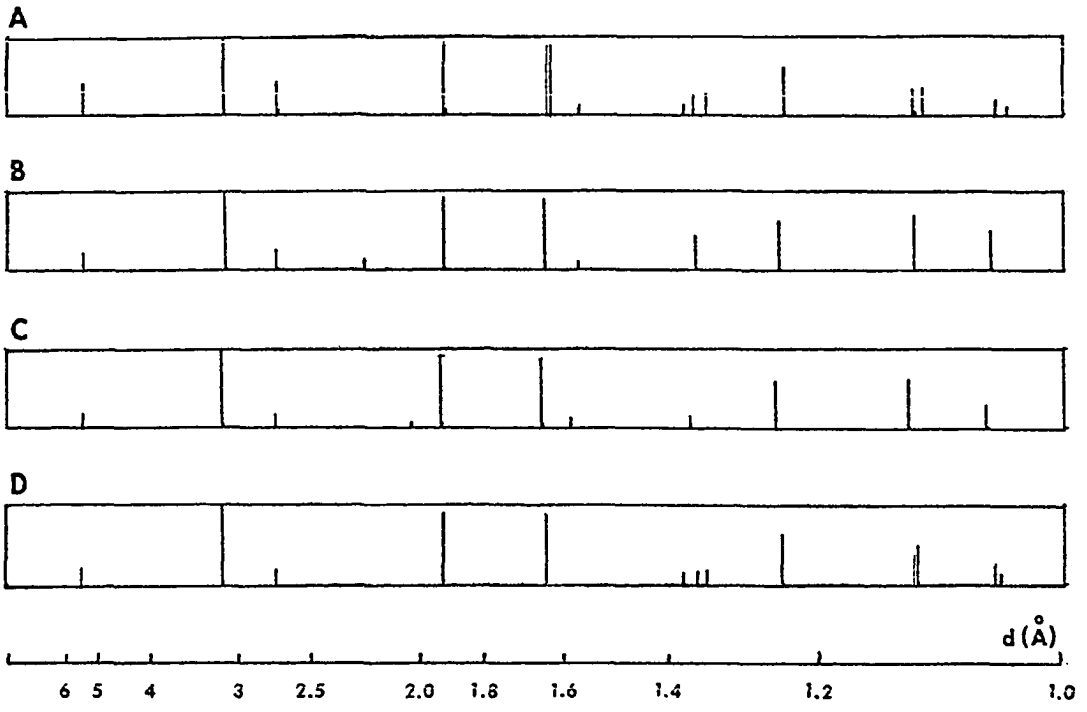

Figure 29 Stannite A) unheated B) at 480°C. C) at 735°C. D) stannite quenched to room temperature.

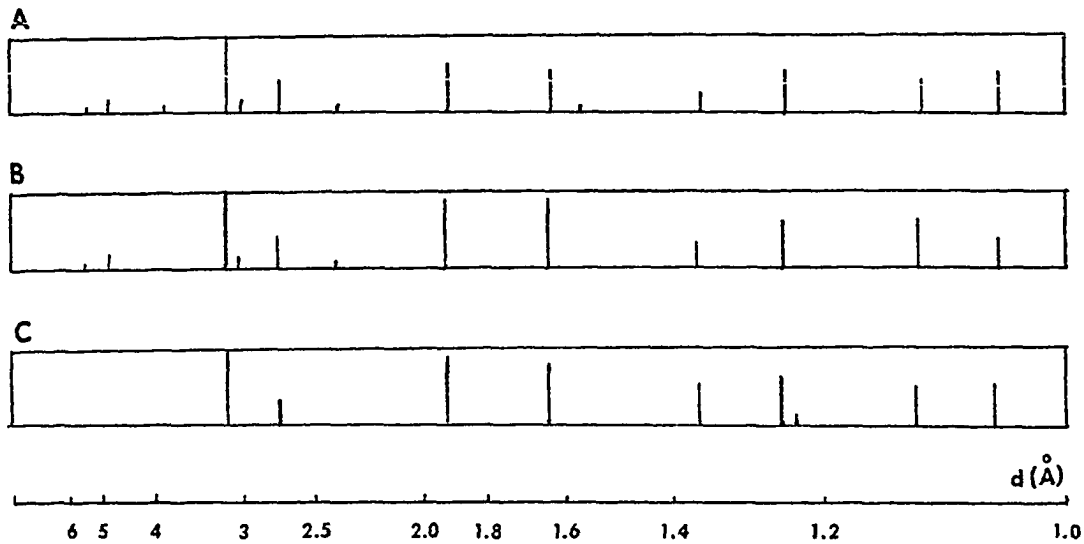

Figure 30 Zincian stannite A) unheated B) at 820°C. C) quenched to room temperature.

cell.

Frueh (1949) indicated that at 600° C (low) stannite changed into (high) stannite (sphalerite-type structure). The expanded stannite gave a diffraction pattern which was very similar to sphalerite however instead of having cubic symmetry, was really tetragonal where $2a_o$ happens to equal or is close to c_o. The expanded stannite was detected at 360° C which was far below Frueh's 600° C.

Structure

Brockway (1934) determined the cell dimensions as follows:

Tetragonal, D_{2d}^{11}-I42m $a = 5.47$, $c = 10.746$, $Z = 2$

and also determined the structure (Fig. 31) which is quite similar to that of chalcopyrite and sphalerite. Each sulfur atom is surrounded by four metal atoms, two copper, one iron, and one tin, located at the corners of an almost regular tetrahedron. The four sulfur atoms similarly surround each metal atom. As opposed to chalcopyrite, the Cu atoms occupy planes by themselves. As Brockway points out, the Cu-S distance of 2.31 $\pm$ .03 Å is smaller than the sum of the tetrahedral radii (2.30 Å), but quite close with observed Cu-S distances in sulvanite (2.28 $\pm$ .014 Å), enargite (2.32 $\pm$ .03 Å), binnite (2.28 $\pm$ .03 Å), wolfsbergite (2.29 $\pm$ .04 Å) and chalcopyrite (2.32 $\pm$ .03 Å). The tin-sulfur distance is 2.43 $\pm$ .03 Å for which the radius sum is 2.44 Å. The iron-sulfur distance of 2.36 $\pm$ .03 Å is quite unusual in that it is much larger than other iron-sulfur compounds (e.g., chalcopyrite 2.20 $\pm$ .03 Å). No satisfactory explanation has been found for the stability of the structure with such an anomalous bond distance. Table 34 gives the atomic parameters for the

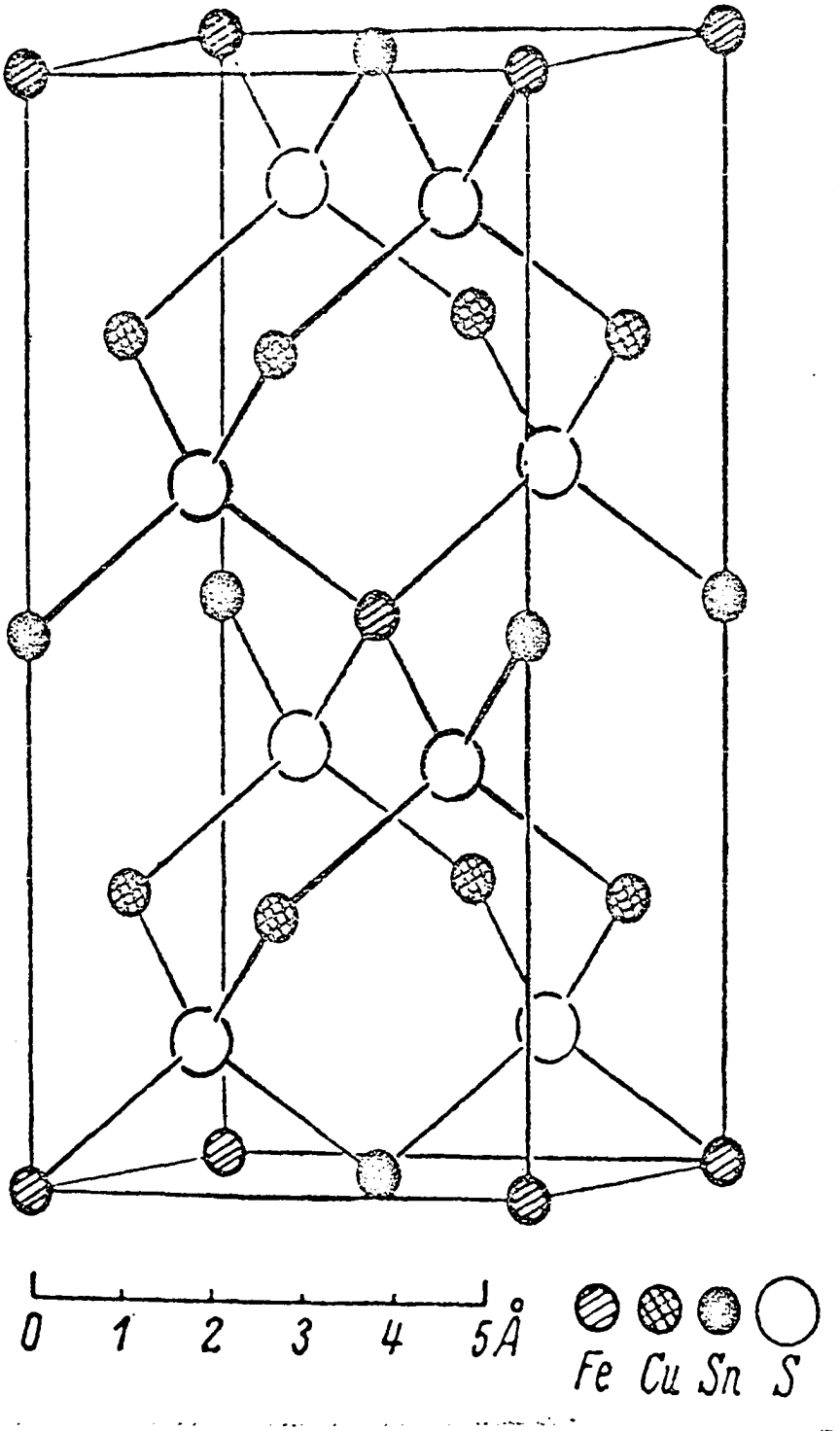

Figure 31 The structure of stannite, Cu_2FeSnS_4 (after Brockway, 1934).

unit cell.

TABLE 34

Atomic Parameters of Stannite

$2Cu_2FeSnS_4$

2Fe in 000, 1/2 1/2 1/2

2Sn in 00 1/2, 1/2 1/2 0

4Cu in 1/2 0 1/4, 1/2 0 3/4, 0 1/2 1/4, 0 1/2 3/4

8S in uuv, $u\bar{u}v$, u+1/2 u+1/2 v+1/2, u+1/2 1/2-u 1/2-v,
$\bar{u}uv$, uuv, 1/2-u 1/2-u v+1/2, 1/2-u u+1/2 1/2-v,

$u = 0.245 \pm 0.002$
$v = 0.132 \pm 0.002$

Least Squares Cell Refinement

Stannite, Mina La Fabulosa, Bolivia

The room temperature cell refinement gave the following results:

Oruro, Bolivia (Brockway, 1934)	Mina La Fabulosa, Bolivia
$a_o = 5.47$	$a_o = 5.457$
$c_o = 10.746$	$c_o = 10.794$

The 490° C and the 735° C patterns could be refined using a cubic or a tetragonal cell. In both cases the tetragonal refinement used more lines with a lower tolerance and in general gave a better fit than the cubic cell.

Room Temperature	480°	735°
$a_o = 5.457$	5.466	5.478
$c_o = 10.794$	10.841	10.837

The 490° C patterns showed expansion of the a_o and c_o directions

over the one at room temperature while the 735° pattern showed a further increase in the a_o direction over the 490° pattern.

Stannite, Snowflake Mine, Revelson, B.C.

The refinement of this Zn-rich stannite was as follows:

Snowflake Mine, B.C. (Berry and Thompson, 1962)	Snowflake Mine, B.C.
$a_o = 5.44$	$a_o = 5.424$
$c_o = 10.88$	$c_o = 10.894$

A pattern of stannite at 585° C was best refined with a cubic cell although a tetragonal cell also worked. Single crystal photographs indicated the stannite was still tetragonal where 2 a_o happened to equal c_o and appear cubic in symmetry. A sample heated to 820° C showed even more expansion of the unit cell. It is probable at very high temperatures just before melting that the metal atoms disorder somewhat causing the loss of weak diffraction lines of the superstructure. See the table below for the refinement.

Room Temperature	585°	820°
$a_o = 5.424$	5.447	5.479
$c_o = 10.894$	10.913	10.911

Note that both stannites show that at the intermediate temperatures the a_o and c_o directions expanded compared to the room temperature cell. At the higher temperatures however, the c_o directions showed no further expansion while the a_o lengths did.

MINERALS FORMING INTERMEDIATE PHASES

ENARGITE

Enargite [$3CuS(As,Sb)_2S_5$] was named after the Greek word for distinct, which refers to the cleavage. Breithaupt (1850), Field (1859), Semmons (1884), and Sandberger were some of the first men to study this mineral which forms tabular {001} and prismatic [001] crystals. The {110} cleavage is perfect with {100} and {010} distinct. Enargite is associated with sphalerite, pyrite, galena, bornite, tetrahedrite, covellite, barite, chalcocite and quartz in vein and replacement deposits formed at moderate temperatures.

Chemical analyses show that Sb substitutes for As to at least 6% by weight and Fe is often present up to 3 wt. %.

The cell dimensions on material from Ouray Co., Colorado are as follows:

orthorhombic $a = 6.41$, $b = 7.42$, $c = 6.15$ Å, $Z = 1$

$C_{2v}^7 = Pnm^2$

In 1934, Pauling and Weinbaum obtained slightly different values:

$a = 6.46$, $b = 7.43$, $c = 6.18$ kX

on samples from the Phillipine Islands.

DTA

A sample of enargite from Ouray Co., Colorado was heated to 700° C, cooled and X-rayed. The diffraction pattern (Fig. 32) showed that the enargite had transformed into tennantite upon heating. The thermogram showed that at approximately 527 ± 5° C an endothermic peak started which continued to increase in size to a maximum at 600° C and then reached a

minimum at 645° C before forming another peak.

Several runs were made at different temperatures to discover the nature of the peaks. One sample was heated to 560° C and held for an hour. The diffractogram showed that the enargite had changed into tennantite and the sample in the cup appeared recrystallized but not melted. A sample that was heated at 660° C had melted into a rather hard ball inside the cup. The first peak on the thermogram therefore, corresponded to the transformation of enargite to tennantite;[1] while the record peak was the melting of tennantite.[2] (It was noted that the arsenic reacted with the stainless steel to produce a yellowish-gold ring on the side of the sample cup.)

The change of enargite into tennantite, according to their chemical formulas, appeared to be of a decompositional nature rather than a polymorphic one. In order to verify the hypothesis, a sample of enargite sealed in evacuated vycor tubing was heated to the melting point and then quenched in cold water. A substantial amount of sulfur condensed on the walls of the tube and where the cold tongs touched the vycor, a reddish-orange substance formed which looked like realgar. (Apparently a small amount of arsenic combined with the sulfur to form the realgar as the tongs quenched the tube.) The sample was X-rayed and found to be a mixture of enargite and tennantite. The enargite decomposed

---

[1]Wernick and Benson (1957) found that enargite melted at 655° C and did not report a transition.

[2]The melting point of 645° C for tennantite is the same as determined by Wernick and Benson (1957).

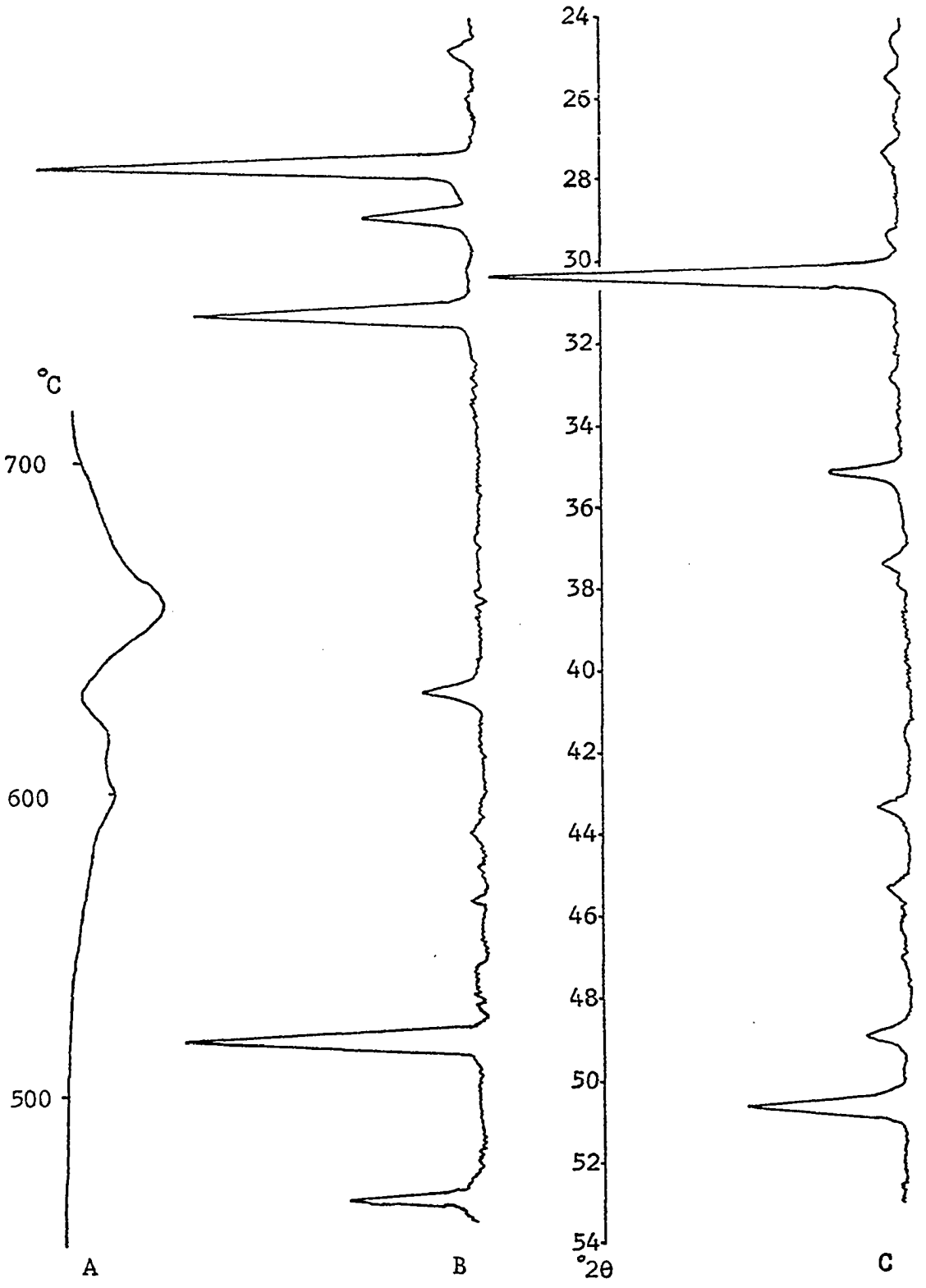

Figure 32 Enargite thermogram(A) and diffractograms of unheated(B) and heated(C) sample. (C is tennantite)

TABLE 35

ENARGITE - $3Cu_2S \cdot (As,Sb)_2S_5$

Orthorhombic, C_{2v}^7 - Pnm2; a= 6.41, b= 7.42, c= 6.15; Z= 1

Taken from Berry and Thompson, (1962).

NS= not scanned
NR= not recorded

I	d(meas.)	hkl	d(calc.)	I	un-heated d(heated)*
½	6.46	100	6.41		NS
½	4.87	110	4.85	½	4.89
½β	3.22	120	3.21		NR
		200	3.20		
10	3.22	120	3.21	10	3.22
		200	3.20		
4	3.08	002	3.07	5	3.08
½	2.97	210	2.94		NR
8	2.87	121	2.85	8	2.85
		201	2.84		
3	2.22	122	2.22	4	2.22
		202	2.22		
½	2.06	310	2.05	1	2.05
½	1.91	222	1.90	½	1.90
9	1.86	040	1.86	8	1.86
		320	1.85		
6	1.73	123	1.73	4	1.73
		203	1.73		

* See tennantite table for d-values obtained from heating enargite.

TABLE 36

TENNANTITE - $(Cu,Zn,Fe)_{12}As_4S_{13}$

Cubic, T_d^3- $I\bar{4}3m$; a= 10.21; Z= 2

Taken from Berry and Thompson, (1962).

NS= not scanned
NR= not recorded

I	d(meas.)	hkl	d(calc.)	I	d(heated)*
1	4.15	112	4.17	½	4.20
½	3.60	022	3.61	½	3.61
½	3.23	013	3.23	½	3.24
10	2.94	222	2.95	10	2.95
1	2.71	123	2.73	½	2.71
3	2.55	004	2.55	2	2.56
2	2.40	{114 / 033}	2.41	1	2.41
½	2.17	233	2.18		NR
½	2.07	224	2.08	1	2.09
2	1.99	{015 / 134}	2.00	1	2.00
2	1.86	125	1.87	2	1.88
8	1.80	044	1.81	5	1.81

* Formed from heating enargite to 550°C.

with the loss of some As and S to form tennantite. More importantly a small grain on the vycor tubing had a small halo where no sulfur was present. The grain had resorbed some of the sulfur, possibly during quenching.

In order to check the reversibility of the reaction, two identical samples of enargite were sealed in vycor tubes and heated to a temperature just below the melting point (640° C). In order to be sure some of the enargite changed into tennantite, one of the tubes was quenched and X-rayed. Once again enargite and tennantite were present. The other tube was cooled very slowly over a period of two days. According to the diffractogram, only a trace of tennantite remained, the rest was enargite.

High Temperature Camera

The enargite from Ouray Co., Colorado was heated in the camera and at 690 ± 10° C melted without transforming into tennantite. (Wernick and Benson [1957] reported the melting point at 655° C). In the tiny quartz tubes very little void space was present which did not allow much arsenic and sulfur to vaporize to form tennantite. The diffraction pattern identified only enargite and if a little tennantite did form, it was not in sufficient quantities to be detected.

Several of the quartz tubes leaked where apparently the vapor pressure was large enough to break the tubes. In such cases the enargite transofrmed into tennantite and at a higher temperature into a very simple pattern cubic in symmetry. In these tubes the arsenic and sulfur could escape changing the bulk composition to a more copper rich phase.

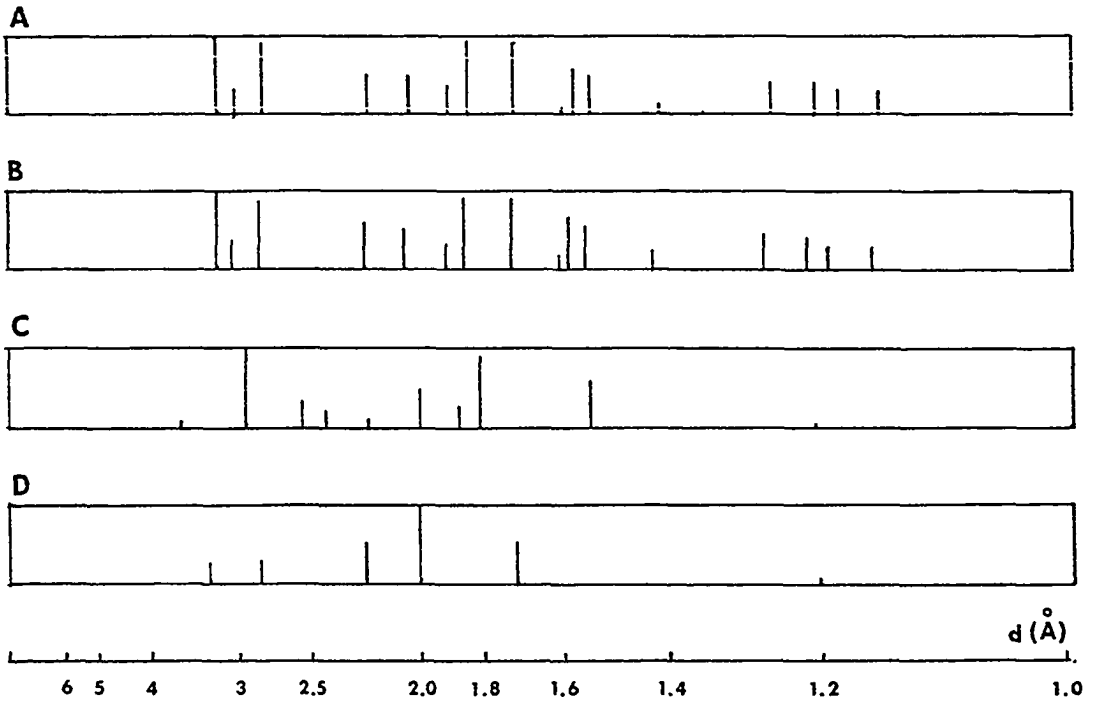

Figure 33 Enargite A) unheated B) at 590°C. C) tennantite formed from heating enargite to 595°C. in an open system D) a cubic phase formed from enargite at 615°C. in an open system.

Structure of Enargite and Tennantite

Pauling and Weinbaum (1934) described the structure of enargite as being very similar to wurtzite with each arsenic or copper atom surrounded by four sulfur atoms at the corners of a nearby regular tetrahedron and each sulfur atom similarly surrounded by a tetrahedron of one arsenic and three copper atoms. The AsS_4 groups share no sulfur atoms with one another and can be thought of as discrete entities. Figure 34 shows the atomic arrangements while Table 37 gives the atomic parameters.

Pauling and Neuman (1934) described tennantite in terms of the sphalerite structure. "In a large cube containing 32 ZnS, replace 8 Zn (at 1/4, 1/4, 1/4, 1/4, 1/4, 1/4, etc.) by As and the remaining 24 by Cu. Then remove 8 S (at 1/8, 1/8, 1/8, etc.), leaving As bonded to 3 S only, and introduce 2 S at 000 and 1/2, 1/2, 1/2, the centers of the two tetrahedra formed by the eight sulfur atoms removed." Table 38 gives the atomic parameters and figure 35 the atomic arrangement.

Enargite has a composition quite similar to tennantite as seen in the following table.

2 unit cells of enargite	1 unit cell of tennanite
2 $3Cu_2S \cdot (As,Sb)_2S_5$	$(Cu,Fe)_{12}As_4S_{13}$
12 Cu	12 (Cu,Fe)
4 (As,Sb)	4 (As)
16 S	13 S

By heating enargite to a temperature of around 530° C, the thermal agitation apparently becomes so large that sulfur is released from the discrete AsS_4 units and forms AsS_3 (arsenic with a coordination number of

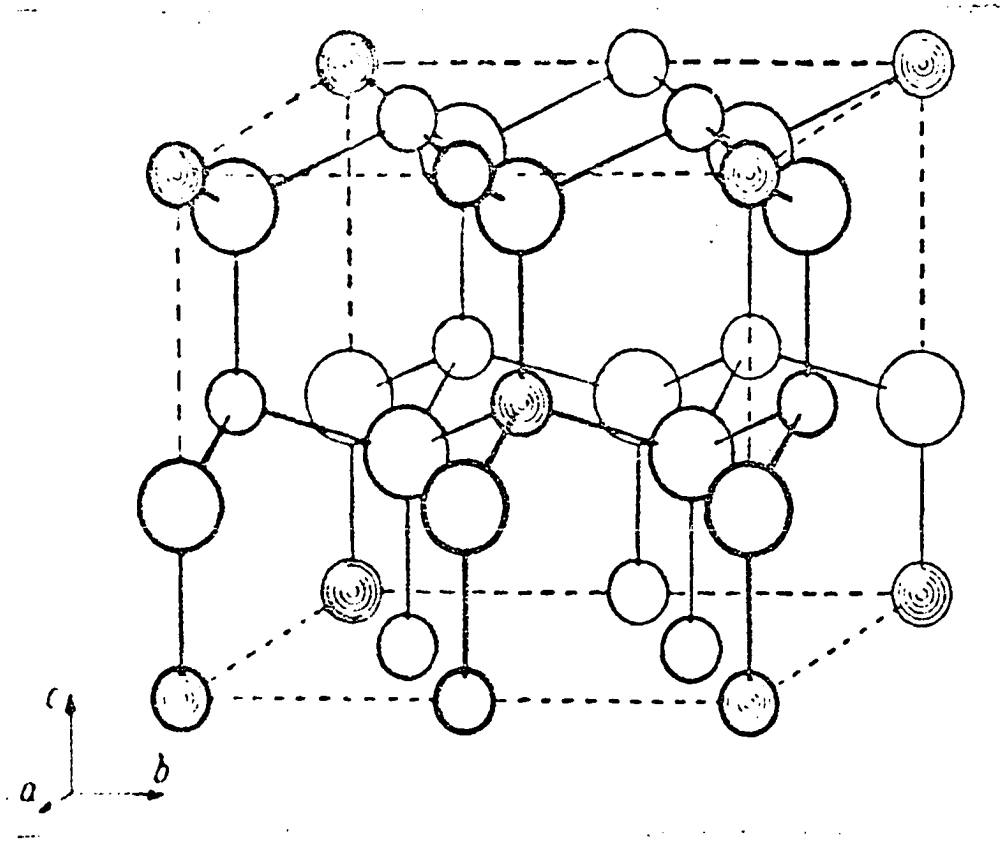

Figure 34 The structure of enargite, Cu_3AsS_4. Large circles represent sulphur, small open circles copper, and small shaded circles arsenic (Pauling and Weinbaum, 1934).

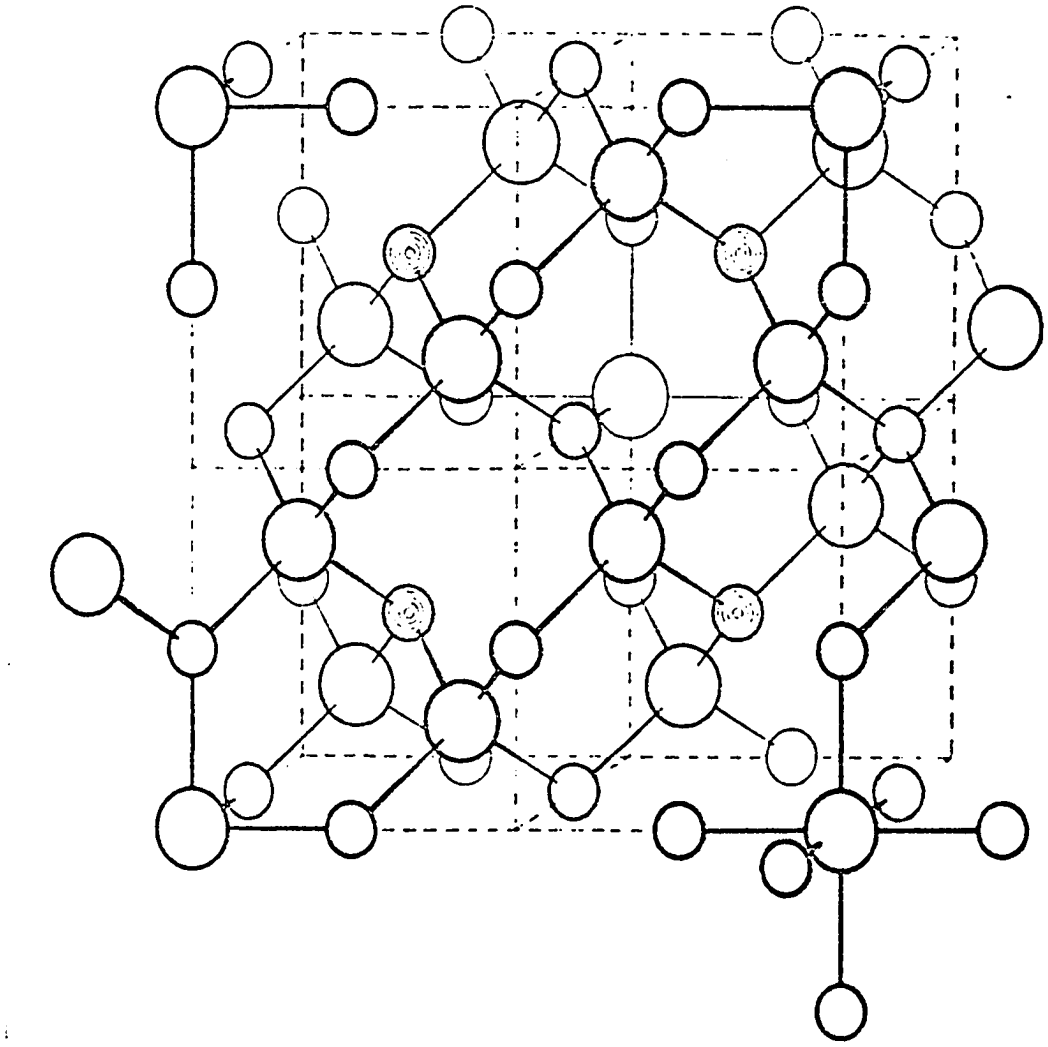

Figure 35 The structure of tennantite, $(Cu,Fe)_{12}As_4S_{13}$. (Only the front half of the unit cell is shown.) Large open circles represent sulphur, small open circles copper, and small shaded circles arsenic (Pauling and Neumann, 1934).

TABLE 37

Atomic Parameters for Enargite.*

	x	y	z
2 As in (a) x,0,z	0.820	0	0
2 Cu in (a)	0.165	0	0.500
4 Cu in (b) x,y,z	0.333	0.245	0.990
2 S in (a)	0.830	0	0.360
2 S in (a)	0.140	0	0.875
4 S in (b)	0.330	0.255	0.367

* Taken from Pauling and Weinbaum, 1934.

TABLE 38

Atomic Parameters for Tennantite*

	x	y	z
8 As in (c) x,x,x	0.255		
12 Cu_I in (d) $\frac{1}{2},\frac{1}{2},0$			
12 Cu_{II} in (e) x,0,0	0.225		
24 S_I in (g) x,x,z	0.122		0.363
2 S_{II} in (a) 0,0,0			

* Taken from Pauling and Neuman, 1934.

3) where a free electron pair fills the sulfur void. Arsenic atoms have two electrons in the 4s orbital and three electrons in the 4s orbital. Normally they form structures by loss of the p- electrons to assume a valency of 3. Enargite is an unusual structure in placing arsenic in a regular tetrahedron. Tennantite has arsenic in the more normal 3-coordination and the 4s orbital as an inert ion pair forming a distorted tetrahedron geometry. Copper can assume two valencies and stabilize this structure at low by not high temperatures. It is interesting that the arsenic tends to resorb the sulfur on cooling to form the discrete AsS_4 units again.

The Cu-S distances in enargite (2.31 and 2.33 Å) are very similar to those in tennantite (2.29 Å) as well as the As-S distances (enargite 2.21 Å and tennantite 2.21 Å).

Least Squares Cell Refinement

The cell refinement showed a very close agreement between the sample used in this study and the published values. (Note that both samples come from Ouray Co., Colorado.)

The mineral luzonite ($Cu_3(As,Sb)S_4$) is very similar to enargite but has about 6% or more antimony substituting for the arsenic. X-ray fluorescence indicated that the sample contained very little antimony (less than 1%) and indeed was "true" enargite.

Table 39 also gives the values for tennantite which showed an expansion from a_o = 10.21 Å at room temperature to a_o = 10.281 at 595° C. The cubic phase which formed at a higher temperature had a_o = 5.711 and was vaguely similar to digenite (Cu_7S_4).

TABLE 39

Least Squares Cell Refinement

Enargite Ouray Co., Colo. (Peacock and Thompson)	Enargite Room temperature
a_o = 6.410	6.409
b_o = 7.420	7.436
c_o = 6.150	6.141

Tennantite Binnental, Switzerland (Pauling and Neuman, 1934)	Tennantite (595° C)
a_o = 10.21	10.281
	Cubic phase (617° C)
	a_o = 5.711

Summary

If enargite is heated in a closed system most of the sulfur released can later on cooling, be resorbed to form enargite. In the case with an open system like the DTA, heating of enargite resulted in tennantite which remained no matter how slowly it was cooled.

The sulfur pressure in the vycor tubing apparently kept the enargite from completely changing into tennantite.[1] No matter how long the sample was heated and how fast the tube was quenched, a mixture of enargite and tennantite remained. The following equation depicts the reaction:

---

[1]Equilibrium here depends on the δP of S in the system. Unfortunately the partial pressure of sulfur was not known and further experimentation is needed.

$$2[3Cu_2S\cdot(As,Sb)_2S_5] \overset{\Delta}{\rightleftharpoons} (Cu,Zn,Fe)_{12}As_4S_{13} + 3S(g)$$

(enargite) (tennantite)

However in the tiny sealed tubes of the high temperature X-ray camera, little void space was present and the partial pressure of sulfur was large enough to prevent enargite from changing into tennantite. In the case of the much larger vycor tubes, significantly more void space allowed some enargite to transform into tennantite before the sulfur pressure became large and the reaction attained equilibrium.

The transformation listed in the equation is not a function of melting and could possibly take place at low temperature with high sulfur pressures. The experiments have established only one temperature (527° C) and pressure (1 atm) for the transformation of enargite into tennantite. With further work at various temperatures and pressures, a phase diagram could be constructed representing the transformation which might have a practical application in geothermometry and in determining sulfur pressure in mineral systems. (Both enargite and tennantite are common and occur in the same mining district.)

EMPLECTITE

Emplectite ($Cu_2S \cdot Bi_2S_3$) received its name from the Greek word meaning entwined, or interwoven in allusion to the intimate association with quartz. The first workers with the mineral include: Selb (1817), Schneider (1853), Kenngott (1853), Dana (1854), and Kobell (1864). Emplectite forms striated [001], flattened {010} prismatic crystals which are associated with siderite, chalcopyrite, wolframite, and molybdenite.

Hofman (1933) determined the following cell dimensions on single crystals from Schwarzenberg, Saxony:

a = 6.137, b = 14.541, c = 3.898, Z = 2, Pnam

He also found the structure to be like chalcostibite ($F5_6$ type) but did not determine the exact atomic positions.

DTA

Figure 36 shows the thermogram for emplectite from Johanngeorgenstadt, Saxony. Three distinct peaks are present, starting at 378° C, 466° C and 506° C. A sample was heated (385° C) just above the temperature where the first endothermic peak started and held for an hour. The X-ray diffraction pattern showed the presence of cuprobismutite which has the formula $Cu_2S \cdot Bi_2S_3$.

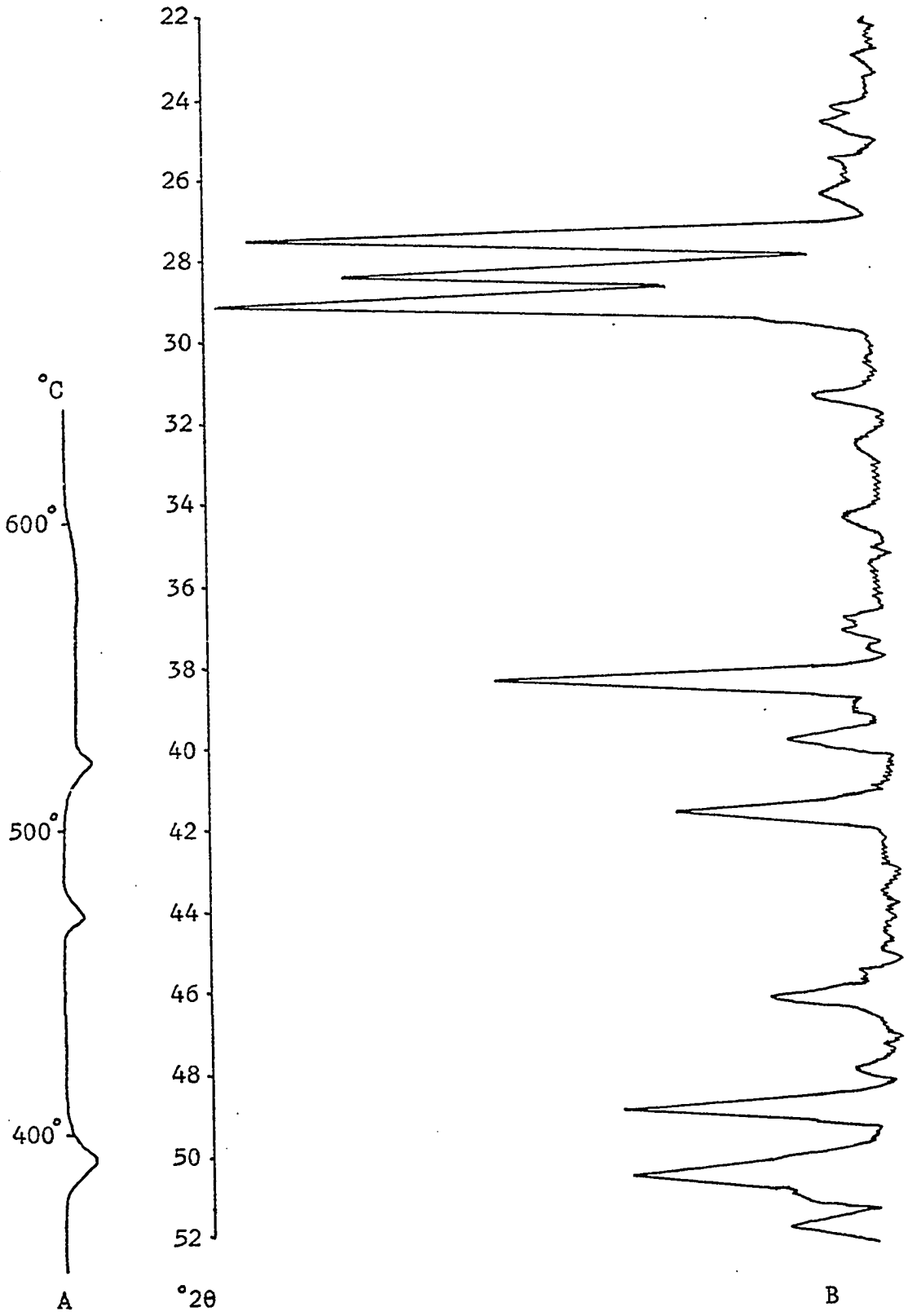

Figure 36 Emplectite thermogram(A) and diffractogram of the unheated(B) specimen.

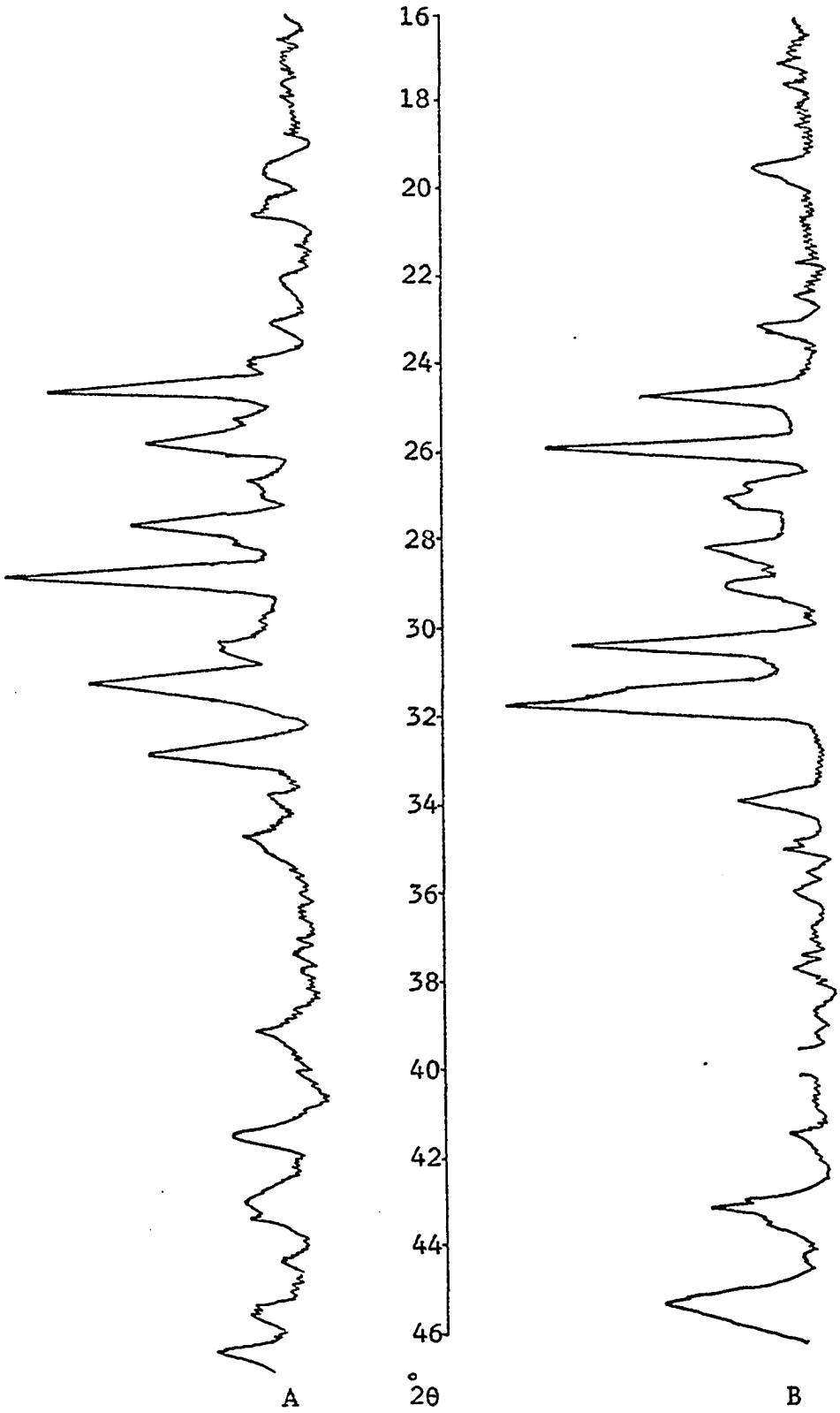

Figure 37 Emplectite heated to 378°C to form (A) cuprobismutite and then to 466°C to produce (B) wittichenite and phase X.

TABLE 40

EMPLECTITE - $Cu_2S \cdot Bi_2S_3$

Orthorhombic, D_{2h}^{16}- Pnam; a= 6.137, b= 14.541, c= 3.898; Z= 2

Taken from Berry and Thompson, (1962).

NS= not scanned
NR= not recorded

I	d(meas.)	hkl	d(calc.)	I	d(unheated)
5	7.38	020	7.27		NS
2	4.72	120	4.69	1	4.69
½	3.65	040	3.64	½	3.60
9	3.23	111	3.21	9	3.23
7	3.13	140	3.13	7	3.13
10	3.05	031	3.04	10	3.06
½	2.83	220	2.83	1	2.83
½	2.73	131	2.72		NR
½	2.61	230	2.59	½	2.59
½	2.42	060	2.42		NR
		201	2.41		
5	2.34	240	2.35	5	2.34
1	2.25	160	2.26	1	2.26
4	2.17	151	2.18	2	2.16
		231	2.16		
2	1.97	320	1.97	2	1.96
		170	1.97		
3	1.86	251	1.86	3	1.86
3	1.80	122	1.80	3	1.80
		311	1.80		
2	1.78	340	1.78	2	1.76

The heated sample changed into cuprobismutite at 378°C.

TABLE 41

CUPROBISMUTITE - $CuS \cdot Bi_2S_3$

Monoclinic, C_{2h}^3- C2/m; a= 17.65, b= 3.93, c= 15.24, β = 100° 30'; Z= 6.

b= broad peak
NS= not scanned
NR= not recorded

Taken from Berry and Thompson, (1962).					
I	d(meas.)	hkl	d(calc.)	I	d(heated)*
2	6.24	$\bar{2}02$	6.26		NS
3	4.31	400	4.34	2	4.34
4b	3.65	$\bar{1}11$	3.68	7	3.65
		$\bar{4}03$	3.62		
1	3.47	402	3.49	3	3.47
		$\bar{1}12$	3.47		
4	3.23	310	3.25	5	3.23
		$\bar{3}11$	3.25		
		204	3.23		
10	3.10	$\bar{3}11$	3.11	10	3.11
		$\bar{1}13$	3.10		
		$\bar{3}12$	3.10		
½b	2.96	$\bar{1}13$	2.98	1	2.95
		$\bar{6}01$	2.94		
1b	2.86	$\bar{6}02$	2.88	6	2.88
		$\bar{3}12$	2.88		
		$\bar{3}13$	2.86		
6	2.73	$\bar{6}01$	2.75	5	2.74
		$\bar{6}03$	2.73		
		$\bar{4}05$	2.71		
1	2.58	$\bar{3}14$	2.59	½	2.58
		$\bar{5}12$	2.57		
½	2.49	$\bar{5}11$	2.51		NR
		006	2.50		
½	2.30	$\bar{6}05$	2.30	1	2.31
		206	2.29		
2	2.17	$\bar{2}07$	2.17	2	2.18
		800	2.17		
2	2.09	710	2.10	2	2.08
		801	2.09		
		$\bar{6}06$	2.09		
		$\bar{3}16$	2.09		
½	2.00	$\bar{2}07$	2.00	½	1.99
		802	1.99		
3	1.96	020	1.97	2	1.96
		$\bar{7}14$	1.96		

* Formed from heating emplectite to 385°C.

TABLE 42

WITTICHENITE - $3Cu_2S \cdot Bi_2S_3$

Orthorhombic, D_2^4 - $P2_12_12_1$; a= 7.68, b= 10.33, c= 6.70
Z= 2

PHASE X - $3Cu_2S \cdot 5Bi_2S_3$

Monoclinic, C2/m; a= 13.08, b= 4.00, c= 14.70
$\beta = 99°24\frac{1}{2}'$; Z= 1

b= broad peak
d_c=d(calculated) NS= not scanned
d_m=d(measured) NR= not recorded
d_h=d(emplectite heated to 650°C.

*Taken from Berry and Thompson, 1962.

Taken from Nuffield, 1947.

		wittichenite*				phase X#			
I	d_h	I	d_m	hkl	d_c	I	d_m	hkl	d_c
	NS	1	5.68	011	5.62				
	NR	1	5.22	020	5.16				
2	4.55	4	4.55	111	4.54				
	NR					$\frac{1}{2}$	4.45	202	4.47
2	3.85	3	3.83	200	3.84				
		1	3.62	121	3.61				
6	3.60			210	3.60	4	3.59	203	3.60
9	3.45					10	3.44	$\bar{1}12$	3.45
1	3.34	1	3.34	002	3.35				
				201	3.33				
	NR					1	3.27	$\bar{4}01$	3.26
2	3.17	3	3.19	012	3.19	1	3.16	$\bar{4}02$	3.14
				211	3.17				
				220	3.08				
2	3.08	8	3.08	102	3.07				
				031	3.06				
	NR					$\frac{1}{2}$	3.04	401	3.04
								$\bar{3}11$	2.94
8	2.94	1	2.96	112	2.94	3	2.93	113	2.93
								310	2.93
								$\bar{3}12$	2.83
10	2.82b	10	2.85	131	2.84	8	2.82	205	2.82
$\frac{1}{2}$	↑	$\frac{1}{2}$	2.81	022	2.81			311	2.81

TABLE 42 (cont.)

		wittichenite				phase X			
I	d_h	I	d_m	hkl	d_c	I	d_m	hkl	d_c
2	2.64	4	2.66	122	2.64	½	2.64	$\bar{3}13$	2.64
								$\bar{4}04$	2.63
½	2.56	2	2.58	040	2.58				
				230	2.56				
½	2.49	½	2.49	310	2.48	½	2.49	403	2.50
								205	2.50
½	2.38	3	2.39	032	2.40				
				231	2.39				
				301	2.39	½	2.36	$\bar{1}15$	2.37
NR								$\bar{4}05$	2.36
NR		½	2.34	311	2.33				
				141	2.30				
NR		½	2.28	320	2.29				
				132	2.29				
				222	2.27				
3	2.26					2	2.25	155	2.26
1	2.18	2	2.17	013	2.18	½	2.17	$\bar{6}01$	2.18
				321	2.17			510	2.17
								$\bar{5}11$	2.10
								$\bar{6}03$	2.10
3	2.10	½	2.10	113	2.10	3	2.09	$\bar{1}16$	2.09
								$\bar{5}13$	2.09
								601	2.08
				330	2.05				
	NR	2	2.05	023	2.05				
				042	2.05				
				241	2.04				
				312	2.00				
4	2.00	2	1.99	150	2.00	3	1.99	-	-
				123	1.98				

Formed from heating emplectite to 650°C.

On further heating of the cuprobismutite (originally emplectite, another sharp endothermic peak occurred at 466° C which represented the transformation into wittichenite and a (see Cu-Bi-S section) phase X.

The endothermic peak on the thermogram representing this transition immediately returns to the baseline which indicates at that temperature neither phase has melted. At 506° C a sharp peak occurs which later decreases in height but extends over a long temperature interval and finally returns to the baseline at 610° C. The larger peak starting at 506° C represents the melting of wittichenite and the lower broad portion represents the extended melting of phase X. At 610° C all the substance has melted and only a liquid phase remains. The slope of the curve allows extrapolation to suggest pure phase X could have a transition or melting point near 635° C.

High Temperature Camera

Emplectite from Johanngeorgenstadt, Saxony made a transition at about 390 ± 10° C into cuprobismutite. The diffraction patterns did not show a real sharp change but more of a gradual altering over a temperature range of 10-15° C. Continued heating caused cuprobismutite to transform into wittichenite and phase X at a temperature of 470 ± 5° C. Wittichenite and phase X then form a melt and a Bi-rich phase at 613 ± 7° C. Diffraction patterns of quenched samples using the Nonius camera identified bismuth, wittichenite and phase X. The successively higher temperatures above 613° C the quenched patterns showed the bismuth lines became more and more intense (Fig. 39). No bismuth lines appeared on the high temperature or the Nonius patterns below 613° C and only on the Nonius films quenched

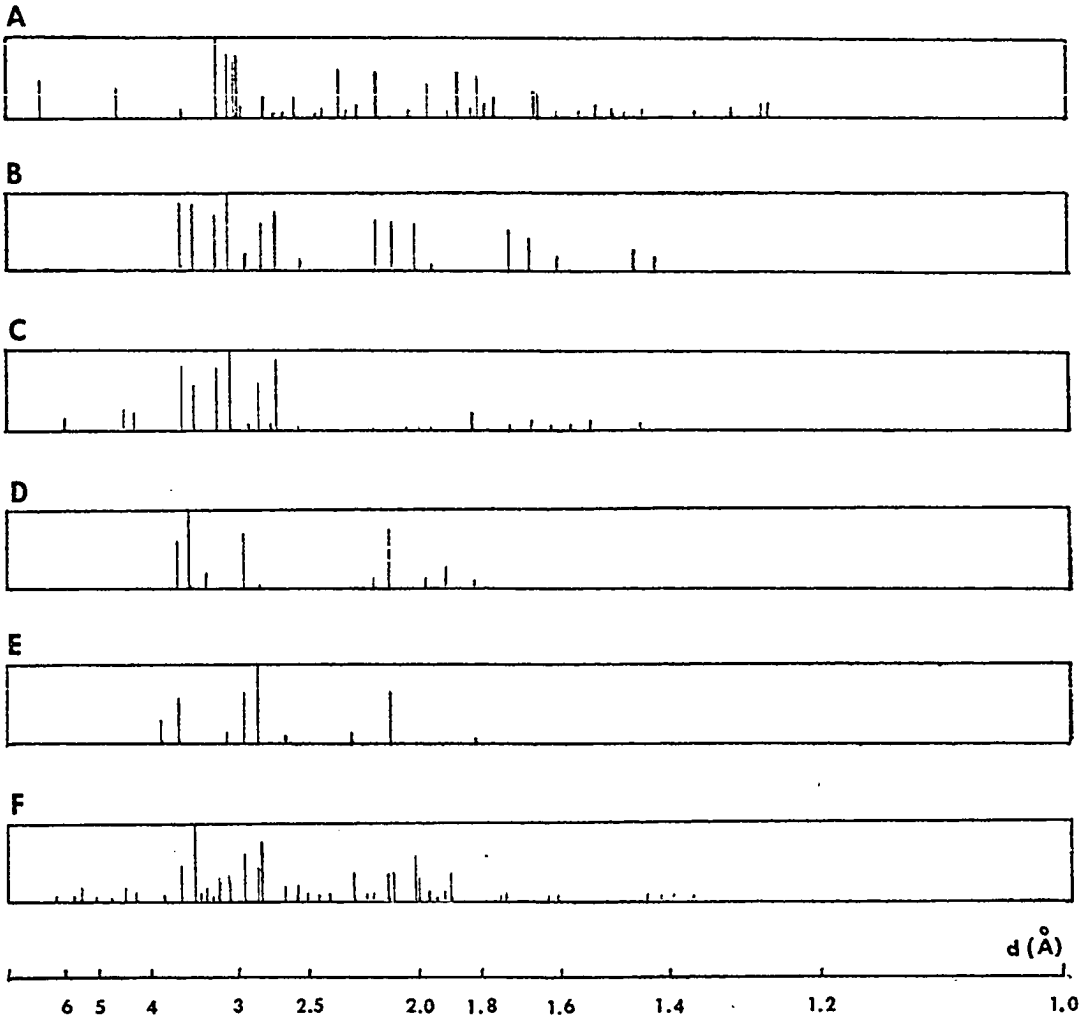

Figure 38 Emplectite A) unheated B) cuprobismutite at 415°C., formed by heating emplectite above 390°C. C) cuprobismutite quenched to room temperature D) phase X and E) wittichenite at 475°C., formed by heating emplectite above 470°C. F) phase X and wittichenite quenched to room temperature.

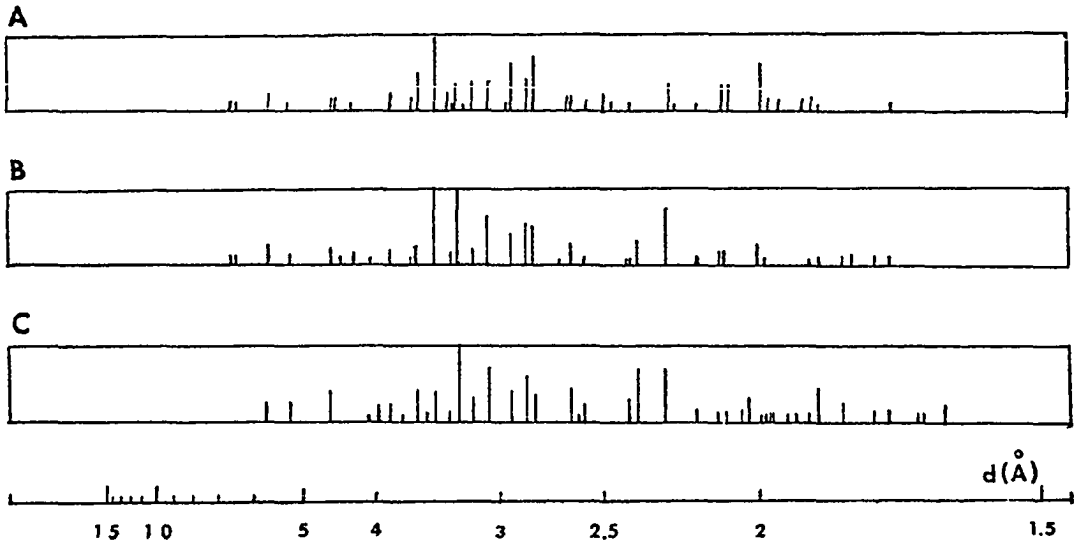

Figure 39 Nonius patterns of emplectite heated to A) 545°C. B) 649°C. C) 675°C. quenched to room temperature and X-rayed. The diffraction lines identify phase X, wittichenite, and bismuth. Refer to table 41 for the measured values of the lines.

TABLE 43

EMPLECTITE HEATED TO A) 545° C, B) 649° C, C) 675° C
[B = bismuth, W = wittichenite, X = phase X]

Only the most intense lines are initialled
Intensities are enclosed in parentheses

A		B		C	
I	d	I	d	I	d
1/2	6.491	1/2	6.549		
1/2	6.348				
1/2	5.619	2	5.613	2	5.613
2	5.565				
1/2	5.197	1	5.208	2	5.202
1	4.525	2	4.541	4	4.533
1	4.463	1/2	4.487		
1/2	4.257	1	4.264		
		1/2	4.050		
				1	3.958 B (1)
2	3.834	1	3.843	1/2	3.837
				1/2	3.737
1	3.641 X (4)	1/2	3.631 X(4)	1/2	3.654 X (4)
4	3.592 X (4)	2	3.602 X (4)	3	3.611 X (4)
				1/2	3.525
10	3.451 X (10)	10	3.456 X (10)	3	3.451 X (10)
1	3.339	1	3.347	1	3.343
2	3.293 B (10)	10	3.279 B (10)	10	3.279 B (10)
1/2	3.243				
3	3.170	2	3.179	3	3.170
3	3.072 W (8)	6	3.077 W (8)	7	3.073 W (8)
			3.063		
1/2	2.950	4	2.944	4	2.940
6	2.932				
4	2.850 W (10)	5	2.858 W (10)	6	2.858 W (10)
8	2.813 X (8)	5	2.815 X (8)	3	2.809 X (8)
		1/2	2.651		
2	2.638	1/2	2.639	4	2.642
				1/2	2.606
1	2.566	1/2	2.576	2	2.571
1	2.500				
1/2	2.469				
1/2	2.436				
1/2	2.399	1/2	2.396	3	2.398
1/2	2.385	1/2	2.382		
		3	2.366 B (7)	7	2.367 B (7)
3	2.261 B (8)	7	2.272 B (8)	7	2.272 B (8)
1/2	2.239				
1/2	2.203				

TABLE 43 - Continued

I	d	I	d	I	d
1/2	2.177	1	2.177	1	2.175
3	2.105	2	2.108	1	2.108
3	2.083	2	2.092	1	2.095
				2	2.051
				3	2.032 B (1)
6	2.002	3	2.007	1	2.007
2	1.993	1	1.995	1	1.995
1	1.976	1/2	1.986	1	1.983
1/2	1.960				
				1	1.938
		1/2	1.922	1	1.924
1	1.907			1	1.895'
3	1.885	2	1.890	1	1.887
1	1.870 B (5)	2	1.867 B (5)	4	1.868 B (5)
1/2	1.840				
1/2	1.820	2	1.821	2	1.822
		1	1.804	1/2	1.808

above 613°. The liquid that formed above the transition temperature of course would not produce a diffraction pattern but could be identified as bismuth from the Nonius films. With higher temperatures more and more liquid formed as indicated by the increased intensities of the bismuth lines from the quenched samples. The bismuth-rich phase could not be identified from the high temperature patterns because only one good line was visible.

Cu-Bi-S SYSTEM

Gaudin and Dicke (1938) experimented with the Cu-Bi-S system and identified the synthetic substances by irridescent filming techniques. Figure 40 shows the sketched diagram for the system in the presence of excess sulfur. They considered phase A the equivalent of cuprobismutite, phase B as klaprothite and phase C as wittichenite. The results obtained in this paper cannot be explained with Gaudin and Dicke's diagram and some doubt exists as to the reliability of their phase identification by irridescent filming.

Nuffield (1947) examined klaprothite from the type localities and found in all cases the specimens were wittichenite; emplectite and wittichenite; or emplectite, wittichenite and native bismuth. From an extensive study, he concluded that klaprothite was not a valid mineral.

In an attempt to synthesize klaprothite ($3Cu_2S \cdot 2Bi_2S_3$) Nuffield found by mixing Cu_2S and Bi_2S_3 in the ratio 3:2 (wt. %) that an intergrowth of phase X with wittichenite resulted. A second mixture with the ratio 1:1 again produced wittichenite but was noticeably richer in phase X. A single crystal of phase X was studied with the Weissenberg camera and gave the following results:

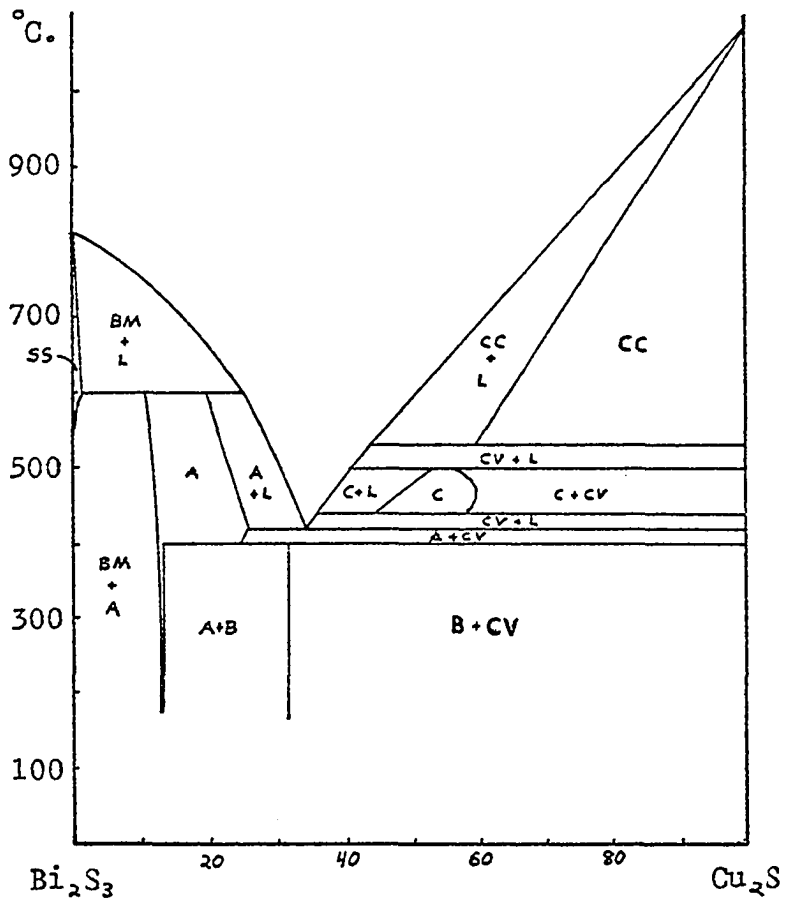

BM= bismuthinite
CC= chalcocite
CV= covellite
L= liquid
A= cuprobismutite
B= klaprothite
C= wittichenite
SS= solid solution

Figure 40 Cu-Bi-S system in the presence of excess sulfur. (Gaudin and Dicke, 1938).

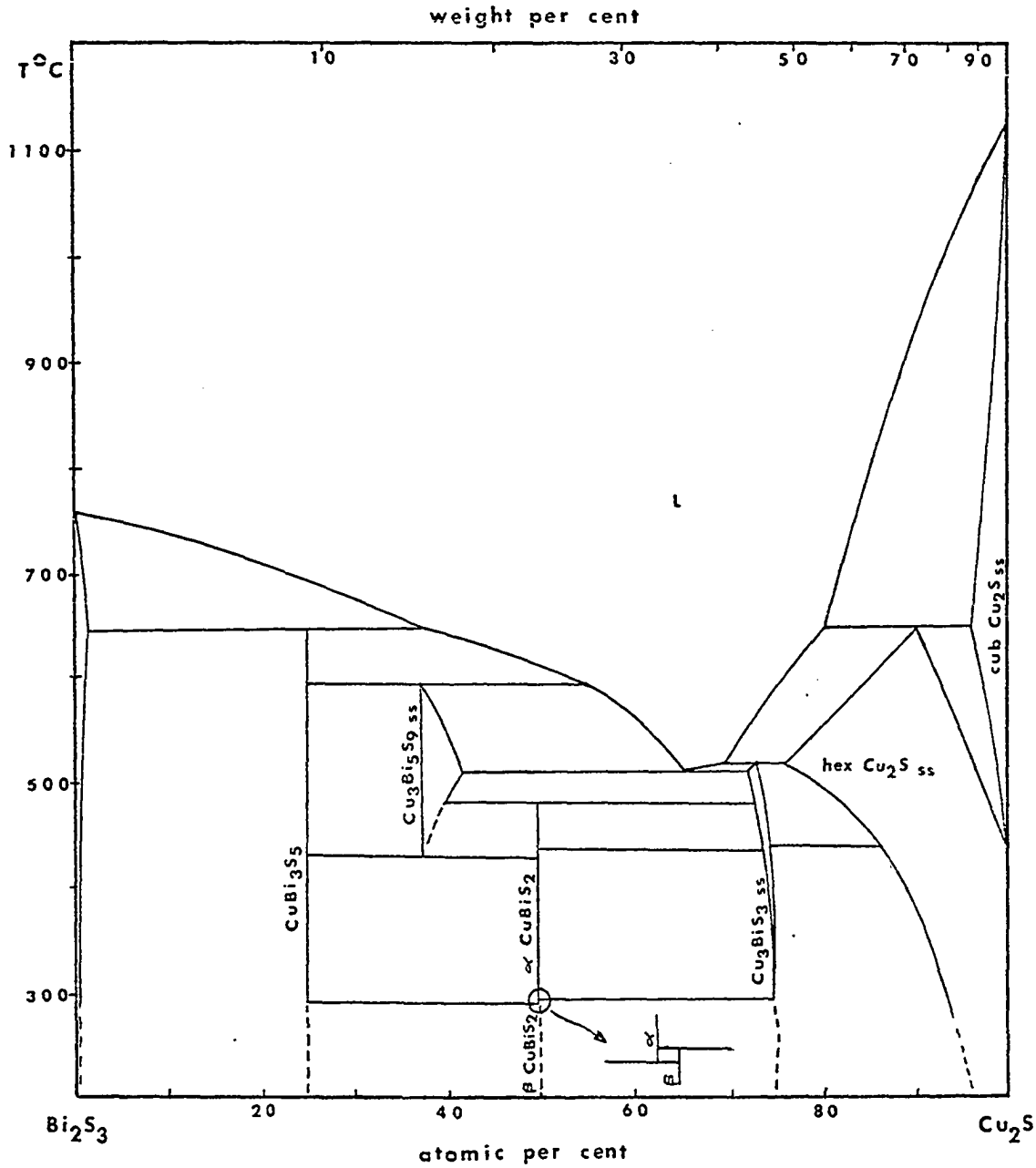

Figure 41 Equilibrium diagram for the Cu-Bi-S System (after Buhlman 1971).

monoclinic lattice with space group C 2/m and dimensions

a = 13.08, b = 4.00, c = 14.70 kX, = 99°24'. The specific gravity of several crystal groups averaged 6.62 and the molecular weight of the cell contents is 3045. Nuffield states that the only simple rational formula which is richer in bismuth than $Cu_2S \cdot Bi_2S_3$ and is at the same time compatible with the known molecular weight is $3Cu_2S \cdot 5Bi_2S_3$, which has a molecular weight of 3049. The composition of phase X is therefore provisionally taken as $3Cu_2S \cdot 5Bi_2S_3$ and may correspond to the mineral dognacskite (Palache, et al., 1944, p. 470), reported to have the composition $Cu_2S \cdot 2Bi_2S_3$ with a specific gravity of 6.79. No specimens of the mineral were available and some doubt exists as to its stability except as a high temperature phase. Table 42 lists the d-values for synthetic phase X which closely corresponds to the d-values of the substance produced by heating emplectite.

Barton and Skinner (1967, p. 271) summarized the work of Vogel (1956) who reported that at 610° C emplectite formed a melt and high digenite. They however did not report any intermediate changes for emplectite as found in this study.

Buhlman (1971) identified a phase with the composition $CuBi_3S_5$. According to his Cu-Bi-S equilibrium diagrams (Fig. 41), phase X melted incongruently at 588 ± 5° C to $CuBi_3S_5$ and a liquid. The diffraction data was not available and could not be compared with the unknown high temperature phase discovered in this study. Buhlman's work with emplectite at lower temperatures produced results similar to the writer's and therefore seems plausible that the unknown high temperature phase found in this study is also similar to his Cu Bi_3S_5 phase and not nearly as copper-rich as high digenite reported by Vogel.

Least Squares Cell Refinement

The unit cell refinement of emplectite gave the following results:

	Schwarzenberg, Saxony (Hofman, 1933)	Johanngeorgenstadt, Saxony
a_o =	6.137	6.149
b_o =	14.541	14.539
c_o =	3.898	3.925

Emplectite transformed into cuprobismutite, which refined as follows:

	(Nuffield, 1952)	Formed from emplectite at 390° C (X-rayed at RT)
a_o =	17.65	17.646
b_o =	3.93	3.935
c_o =	15.24	15.258
β =	100°30'	100°31'

Emplectite has orthorhombic symmetry and changes into cuprobismutite which is monoclinic at room temperature. Such a symmetry change with increase in temperature is not very plausible. At high temperatures the writer believes cuprobismutite is actually orthorhombic. In order to substantiate this, cuprobismutite was refined with an orthorhombic cell and compared with the monoclinic cell. (Refer to least square tables in the appendix.)

The orthorhombic cell used more lines and had a much smaller tolerance than the monoclinic cell. The orthorhombic cell was tried for the room temperature pattern, but the refinement was not very successful and the monoclinic cell gave the best fit.

The next table gives the refinements for wittichenite and phase X at room and high temperatures.

TABLE 44

Wittichenite

Schepbachthal, Baden, Germany (Nuffield, 1947)	Formed from emplectite at 490° C (X-rayed at RT)	High temperature pattern at 480°
a_o = 7.68	7.670	7.723
b_o = 10.33	10.363	10.295
c_o = 6.70	6.692	6.741

Phase X

Synthetic mixture by (Nuffield, 1947)	Formed from emplectite at 490° C (X-rayed at RT)	High temperature pattern at 480°
a_o = 13.08	13.075	13.072
b_o = 4.00	4.006	4.005
c_o = 14.70	14.705	14.687
β = 99°24'	99°20'	99°18'

Structure

Hofman (1933) found that emplectite has a structure like chalcostibite ($CuSbS_2$) where bismuth occupies the same atomic position as antimony. The following table shows the close similarity between the two minerals.

	Composition	System	Space group	a	b	c	Z
Emplectite	$CuBiS_2$	ortho.	D_{2h}^{16}-Pnam	6.137	14.541	3.898	2
Chalcostibite	$CuSbS_2$	ortho.	D_{2h}^{16}-Pnam	6.02	14.49	3.79	2

A structural diagram of chalcostibite, constructed by

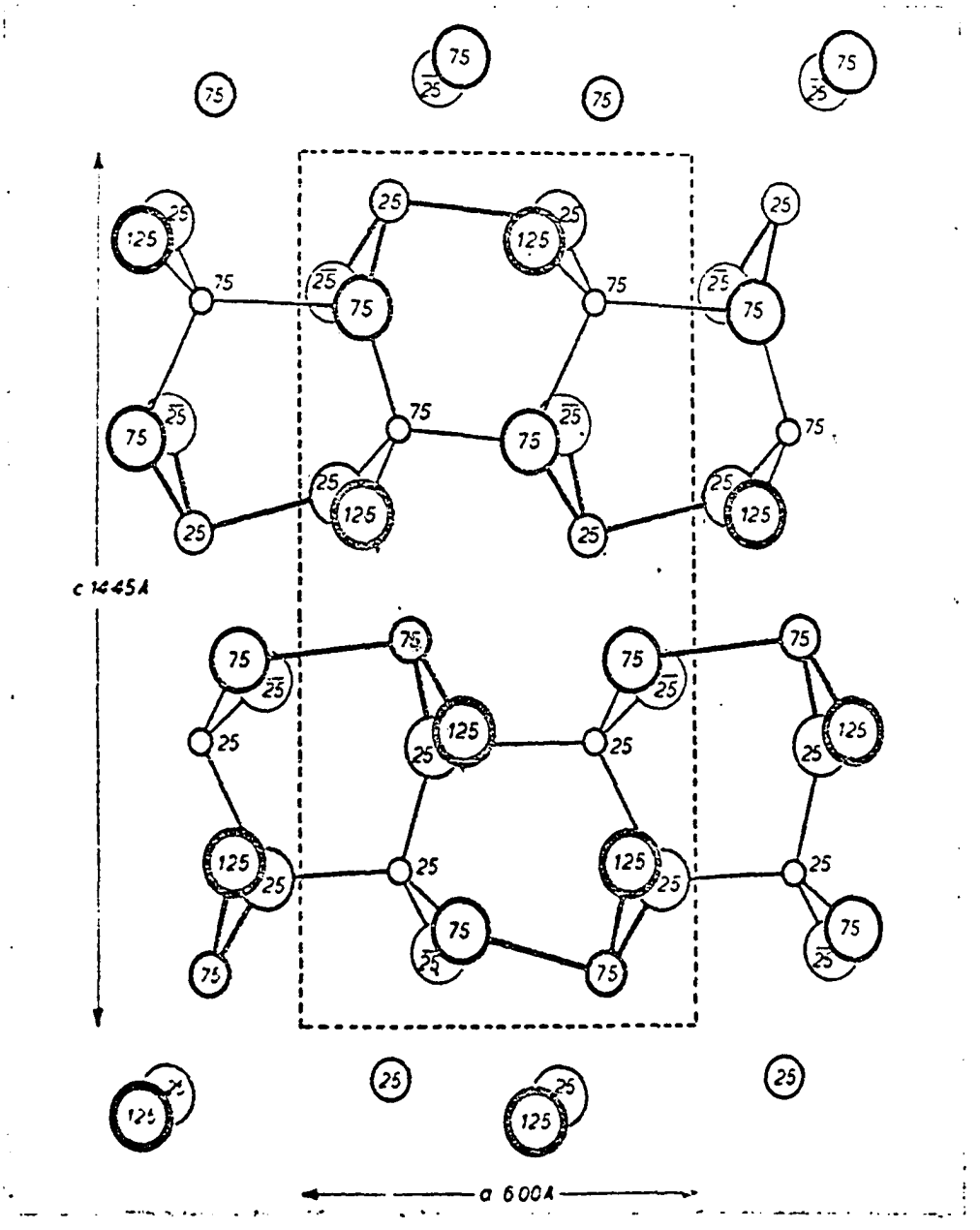

Figure 42 The structure of emplectite, $CuBiS_2$, projected on (010). Largest circles represent sulphur, intermediate circles antimony, and smallest circles copper. (Hofmann, 1933)

Hofman, has the b and c crystallographic axes interchanged with respect to the above lattice parameters. The atoms all lie on mirror planes at heights 1/4 and 3/4. (In the figure some of the sulfur, at a height of 1/4, are slightly offset to better show the structural relationship.) Copper atoms are located between tetrahedral groups of sulfur atoms at an average distance of 2.3 Å. Each antimony atom is bonded to two sulfur atoms at a distance of 2.57 Å and at a distance of 3.44 Å forming a flattened SbS_3 pyramid. The SbS_3 groups are linked by copper atoms in sheets parallel to (001). (Hofman found the structure of emplectite, but did not determine the parameters for the atoms.)

With the heating of emplectite, one would expect higher symmetry to be imparted on the structure and the distorted BiS_3 pyramids should become more regular. Unfortunately the structure of cuprobismutite, phase X, and wittichenite are unknown so that the structural nature of the transitions are indeterminable.

In the case of enargite, the arsenic changes from four coordination (AsS_4) into 3 coordination (AsS_3 in tennantite) on heating. In emplectite however, the bismuth already has a coordination number of 3. The author could not find any Bi-S or Sb-S high temperature polymorphs where the structure has been determined which might suggest the type of coordination of Sb and Bi at elevated temperatures.

Summary

The transition of emplectite into cuprobismutite can be expressed by the following equation:

$$\underset{\text{(emplectite)}}{Cu_2S{\cdot}Bi_2S_3} \xrightarrow{390^\circ} \underset{\text{(cuprobismutite)}}{Cu_2S{\cdot}Bi_2S_3}$$

This transition was not decompositional in nature and cuprobismutite is the high temperature polymorph of emplectite. Muffield (1947) discovered that synthetic mixtures of the appropriate composition always formed cuprobismutite and not emplectite. This would be expected if cuprobismutite was the stable high temperature phase. The writer believes cuprobismutite is orthorhombic above 390° C and "collapses" into monoclinic symmetry on cooling. The following table shows the high degree of similarity between emplectite and cuprobismutite at room temperatures. (Note that the b_o and c_o directions have been interchanged for cuprobismutite for the sake of comparison.)

	a	b	c	β	cell volume	density
emplectite	6.149	14.539	3.925		348.2	6.43 calc.
cuprobismutite	3x5.882	15.258	3.935	100°31'	3x346.5	6.47 meas.

The cell lengths in this transition did not have to undergo much of a change to form cuprobismutite, which indicated the atomic structural arrangement was quite similar.

The following equation represents the transition in the solid state of cuprobismutite into wittichenite and phase X.

$$\underset{\text{(cuprobismutite)}}{6[Cu_2S{\cdot}Bi_2S_3]} \xrightarrow{470°} \underset{\text{(wittichenite)}}{3Cu_2S{\cdot}Bi_2S_3} + \underset{\text{(phase X)}}{3Cu_2S{\cdot}5Bi_2S_3}$$

At approximately 613° C wittichenite and phase X melted to produce a bismuth-rich melt and a phase similar to $CuBi_3S_5$.

CONCLUSIONS

The invariant points of selected sulfosalt minerals were determined in an open system at one atmosphere nitrogen pressure in the DTA apparatus and in a closed system at elevated temperatures in a high temperature powder camera. For DTA, the invariant points were determined in a large closed system where a slight partial pressure due to loss of volatile components would be unnoticed, but the loss prevented reversibility of the system. Many of these points were rechecked in small closed rigid glass tubes where intimate vapor-melt relations could be maintained. Slow cooling determinations were also made to test the reversibility of the phases described. For the high temperature camera, samples were sealed at one atmosphere in .7 mm O.D. quartz capillary tubes where any volatile components were kept in very close contact with the sample.

The following list summarizes the conclusions derived from the results in this study.

(1) The minerals jamesonite and meneghinite made no transitions on heating and after melting, recrystallized as the initial mineral.

(2) Zinckenite melts (540 $\pm$ 5° C) incongruently with the transformation into robinsonite. (Synthetic robinsonite with excess stibnite after cooling, converts back into zinckenite.) Robinsonite as found in nature, probably represents a metastable high temperature mineral unless further work indicates that it can be stabilized by impurity ions.

(3) Synthetic robinsonite melts (575 $\pm$ 5° C) incongruently into a liquid and phase II which Craig (1969) assigned the composition

$5PbS \cdot 3Sb_2S_3$.

(4) Plagionite melts (575 ± 5° C) incongruently into phase II which in turn transforms (595 ± 5° C) into boulangerite and liquid. At 643 ± 5° C boulangerite reacts with the liquid to form another liquid and galena, some of which remains until 60° C.

(5) Semseyite transforms (575 ± 5° C) in the solid state into boulangerite and phase II. At 595 ± 5° C phase II melts and forms a liquid and boulangerite which then melts (547 ± 5° C) incongruently to galena and a liquid.

(6) Boulangerite at high temperatures probably is orthorhombic in symmetry and melts (643 ± 5° C) incongruently into galena and liquid.

(7) Electronmicroprobe studies by Fredrikson (1964) have shown that meneghinite contains tiny particles of galena which exsolved from the meneghinite with cooling and implies that the mineral has an open structure at high temperatures which can accommodate excess PbS. In this study the unheated diffractogram showed the presence of galena and with heating in the open system, Sb_2S_3 was vaporized from the melt resulting in excess PbS as indicated by the intense galena X-ray diffraction peaks.

(8) Stannite (Cu_2FeSnS_4) at room temperature produces an X-ray diffraction pattern distinctly tetragonal in symmetry while zincian stannite [$Cu_2(Zn,Fe)SnS_4$] gives a diffraction pattern much less tetragonal in appearance. Above 360 ± 5° C thermal

expansion of the cell dimensions happens to result in 2 c_o = c_o producing a "cubic" resembling pattern. Single crystal work by Koucky (1959), however identifies the true tetragonal symmetry at elevated temperatures.

Stannite on cooling from a melt in an open system, crystallized into a high temperature disordered Sn-S type structure which on further cooling, reorders into stannite.

(9) Enargite, with the release of sulfur on heating, forms the high temperature mineral tennantite. With slow cooling in a closed system, tennantite resorbs most of the sulfur again to form enargite. Equilibrium of the transition depends on the partial pressure of sulfur. The transformation is not a function of melting, but a solid-solid transition and could occur at low temperatures with high sulfur pressure.

The occurrence of "green enargite", which is a pseudomorph of tennantite after enargite, has been reported in several mineralogy texts. This type of pseudomorphic relationship is to be expected if the sulfur pressure is released at high temperatures during crystallization. Enargite initially crystallized under high sulfur pressures and temperature, however with the release of the pressure, it is no longer stable and transforms into tennantite which is stable under the low sulfur pressure. If the temperature of crystallization of an ore deposit can be determined from other temperature indicators, the enargite-tennantite transition could have a practical application in determining the partial sulfur pressure. First,

though, more experimentation is needed to obtain the slope of the univariant curve for the transition under various temperatures and pressures.

(10) Emplectite transforms (390 ± 10° C) into the high temperature polymorph cuprobismutite which with continued heating (470 ± 5° C) transfers into the solid state to wittichenite and phase X. According to DTA data, wittichenite melts at 506° C while phase X melts over the range 506-610° C. At 613 ± 5° C in the closed system of the high temperature camera a phase formed which most likely has the composition $CuBi_3S_9$ as reported by Buhlman (1971). The reverse transformations of various compositions from the wittichenite-phase X to cuprobismutite and cuprobismutite to emplectite phase fields are probably sluggish since the transformation temperatures are relatively low, 466° C and 380° C respectively. The experiments with emplectite in this study and the work of Nuffield (1947) and Buhlman (1971) with synthetic mixtures, have found phase X, but no natural occurrence of the substance has yet been reported. Most likely though, phase X is mistaken for bismuthinite or some related mineral and with X-ray diffraction techniques employed for identifications, phase X may be expected to be found in ore deposits.

With several of the sulfosalt minerals studied, the high temperature quenched modification had a more complex symmetry and often equal or greater density than the low temperature form. This is not expected if the true symmetry of the high temperature form was preserved, but might

result from the "collapse" of a lower density, more symmetrical high temperature form. High temperature X-ray diffraction of boulangerite, robinsonite, and cuprobismutite suggests that this is indeed the case.

GEOLOGIC APPLICATIONS

Although differential thermal analysis and high temperature X-ray diffraction at low pressures probably does not reflect conditions of formation in many ore deposits, they are useful in outlining phase fields that can later be studied under greater pressure in hydrothermal systems. With increased pressure the transition temperatures will probably vary from the dry conditions, but the phase field boundaries should be approximately the same.

The Pb-Sb-S phase equilibrium diagram (Fig. 24) can be used to predict the relative abundance of minerals in nature. Stibnite and zinckenite is the stable assemblage over a wide range of composition and in nature are very common. The minerals robinsonite, plagionite, and semseyite have very limited stability fields in the diagram and as expected are rather rare in nature. Boulangerite and galena are very common associations in nature as one would predict by the large stability field in the equilibrium diagram.

The occurrence of high temperature polymorphs in ore deposits can be useful in assigning temperature ranges of crystallization. For example the emplectite - cuprobismutite transition occurs at 390° C. If an ore deposit contains only cuprobismutite and no emplectite, the temperature of crystallization must have been above 390° C. If the deposit contains only emplectite, the crystallization temperature was below 390° C unless cuprobismutite reequilibrates at low temperatures into emplectite. Experimental work with cuprobismutite does not indicate any tendency for such an equilibration and appears stable at low temperatures. The polymorphic transition is independent of low pressure in

that the temperature was identical whether heated in the open system of the DTA or a closed system of the high temperature camera. More experimentation must be done however, to determine the effects of high total pressure and high sulfur pressure.

Phase X which also belongs to the Cu-Bi-S system was produced both synthetically (Nuffield, 1947) and from the mineral emplectite by heating above 470° C. No natural occurrence of phase X has yet been reported however the increased use of X-ray diffraction for identification may discover a mineral which previously was misidentified. The equilibrium diagram constructed by Buhlman (1971) (Fig. 41) indicates that at 435° C phase X changes into $CuBi_3S_5$ and cuprobismutite and would not be stable at low temperatures which most likely explains why it has not been found naturally.

If the temperature of crystallization of an ore deposit can be determined from other temperature indicators, the enargite-tennantite transition could have a practical application in determining the partial sulfur pressure. Equilibrium of the transition depends on the partial pressure of sulfur and it is not a function of melting, but a solid-solid transition which could occur at low temperatures with high sulfur pressure.

The occurrence of "green enargite", which is a pseudomorph of tennantite after enargite, could be explained if the sulfur pressure is released at high temperatures during crystallization. Enargite initially crystallized under high sulfur pressure and temperature however with the release of pressure, transforms into tennantite which is stable under low sulfur pressure.

In the Butte, Montana mining district, enargite is found at depth with tennantite near the surface. This type of mineral zoning could be explained as follows. At depth the sulfur pressure is high and enargite is the stable phase while closer to the surface the sulfur pressure would be lower and tennantite would be the stable phase.

Before the enargite-tennantite transition can be used as an indicator of partial sulfur pressure, more experimentation is needed to obtain the slope of the univariant curve for the transition under various temperatures and pressures. Other factors also need to be studied which might effect the transition such as impurities, compositional ranges of the minerals, trace element partitioning and total pressure.

REFERENCES CITED

Barshad, Issac (1952) Temperature and heat of reaction calibration of the differential thermal analysis apparatus. Am. Mineral., vol. 37, pp. 667-694.

Barton, Jr., P. B. and B. J. Skinner (1967) Geochemistry of Hydrothermal Ore Deposits, Chapt. 7 "Mineral Stabilities", Barnes, H. L. ed., Holt, Rinehart, and Winston, New York, 685 p.

Berry, L. G. (1940a) Studies of mineral sulpho-salts, III. Boulangerite and "epiboulangerite", Univ. Toronto Studies, Geol. Ser. 44, pp. 5-19.

_____(1940b) Studies of mineral sulpho-salts, II. Jamesonite from Cornwall and Bolivia. Min. Mag., vol. 26, p. 597.

_____(1941) Studies of mineral sulpho-salts, V. Meneghinite from Ontario and Tuscany, Univ. Toronto Studies, Geol. Ser. 46, pp. 5-17.

_____(1965) Recent advances in sulfide mineralogy. Am. Mineral., vol. 50, pp. 301-313.

Berry, L. G., J. J. Fahey, and E. H. Bailey (1952) Robinsonite, a new lead antimony sulphide. Am. Mineral., vol. 37, pp. 438-446.

Berry, L. G. and D. A. Moddle (1941) Studies of Mineral Sulphosalts: V. Meneghinite from Ontario and Tuscany, Univ. Toronto Studies, Geol. Ser. 44, pp. 5-19.

Berry, L. G. and R. M. Thompson (1962) X-ray powder data for the ore minerals. The Peacock Atlas, Geol. Soc. Am. Mem. 85, 281 p.

Bokii, G. B. and E. M. Romanova (1962) Polyhedra in the Structures of Sulfoarsenides. Soviet Physics - Crystallography, vol. 6, no. 6, May-June, pp. 701-02.

Born, L. and E. Hellner (1960) A structural proposal for boulangerite. Am. Mineral., vol. 45, pp. 1266-1271.

Brockway, L. O. (1934) The crystal structure of stannite, Cu_2FeSnS_4. Zeit. Krist, 89, pp. 434-441.

Buhlman, Eckart (1971) Untersuchurgen im System Bi_2S_3- Cu_2S und geologische Schluß folgerungen. Neues Jahrb. Min., Mh., pp. 137-141.

Cho, Seung-Am and B. J. Wuensch (1970) Crystal Chemistry of the Plagionite Group. Nature, vol. 225, January 31, pp. 444-445.

Craig, James (1969) Personal Communication, Texas Tech University.

Euler, R. and E. Hellner (1960) Uber komplex zusammengesetzte sulfidische Erze. VI. Zur kristallstrukture des menighinits, $CuPb_{13}Sb_7S_{24}$. Zeit. Krist. 113, pp. 345-372.

Fredrikson, K. and C. A. Anderson (1964) Electron probe analysis of copper in meneghinite. Am. Mineral., vol. 49, pp. 1467-1468.

Frueh, Jr., Alfred J. (1949) A study of disorder in minerals, Ph.D. Thesis, Massachusetts Institute of Tech.

Gaudin, A. M. and G. Dicke (1938) The pyrosynthesis, microscope study and irridescent filming of sulfide compounds of copper with arsenic, antimony, and bismuth, Part II: Copper-Bismuth-Sulfide System. Ec. Geol., vol. 34, pp. 214-232.

Hellner, E. (1958) Crystal structure classification. Jour. of Geol., vol. 66, no. 5, pp. 503-525.

Hofman, W. (1933) Strukturelle und morphologische zusammenhange bei erzen vom formeltyp ABC_2. I. Die struktur von wolfsbergite, $CuSbS_2$ and emplektit, $CuBiS_2$ and deren beziehungen zu der struktur von antimonit Sb_2S_3. Zeit. Krist. 84, pp. 177-203.

Iitsuka, D. (1919) Metallographic enquiry into the antimony sulphide lead sulphide system (trans.). Kyoto Imp. Univ., Coll. Sci., Men., vol. 4, no. 2, p. 61.

Jaeger, F. M. and H. S. Van Klooster (1912) Studien uber naturliche und kunstliche Sulfantimonite und Sulfarsenite. Zeitschr. Anorg. Chemie, vol. 78, pp. 245-269.

Jambor, J. L. (1969a) Dadsonite (Minerals Q and QM) a new lead sulphantimonide. Min. Mag., vol. 37, pp. 437-441.

_____(1969b) Sulphosalts of the Plagionite Group. Min. Mag., vol. 37, pp. 442-446.

Kitakawa, A. (1968) Unpublished Masters Thesis, Yamagachi University, Japan.

Koucky, F. L. (1959) Stannite Series. Geol. Soc. Am. (abs.), vol. 70, p. 1632.

Nuffield, E. W. (1945) Studies of mineral sulpho-salts. XII. Fülöppite and zinckenite. Univ. Toronto Studies, Geol. Ser. 50, pp. 49-62.

_____(1947) Studies of mineral sulpho-salts. XI. Wittichenite (klaprothite). Ec. Geol., vol. 42, pp. 147-160.

Nuffield, E. W. (1952) Studies of mineral sulpho-salts. XVI. Cupro-bismutite. Am. Mineral., vol. 37, pp. 447-452.

Nuffield, E. W. and M. A. Peacock (1944) Studies of mineral sulpho-salts. VIII. Plagionite and semseyite. Univ. Toronto Studies, Geol. Ser. 49, pp. 17-39.

Nuzeki, N. (1957) The crystal structure of jamesonite, $FePb_4Sb_6S_{14}$. Zeit. Krist. 109, pp. 161-183.

Palache, C., H. Berman and C. Frondel (1944) Dana's System of Mineralogy. Vol. I. 7th ed., John Wiley and Sons, Inc., New York.

Pauling, L. and E. W. Neuman (1934) The crystal structure of binnite $(Cu,Fe)_{12}As_4S_{13}$ and the chemical composition and structure of minerals of the tetrahedrite group. Zeit. Krist. 88, pp. 54-62.

Pauling, L. and S. Weinbaum (1934) The crystal structure of enargite, Cu_3AsS_4. Zeit. Krist. 88, pp. 48-53.

Robinson, S. C. (1948) Studies of mineral sulpho-salts. XI. Artificial sulphantimonites of lead. Univ. Toronto Studies, Geol. Ser. 52, pp. 54-69.

Ross, V. F. (1957) Geochemistry, crystal structure and mineralogy of the sulfides. Ec. Geol., vol. 52, pp. 755-774.

Schaber, G. G. (1965) Mineralogy and crystal chemistry of the sulfosalt minerals: bournonite, seligmannite, aikinite, diaphorite and freieslebenite. Unpublished Ph.D. Dissertation, Univ. of Cincinnati, Cincinnati, Ohio.

Schenk, R., I. Hoffman, W. Knepper, and H. Vogler (1939) Gleichgewigh studien über erzbildende sulphide. I. S. Anorg. Allg. Chemie, vol. 240, pp. 173-197.

Skinner, B. J. (1960) Assemblage enargite-famatinite, a possible geologic thermometer (abs.). Bull. Geol. Soc. Am., 71, p. 1975.

Smith, G. F. H. (1919) Semseyite from Dumfriesshire. With a chemical analysis by G. T. Prior, Min. Mag., vol. 18, pp. 354-359.

Sommerlad, H. (1898) Experiments on the preparation of sulphantimonites and sulpharsenites of silver, copper and lead by dry methods (trans.). Zeitschr. Anorg. Chemie, vol. 18, p. 420.

Springer, G. (1968) Electronprobe analyses of stannite. Min. Mag., vol. 36, p. 1045.

Strock, L. W. (1936) A classification of the crystal structures with defect lattices. Zeit. Krist. 93, pp. 285-311.

Traill, R. J. (1970) A Catalogue of Canadian Minerals, Geol. Surv. of Canada, Dept. of Energy, Mines and Resources, Paper 69-45, pp. 97-101.

Vaux, G. and F. A. Bannister (1938) The identity of zinckenite and keeleyite. Min. Mag., vol. 25, pp. 221-227.

Vogel, R. (1956) The system bismuth sulfide-copper sulfide and the ternary system Bi-Bi_2S_3-Cu_2S-Cu. Zeits. für Metallkunde 47, pp. 694-699.

Weast, G. editor, (1965-1966) Handbook of Chemistry and Physics, 46th ed., The Chemical Rubber Co.

Wernick, J. H. and K. E. Benson (1957) New semiconducting ternary compounds. J. Phys. Chem. Solids, 3, pp. 157-159.

APPENDIX

The following section contains the tables for the least square cell refinements.

The 'theta measured' value is listed opposite the 'theta calculated' value which gives the closest fit for that reflection. Brackets indicate that more than one hkl can be assigned for that particular measured diffraction line. The letter R in the last column indicates the 'theta difference' value is larger than the theta tolerance and is therefore rejected in the least squares refinement. Lines which do not have a 'theta difference' value were not used in the refinement.

TABLE 45

Zinckenite $PbS \cdot Sb_2S_3$ (Pribram, Bohemia)

Hexagonal: $P6_3$ $\lambda = Co_{k\alpha} = 1.7902$

Refined parameters (Å): a = 44.116 ± .008, c = 8.622 ± .002
Conditions for non-extinction: none
Theta tolerance = .021
Unheated sample from the Nonius camera

I	d (meas.)	hkil	d (calc.)	theta (calc.)	theta (meas.)	theta diff.	
1	11.137	$22\bar{4}0$	11.029	4.655	4.610	.045	R
1	5.510	$44\bar{8}0$	5.514	9.341	9.350	-.009	
1/2	5.291	$62\bar{8}0$	5.298	9.727	9.740	-.013	
1	4.385	$64\cdot\bar{10}\cdot0$	4.382	11.785	11.780	.005	
1/2	4.016	$22\bar{4}2$	4.015	12.881	12.870		
4	3.926	$40\bar{4}2$	3.929	13.167			
		$55\cdot\bar{10}\cdot1$	3.927	13.174	13.180	-.006	
2	3.697	$42\bar{6}2$	3.702	13.994	14.010	-.016	
2	3.570	$60\bar{6}2$	3.570	14.521	14.520	.001	
10	3.432	$10\cdot2\cdot\bar{12}\cdot0$	3.431	15.123	15.120	.003	
5	3.345	$62\bar{8}2$	3.344	15.526	15.520	.006	
		$10\cdot1\cdot\bar{11}\cdot1$	3.343	15.532			
1/2	3.203	$80\bar{8}2$	3.200	16.243	16.230	.013	
1	3.141	$86\cdot\bar{14}\cdot0$	3.140	16.560	16.560	.000	
		$85\cdot\bar{13}\cdot1$	3.134	16.597			
3	3.070	$64\cdot\bar{10}\cdot2$	3.073	16.932	16.950	-.018	
6	3.000	$82\cdot\bar{10}\cdot2$	2.997	17.379	17.360	.019	
1/2	2.917	$74\cdot\bar{11}\cdot2$	2.917	17.869	17,870	-.001	
		$12\cdot2\cdot\bar{14}\cdot0$	2.913	17.894			
6	2.798	$66\cdot\bar{12}\cdot2$	2.798	18.662	18.660	.002	
6	2.769	$84\cdot\bar{12}\cdot2$	2.768	18.868	18.860	.008	
		$96\cdot\bar{15}\cdot1$	2.767	18.873			
1/2	2.688	$50\bar{5}3$	2.690	19.435	19.450	-.015	
		$10\cdot2\cdot\bar{12}\cdot2$	2.685	19.477			
		$13\cdot1\cdot\bar{14}\cdot1$	2.684	19.482			
1/2	2.535	$86\cdot\bar{14}\cdot2$	2.538	20.648	20.660		
1/2	2.409	$55\cdot\bar{10}\cdot3$	2.408	21.820	21.810	.010	
		$12\cdot6\cdot\bar{18}\cdot0$	2.407	21.834			
1/2	2.322	$88\cdot\bar{16}\cdot2$	2.323	22.665	22.66		
		$10\cdot9\cdot\bar{19}\cdot0$	2.321	22.686			
1/2	2.307	$8\cdot3\cdot\bar{11}\cdot3$	2.309	22.805			
		$10\cdot6\cdot\bar{16}\cdot2$	2.306	22.842	22.830	.012	
2	2.258	$12\cdot4\cdot\bar{16}\cdot2$	2.257	23.365	23.350	.015	
1/2	2.234	$16\cdot2\cdot\bar{18}\cdot0$	2.236	23.600	23.60		
		$11\cdot8\cdot\bar{19}\cdot1$	2.233	23.627			
1	2.183	$14\cdot2\cdot\bar{16}\cdot2$	2.182	24.217	24.210	.007	
		$17\cdot1\cdot\bar{18}\cdot0$	2.180	24.236			

I	d (meas.)	$\bar{h}kil$	d (calc.)	theta (calc.)	theta (meas.)	theta diff.
3	2.159	16·3·19·0	2.159	24.487	24.490	-.003
3	2.129	99·18·2	2.131	24.841	24.860	-0.19
		10·8·18·2	2.127	24.882		
1/2	2.084				25.440	
2	2.054				25.830	
3	1.983				26.840	
1	1.878				28.470	
4	1.826				29.360	

TABLE 46

Zinckenite $PbS \cdot Sb_2S_3$

$\lambda = Cu_{k\alpha} = 1.5405$

Hexagonal: $P6_3$

Refined parameters (Å): a = 44.337 ± .007, c = 8.626 ± .004

Conditons for non-extinction: none

Theta tolerance = .022

Temperature: 527° C

I	d (meas.)	hhil	d (calc.)	theta (calc.)	theta (meas.)	theta diff.	
1	3.818	$90\bar{9}1$	3.824	11.620	11.640	-.020	
10	3.450	$10\cdot2\cdot\bar{12}\cdot0$	3.448	12.908	12.900	.008	
1	3.346	$62\bar{8}2$	3.352	13.286			
		$84\cdot\bar{12}\cdot1$	3.344	13.315	13.310	.005	
2	3.095	$55\cdot\bar{10}\cdot2$	3.092	14.427	14.410	.017	
4	2.803	$66\cdot\bar{12}\cdot2$	2.806	15.932	15.950	-.018	
		$75\cdot\bar{12}\cdot2$	2.799	15.976			
1	2.275	$66\cdot\bar{12}\cdot3$	2.269	19.842	19.790	.052	R
2	2.213	$11\cdot9\cdot\bar{20}\cdot0$	2.213	20.367	20.370	-.003	
3	2.157	$13\cdot4\cdot\bar{17}\cdot2$	2.159	20.900			
		0004	2.157	20.926	20.920	.006	
1	2.072	$14\cdot7\cdot\bar{21}\cdot0$	2.073	21.809			
		$18\cdot0\cdot\bar{18}\cdot1$	2.071	21.836	21.820	.016	
5	2.004	$13\cdot9\cdot\bar{22}\cdot0$	2.004	22.600	22.600	.000	
1	1.895	$11\cdot10\cdot\bar{21}\cdot2$	1.896	23.973	23.980	-.007	
5	1.839	$14\cdot10\cdot\bar{24}\cdot0$	1.839	24.763	24.760	.003	
		$16\cdot7\cdot\bar{23}\cdot1$	1.837	24.788			
1/2	1.794	$15\cdot7\cdot\bar{22}\cdot2$	1.794	25.431	25.430	.001	
2	1.736	$13\cdot12\cdot\bar{25}\cdot1$	1.737	26.328			
		$17\cdot8\cdot\bar{25}\cdot0$	1.736	26.333	26.340	-.007	
2	1.682	$14\cdot7\cdot\bar{21}\cdot3$	1.682	27.259	27.250	.009	
1/2	1.629	$20\cdot6\cdot\bar{26}\cdot0$	1.628	28.230	28.220	.010	
1/2	1.475				31.480		
1/2	1.415				32.980		

TABLE 47

Zinckenite $PbS \cdot Sb_2S_3$ (Julcani, Peru)

$\lambda = Co_{k\alpha} = 1.7902$

Hexagonal: $P6_3$

Refined parameters (Å): a = 44.221 ± .009, c = 8.624 ± .003

Conditions for non-extinction: none

Theta tolerance = .029

Unheated sample from the Nonius camera

I	d (meas.)	hkil	d (calc.)	theta (calc)	theta (meas.)	theta diff.	
1/2	11.137	$22\bar{4}0$	11.055	4.664	4.610	.034	
1/2	5.513	$44\bar{8}0$	5.528	9.319	9.340	-.021	
1/2	5.302	$62\bar{8}0$	5.311	9.703	9.720	-.017	
1/2	4.399	$64\cdot\bar{1}0\cdot0$	4.393	11.757	11.740	.017	
1/2	4.017	$22\bar{4}2$	4.017	12.875	12.870		
		$65\cdot\bar{1}1\cdot0$	4.015	12.883			
4	3.935	$55\cdot\bar{1}0\cdot1$		13.148	13.150	-.002	
		$40\bar{4}2$		13.160			
1	3.705	$42\bar{6}2$	3.704	13.983	1.3980	.003	
3	3.577	$60\bar{6}2$	3.573	14.508	14.490	.018	
10	3.438	$10\cdot2\cdot\bar{1}2\cdot0$	3.439	15.086	15.090	-.004	
4	3.341	$84\cdot\bar{1}2\cdot1$	3.337	15.560	15.540	.020	
1/2	3.201	$80\bar{8}2$	3.204	16.224	16.240	-.016	
2	3.141	$85\cdot\bar{1}3\cdot1$	3.140	16.561	16.560	.001	
5	3.074	$64\cdot\bar{1}0\cdot2$	3.077	16.911	16.930	-.019	
6	3.002	$82\cdot\bar{1}0\cdot2$	3.001	17.355	17.350	.005	
		$11\cdot3\cdot\bar{1}4\cdot0$	3.000	17.362			
1/2	2.912	$12\cdot2\cdot\bar{1}4\cdot0$	2.920	17.850	17.900	-.050	R
7	2.801	$6\cdot6\cdot\bar{1}2\cdot2$	2.801	18.634	18.640	-.006	
		$7\cdot5\cdot\bar{1}2\cdot2$	2.794	18.686			
5	2.769	$84\cdot\bar{1}2\cdot2$	2.772	18.839	18.860	-.020	
		$12\cdot2\cdot\bar{1}4\cdot1$	2.766	18.882			
1	2.695	$50\bar{5}3$	2.691	19.426	19.400	.026	
1	2.544	$53\bar{8}3$	2.545	20.595	20.600	-.005	
		$86\cdot\bar{1}4\cdot2$	2.542	20.613			
1	2.408	$55\cdot\bar{1}0\cdot3$	2.410	21.802	21.820	=.018	
		$64\cdot\bar{1}0\cdot3$	2.405	21.847			
1	2.311	$83\cdot\bar{1}1\cdot3$	2.312	22.783	22.790	-.007	
		$10\cdot6\cdot\bar{1}6\cdot2$	2.310	22.800			
1	2.264	$75\cdot\bar{1}2\cdot3$	2.263	23.304	23.290	.014	
1/2	2.234	$93\cdot\bar{1}2\cdot3$	2.232	23.647	23.620	.027	
1/2	2.194	$76\cdot\bar{1}3\cdot3$	2.195	24.070	24.080	-.010	
4	2.154	$13\cdot4\cdot\bar{1}7\cdot2$	2.155	24.545			
		$14\cdot6\cdot\bar{2}0\cdot0$	2.154	24.550	24.560	-.010	
		$10\cdot3\cdot\bar{1}3\cdot3$	2.153	24.570			
		$10\bar{1}4$	2.152	24.572			
4	2.132	$21\bar{3}4$	2.132	24.820			
		$10\cdot7\cdot\bar{1}8\cdot2$	2.131	24.834	24.830	.004	

I	d (meas.)	hhīl	d (calc.)	theta (calc.)	theta (meas.)	theta diff.
1/2	2.091				25.350	
1/2	20.55				25.830	
3	1.987				26.780	
1/2	1.878				28.470	
4	1.826				29.350	

TABLE 48

Robinsonite $7PbS \cdot 6Sb_2S_3$

Triclinic: $P\bar{1}$ $\lambda = Co_{k\alpha} = 1.7902$

Refined parameters (Å): a = 16.473 ± .003, b = 17.637 ± .004,
c = 3.970 ± .0008, α = 96°11' ± 1.4',
β = 96°16' ± 1.2', γ = 91°8' ± 1.2'

Conditions for non-extinction: none

Theta tolerance = .020

Formed from heating zinckenite to 562° C and X-rayed at room temperature on the Nonius camera

I	d (meas.)	hkl	d (calc.)	theta (calc.)	theta (meas.)	theta diff.	
1/2	4.388	040	4.381	11.789	11.770	.019	
1	4.053	-330	4.052	12.762	12.760	.002	
5	3.955	410	3.957	13.075	13.080	-.005	
5	3.917	-240	3.915	13.217	13.210	.007	
		-101	3.915	13.218			
5	3.809	240	3.812	13.580	13.590	-.010	
8	3.705	-201	3.702	13.992	13.980	.012	
1/2	3.662	420	3.663	14.145	14.150	-.005	
5	3.575	1-21	3.572	14.512	14.500	.012	
1/2	3.504	050	3.505	14.796	14.800	-.004	
10	3.438	021	3.441	15.079	15.090	-.011	
		0-31	3.437	15.095			
1/2	3.418	-1-31	3.419	15.178	15.180	-.002	
1/2	3.354	-3-11	3.355	15.474	15.480	.006	
1/2	3.243	-510	3.236	16.056	16.020	.036	R
1	3.199	510	3.199	16.247	16.250	-.003	
1/2	3.081	2-31	3.083	16.879			
		-1-41	3.081	16.890	16.890	.000	
7	3.037	-440	3.039	17.129			
		3-11	3.037	17.143	17.140	.003	
		520	3.035	17.155			
6	3.007	1-41	3.008	17.314	17.320	.006	
		-231	3.007	17.318			
		-401	3.004	17.333			
1	2.901	-4-21	2.897	17.997	17.970	.027	R
3	2.836	2-41	2.836	18.400	18.400	.000	
1	2.803	231	2.804	18.618	18.620	.002	
9	2.770	041	2.774	18.830	18.850	.020	
		-3-41	2.773	18.851			
3	2.684	401	2.685	19.472	19.480	.008	
		610	2.682	19.494			
1/2	2.585	-5-21	2.585	20.263	20.260	.003	
		540	2.583	20.275			
1/2	2.543	360	2.541	20.622	20.610	.012	
1/2	2.430	-550	2.431	21.602	21.610	.008	

I	d (meas.)	hkl	d (calc.)	theta (calc.)	theta (meas.)	theta diff.
1/2	2.345	2-61	2.343	22.458	22.440	.018
		460	2.342	22.468		
		-6-21	2.308	22.819		
1	2.309	710	2.308	22.821	22.810	.011
1	2.276	-720	2.277	23.146	23.160	.014
1/2	2.239	4-51	2.239	23.568	23.560	.008
1	2.136	6-11	2.137	24.767	24.770	-.003
1	2.109				25.120	
1	2.060				25.750	
7	1.987				26.770	
1/2	1.887				28.310	
1/2	1.871				28.590	
1/2	1.832				29.250	
1/2	1.798				29.850	

TABLE 49

Plagionite $5PbS \cdot 4Sb_2S_3$ (Wolfsberg, Harz, Germany)

Monoclinic: C2/c $\lambda = Co_{K\alpha} = 1.7902$

Refined parameters (Å): a = 13.472 ± .005, b = 11.832 ± .005,
c = 20.009 ± .007, β = 107°10' ± 1.7'

Conditions for non-extinction: hkl h+k = 2 n
hol l = 2 n
oko k = 2 n

Theta tolerance = .023

Unheated sample from the Nonius camera

I	d (meas.)	hkl	d (calc.)	theta (calc.)	theta (meas.)	theta diff.	
1/2	9.505	002	9.559	5.373	5.400		
1/2	7.360	111	7.389	6.958	6.980		
1/2	6.276	-202	6.263	8.216	8.200		
1/2	5.871	112	5.880	8.756	8.770		
1/2	5.666	021	5.652	9.113	9.090		
1/2	4.536	-204	4.530	11.396	11.380	.016	
1/2	4.330	023	4.336	11.914	11.930		
5	3.874	114	3.876	13.351	13.360	-.009	
1	3.771	130	3.771	13.731	13.730	.001	
1	3.718	024	3.718	13.931	13.930	.001	
1/2	3.639	131	3.640	14.234	14.240		
2	3.580	-224	3597	14.410	14.480	.070	R
1	3.407	132	3.409	15.224	15.230	-.006	
2	3.369	-402	3.365	15.428	15.410	.018	
2	3.304	223	3.302	15.730	15.720		
10	3.263	-206	3.264	15.915			
		-315	3.264	15.918	15.920	-.002	
1/2	3.206	-225	3.209	16.198			
		-116	3.206	16.211	16.210	.001	
3	2.960	-331	2.960	17.603	17.600	.003	
		040	2.958	17.614			
2	2.941	224	2.940	17.725	17.720	.005	
1	2.901	330	2.904	17.955	17.970	-.015	
4	2.874	-423	2.875	18.140	18.150	-.010	
5	2.857	-226	2.858	18.251	18.260	-.009	
2	2.762	-424	2.768	18.869	18.910	-.041	R
1	2.714	-241	2.708	19.302	19.260	.042	R
1	2.696	-406	2.697	19.384	19.390	-.006	
1/2	2.635	332	2.636	19.853	19.860		
1/2	2.489	-208	2.493	21.039	21.080		
1	2.453	-426	2.454	21.393	21.400	-.007	
		-515	2.451	21.420			
1/2	2.365	404	2.365	22.237			
		-318	2.364	22.253	22.240		

I	d (meas.)	hkl	d (calc.)	theta (calc.)	theta (meas.)	theta diff.
1/2	2.340	045	2.340	22.494	22.490	
		-245	2.339	22.503		
2	2.225	153	2.2225	23.724	23.720	.004
		532	2.224	23.731		
4	2.152	-444	2.150	24.598	24.58	.018
		153	2.150	24.609		
1/2	2.143	600	2.145	24.661	24.690	
		-319	2.140	24.722		
1/2	2.081				25.480	
1	2.000				26.600	
1/2	1.948				27.350	
1/2	1.893				28.220	
1/]	1.856				28.830	

TABLE 50

Semseyite $9PbS \cdot 4Sb_2S_3$ (Kisbarya, Hungary)
Monoclinic: C2/c $\lambda = Co_{k\alpha} = 1.7902$
Refined parameters (Å): a = 13.644 ± .002, b = 12.004 ± .002,
c = 24.560 ± .005, β = 105° 49' ± 1.0'
Conditions for non-extinction: hkl h+k = 2 n
hol l = 2 n
oko k = 2 n
Theta tolerance = .020
Unheated sample from the Nonius camera

I	d (meas.)	khl	d (calc.)	theta (calc.)	theta (meas.)	theta diff.	
1/2	6.529	200	6.564	7.838			
		-202	6.545	7.860			
		112	6.534	7.874	7.880	-.006	
		-113	6.511	7.902			
1/2	5.390	113	5.413	9.519			
		-114	5.394	9.552	9.560		
1/2	5.155	202	5.171	9.969			
		-204	5.143	10.023	10.000		
1/2	4.533	114	4.544	11.360			
		-115	4.530	11.396	11.390	.006	
1/2	4.418	-222	4.424	11.674	11.690	-.016	
1	4.222	-312	4.234	12.205			
		221	4.215	12.260	12.240	.020	
2	3.882	311	3.886	13.318			
		115	3.884	13.326	13.330	-.004	
		-206	3.875	13.355			
4	3.826	130	3.827	13.525			
		-131	3.826	13.528	13.530	-.002	
2	3.731	131	3.732	13.879	13.880	-.001	
		-132	3.729	13.889			
1	3.580	223	3.589	14.442			
		-225	3.577	14.493	14.480	.013	
1	3.556	132	3.560	14.566			
		-133	3.555	14.582	14.580	.002	
2	3.414	-402	3.411	15.213	15.200	.013	
2	3.364	-117	3.367	15.416	15.430	-.014	
2	3.306	313	3.313	15.674	15.710	-.036	R
10	3.271	-404	3.273	15.874	15.88	-.006	
		224	3.267	15.901			
		-226	3.256	15.959	15.950		
2	3.027	314	3.030	17.181	17.200	-.019	
1	2.995	-332	2.997	17.375	17.390		
6	2.960	402	2.961	17.596	17.600	-.004	
		-227	2.960	17.601			
6	2.954	008	2.954	17.640	17.640	.006	
		330	2.953	17.646			
1	2.875	-424	2.873	18.152	18.140	.012	

I	d (meas.)	hkl	d (calc.)	theta (calc.)	theta (meas.)	theta diff.	
		-136	2.861	18.233			
6	2.858	-334	2.860	18.238	18.250	-.012	
1/2	2.785	421	2.780	18.785	18.750		
		-425	2.771	18.845	18.830	.015	
3	2.773	315	2.770	18.851			
		332	2.748	19.008	10.010		
1/2	2.748	-241	2.747	19.018			
		240	2.729	19.146	19.140	.006	
3	2.730	-242	2.728	19.156			
3	2.697	-228	2.697	19.383	19.380	.003	
1	2.650	028	2.650	19.740	19.740	.000	
1	2.451	208	2.455	21.385	21.420	.035	R
1/2	2.368	-517	2.369	22.204	22.210		
		-532	2.252	23.416	23.420	-.004	
		-533	2.251	23.427			
3	2.252	-247	2.251	23.434			
		-139	2.250	23.441			
1	2.227	-40·10	2.227	23.669	23.700	-.001	
		-155	2.155	24.540	24.550	-.010	
4	2.154	514	2.153	24.571			
1/2	2.100				25.230		
1/2	2.075				25.560		
1	2.055				25.820		
1/2	2.025				26.230		
1/2	2.004				26.530		
1/2	1.971				27.010		
1	1.919				27.810		
1/2	1.891				28.260		
1/2	1.857				28.810		
1/2	1.853				28.890		
1/2	1.811				29.630		
1/2	1.789				30.020		
1	1.769				30.390		

TABLE 51

Galena PbS
Cubic: Fm3m $\lambda = Cu_{k\alpha} = 1.5405$
Refined parameters (Å): a = 6.010 ± .001
Conditions for non-extinction: hkl h+k = 2n
hkl h+l = 2n
hkl k+l = 2n
hhl h+l = 2n
0kl k = 2n
0kl l = 2n
h0l h = 2n
h0l l = 2n
hk0 h = 2n
hk0 k = 2n
hll h+l = 2n
Temperature: 657° C. Formed from heating semseyite

I	d (meas.)	hkl	d (calc.)	theta (calc.)	theta (meas.)	theta diff.
9	3.469	111	3.470	12.826	12.830	-.004
10	3.021	200	3.005	14.853	14.770	.083
3	2.132	220	2.125	21.255	21.180	.075
8	1.811	311	1.812	25.156	25.170	-.014
5	1.735	222	1.735	26.359	26.360	-.001
4	1.379	331	1.379	33.965	33.960	.005
6	1.346	420	1.344	34.973	34.910	.063
4	1.229	422	1.227	38.896	38.810	.086

TABLE 52

Boulangerite $5PbS \cdot 2Sb_2S_3$ (St. Antonia, California)

Monoclinic: $P2_1/a$

Refined parameters (Å): $a = 21.558 \pm .006$, $b = 23.490 \pm .006$,
$c = 8.074 \pm .004$, $\beta = 100°40' \pm 2'$

Conditions for non-extinction: h0l h = 2n
0k0 k = 2n

Theta tolerance = .025

Unheated sample from the Nonius camera

I	d (meas.)	hkl	d (calc.)	theta (calc.)	theta (meas.)	theta diff.
1/2	6.063	320	6.052	8.505	8.490	.015
1/2	4.585	150	4.587	11.254	11.250	.004
1/2	4.392	430	4.387	11.773	11.750	
1/2	3.941	440	3.933	13.155	13.120	
4	3.908	350	3.911	13.229	13.240	-.011
		-212	3.909	13.238		
1	3.851	160	3.850	13.445	13.440	.005
		421	3.846	13.457		
10	3.721	112	3.727	13.896		
		530	3.726	13.898	13.720	-.022
		-312	3.722	13.916		
2	3.670	260	3.672	14.108	14.120	-.012
		251	3.663	14.142		
1/2	3.585	-322	3.589	14.441	14.460	
2	3.465	212	3.470	14.951		
		-412	3.463	14.979	14.970	.009
2	3.443	511	3.442	15.073	15.070	.003
2	3.354	222	3.361	15.444		
		441	3.346	15.472	15.480	
2	3.316	170	3.314	15.668	15.660	.008
2	3.222	630	3.319	16.146	16.130	.016
2	3.195	-432	3.196	16.262	16.270	.008
1/2	3.086	071	3.091	16.835		
		-171	3.093	16.837	16.860	-.023
3	3.024	640	3.026	17.205	17.220	-.015
		601	3.025	17.214		
5	3.007	-442	3.007	17.315	17.320	-.005
2	2.970	332	2.973	17.520		
		-532	2.968	17.553	17.540	.013
1/2	2.941	152	2.943	17.709		
		-352	2.940	17.725	17.720	.005
9	2.814	-542	2.815	18.542		
		252	2.811	18.569		
		-162	2.810	18.572	18.550	.022
7	2.783	-262	2.785	18.744	18.760	-.016

I	d (meas.)	hkl	d (calc.)	theta (calc.)	theta (meas.)	theta diff.
1	2.708	181	2.709	19.297	19.300	-.003
		-281	2.708	19.303		
1	2.688	740	2.690	19.434	19.450	
1/2	2.649	-552	2.649	19.750	19.750	.000
1/2	2.582	820	2.583	20.273	20.280	.007
1/2	2.509	-481	2.510	20.891	20.900	
		123	2.507	20.914		
1	2.421	-472	2.423	21.682		
		-742	2.419	21.716	21.700	.016
2	2.368	-822	2.369	22.197	22.210	-.013
1	2.341	910	2.342	22.468		
		490	2.341	22.478	22.480	
		-662	2.340	22.485		
1	2.318	182	2.318	22.718	22.720	.002
		632	2.316	22.739		
1	2.254	153	2.252	23.415	23.400	
1/2	2.176	722	2.178	24.265		
		-553	2.177	24.274	24.290	-.016
		-922	2.174	24.316		
1	2.148	-10·01	2.148	24.623		
		4·10·0	2.147	24.636	24.630	
1/2	2.055				25.820	
1/2	2.038				26.060	
5	2.018				26.330	
1	1.921				27.770	
4	1.863				28.710	

TABLE 53

Boulangerite $5\ PbS \cdot 2Sb_2S_3$ (St. Antonio, California)

Monoclinic: $P2_1/a$

Refined parameters (Å): $a = 21.512 \pm .016$, $b = 23.707 \pm .029$
$c = 8.103 \pm .018$, $\beta = 99°45' \pm 6'$

Conditions for non-extinction: hOl h = 2n
0k0 k = 2n

Theta tolerance = .049

Temperature: 593° C. Compare this refinement with Tables 54 and 55

I	d (meas.)	hkl	d (calc.)	theta (calc.)	theta (meas.)	theta diff.	
2	41.22	401	4.107	10.808	10.770	.038	
		-431	4.107	10.810			
10	3.732	530	3.736	11.897	11.910	-.013	
		-441	3.733	11.906			
1/2	3.445	540	3.449	12.906	12.920	-.014	
		-261	3.437	12.949			
3	3.234	232	3.234	13.780			
		630	3.226	13.815	13.780	.035	
5	3.033	640	3.035	14.701	14.710	-.009	
8	2.831	650	2.833	15.775			
		-162	2.828	15.803	15.790	.013	
5	2.710	380	2.733	16.370	16.510	-.140	R
		641	2.709	16.517			
1/2	2.385	811	2.385	18.844	18.840	.004	
1/2	2.335	490	2.359	19.058	19.260	-.202	R
		751	2.337	19.248			
1/2	2.256	-482	2.258	19.948			
		930	2.258	19.949	19.960	-.011	
2	2.161	-922	2.161	20.877	20.880	-.003	
2	2.071	-682	2.073	21.811			
		5·10·0	2.069	21.853	21.830	.023	
2	2.024	2·11·1	2.025	22.357			
		752	2.024	22.373			
		960	2.023	22.375	22.370	.005	
1	1.976	0·12·0	1.976	22.947	22.940	.007	
2	1.942	2·12·0	1.942	23.365			
		842	1.941	23.386	23.370	.016	
2	1.879	592	1.882	24.165	24.200	-.035	
		791	1.880	24.181			
1	1.840	932	1.841	24.727			
		6·11·0	1.840	24.747	24.750	.003	
1	1.785	11·50	1.786	25.556			
		-12·11	1.785	25.562	25.560	.002	

TABLE 54

Boulangerite $5PbS \cdot 2Sb_2S_3$ (St. Antonia, California)

Orthorhombic: $Bb2_1m$ $\lambda = Cu_{k\alpha} = 1.5405$

Refined parameters (Å): a = 42.713 ± .025, b = 23.545 ± .012, c = 8.021 ± .004

Conditions for non-extinction:

hkl	k+l = 2n
0kl	k+l = 2n
h0l	l = 2n
hk0	h = 2n
h00	h = 2n

Theta tolerance = .034

Temperature 593° C. Compare this refinement with Tables 53 and 55

I	d (meas.)	hkl	d (calc.)	theta (calc.)	theta (meas.)	theta diff.
2	4.122	731	4.130	10.750	10.770	-.020
10	3.738	222	3.732	11.893	11.910	-.017
1/2	3.445	10·40	3.457	12.874		
		660	3.437	12.952	12.920	.032
3	3.234	851	3.232	13.787		
		342	3.228	13.805	13.780	.025
5	3.033	371	3.033	14.723	14.710	.013
8	2.821	14·11	2.831	15.788		
		842	2.816	15.875	15.790	.095
5	2.710	11·22	2.714	16.484	16.510	-.036
		462	2.713	16.495		
		14·40	2.709	16.521		
1/2	2.385	17·11	2.385	18.839		
		633	2.385	18.845	18.840	.005
1/2	2.335	13·42	2.333	19.275	19.260	.015
1/2	2.256	10·13	2.256	19.965	19.960	.005
		13·71	2.256	19.968		
2	2.161	15·42	2.160	20.893	20.880	.013
2	2.071	373	2.071	21.837	21.830	.007
		0·11·1	2.068	21.867		
2	2.024	11·82	2.025	22.360	22.370	-.010
		16·71	2.023	22.375		
1	1.976	5·10·2	1.975	22.949	22.940	
		124	1.975	22.959		
2	1.942	15·13	1.942	23.361	23.370	-.009
		22.00	1.941	23.374		
2	1.879	10·73	1.879	24.194	24.200	-.006
		804	1.877	24.225		
1	1.840	8·12·0	1.842	24.723	24.750	
1	1.785	064	1.786	25.554		
		164	1.784	25.578	25.560	.018
1	1.752	22·51	1.752	26.087	26.080	

TABLE 55

Boulangerite $5PbS \cdot 2Sb_2S_3$ (St. Antonio, California)

Orthorhombic: $Bb2_1m$ $\lambda = Cu_{K\alpha} = 1.5405$

Refined parameters (Å): a = 21.160 ± .027, b = 23.472 ± .031, c = 8.065 ± .006

Conditions for non-extinction:

hkl	k+l = 2n
0kl	k+l = 2n
h0l	l = 2n
0k0	k = 2n
00l	l = 2n

Theta tolerance = .076

Temperature: 593° C. Compare this refinement with Tables 53 and 54 a_o dimension is divided by two.

I	d (meas.)	hkl	d (calc.)	theta (cal.)	theta (meas.)	theta diff.	
2	4.122	051	4.057	10.944	10.770	.174	R
10	3.732	122	3.753	11.842	11.910	-.072	
1/2	3.445	540	3.433	12.968	12.920	.048	
3	3.234	451	3.219	13.842	13.780	.062	
5	3.033	700	3.023	14.762			
		640	3.023	14.763	14.710	.053	
8	2.831	371	2.835	15.764	15.790	-.026	
		522	2.833	15.776			
		280	2.827	15.809			
5	2.710	262	2.714	16.488	16.510	-.022	
		380	2.709	16.519			
1/2	2.385	413	2.385	18.847	18.840	.007	
1/2	2.335	053	2.333	19.278	19.261	.017	
		1·10·0	2.333	19.279			
1/2	2.256	513	2.259	19.938	19.960	-.022	
		680	2.256	19.968			
2	2.161	771	2.163	20.861	20.880	-.019	
2	2.071	842	2.070	21.850			
		582	2.070	21.851	21.830	.021	
2	2.024	2·11·1	2.025	22.360	22.370	-.010	
1	1.976	10·31	1.980	22.892	22.942	-.050	
		124	1.979	22.911			
2	1.942	304	1.939	23.410	23.370	.040	
2	1.879	813	1.879	24.194	24.200	-.006	
		573	1.879	24.195			
1	1.840	344	1.841	24.735	24.750	-.015	
1	1.785	164	1.786	25.550	25.560	-.010	
		10·42	1.785	25.564			
1	1.752	604	1.750	26.106	26.080	.026	

TABLE 56

Galena PbS
Cubic: Fm3m $\lambda = Cu_{k\alpha} = 1.5405$
Refined parameters (Å): a = 6.014 ± .0007
Conditions for non-extinction: see table
Theta tolerance = .036
Temperature: 646°C. Formed from heating boulangerite

I	d (meas.)	hkl	d (calc.)	theta (calc.)	theta (meas.)	theta diff.
9	3.474	111	3.472	12.818	12.810	.008
10	3.005	200	3.007	14.843	14.850	-.007
8	2.127	220	2.126	21.240	21.230	.009
8	1.812	311	1.813	25.139	25.160	-.021
5	1.737	222	1.736	26.340	26.320	.020
1/2	1.500	400	1.503	30.820	30.900	-.080
4	1.380	331	1.380	33.939	33.930	.009
6	1.345	420	1.345	34.947	34.940	.007
4	1.228	422	1.228	38.865	38.850	.015
3	1.158	511	1.157	41.725	41.690	.035
1/2	1.063	440	1.063	46.433	46.440	.007
1	1.016	531	1.016	49.268	49.300	-.032
1	1.002	442	1.002	50.221	50.240	-.019

TABLE 57

Meneghinite $Cu_2S \cdot 26PbS \cdot 7Sb_2S_3$ (Bottino, Tuscany, Italy)
Orthorbombic: Pbnm $\lambda = Co_{K\alpha} = 1.7902$
Refined parameters (Å): a = 11.379 ± .005, b = 24.097 ± .011,
c = 4.144 ± .002
Conditions for non-extinction: hol l = 2n
hoo h = 2n
hko h+k = 2 n
ool l = 2n
Unheated sample from the Nonius camera

I	d (meas.)	hkl	d (calc.)	theta (calc.)	theta (meas.)	theta diff.	
1/2	4.452	150	4.438	11.637	11.600	.037	
2	4.142	240	4.136	12.498	12.480	.018	
1	3.897	021	3.919	13.203	13.280	-.077	R
9	3.747	310	3.747	13.821	13.820	.001	
4	3.690	031	3.683	14.066	14.040	.026	
9	3.497	131	3.504	14.800	14.830	-.030	
1/2	3.430	330	3.430	15.128	15.130	-.002	
10	3.292	170	3.295	15.763	15.780	-.017	
	3.269	141	3.270	15.885	15.890	-.005	
5	3.086	231	3.092	16.829	16.860	-.031	
9	2.923	241	2.928	17.803	17.830	-.027	
1/2	2.790	161	2.796	18.673	18.710	-.037	
5	2.773	420	2.769	18.862	18.830	.032	
5	2.751	251	2.751	18.991	18.990	.001	
1/2	2.730	321	2.726	19.173	19.140	.033	
4	2.666	280	2.662	19.648	19.620	.028	
1	2.300	421	2.302	22.880	22.900	-.020	
4	2.250	431	2.251	23.427	23.440	-.013	
		091	2.249	23.454			
1	2.187	390	2.187	24.156	24.160	-.004	
		441	2.186	24.176			
5	2.083	0·10·1	2.083	25.448	25.450	-.002	
5	2.057				25.800		
1/2	2.025				26.240		
3	1.978				26.240		
3	1.978				26.900		
1	1.931				27.610		
1/2	1.904				28.040		
3	1.894				28.210		
2	1.852				28.900		
3	1.809				29.650		

TABLE 58

Jamesonite $4PbS \cdot FeS \cdot 3Sb_2S_3$ (Huanuni, Bolivia)

Monoclinic: $P2_1/a$ $\lambda = Co_{k\alpha} = 1.7902$

Refined parameters (Å): a = 15.716 ± .003, b = 19.177 ± .003,
c = 4.037 ± .0006, β = 91°45' ± 1.0'

Conditons for non-extinction: hol h = 2n
oko k = 2n

Theta tolerance = .020

Unheated sample from the Nonius camera

I	d (meas.)	hkl	d (calc.)	theta (calc.)	theta (meas.)	theta diff.	
1	8.170	120	8.184	6.279	6.290	-.011	
1/2	6.084	220	6.076	8.472	8.460	.012	
1/2	5.924	130	5.921	8.695	8.690	.005	
1/2	5.060	310	5.051	10.207	10.190	.017	
4	4.091	240	4.092	12.635	12.640	-.005	
1	4.031	001	4.035	12.817	12.830	-.013	
1	3.926	400	3.927	13.175	13.180	-.005	
5	3.854	-111	3.857	13.420	13.430	-.010	
		410	3.847	13.454			
1	3.807	111	3.803	13.614	13.600	.014	
5	3.718	021	3.719	13.927	13.930	-.004	
5	3.594	121	3.597	14.411	14.420	-.009	
1	3.539	340	3.536	14.664	14.650	.014	
10	3.443	250	3.446	15.053	15.070	-.017	
2	3.352	-131	3.352	15.486	15.490	-.004	
		430	3.346	15.516			
1/2	3.326	221	3.325	15.615	15.610	.005	
6	3.159	-231	3.159	16.458	16.460	-.002	
7	3.097	510	3.100	16.781	16.800	-.019	
		350	3.094	16.815			
1/2	3.049	-141	3.043	17.109	17.070	.039	R
2	2.992	321	2.993	17.403	17.410	-.007	
1	2.959	260	2.960	17.600	17.610	-.011	
2	2.894	-331	2.893	18.023	18.020	.003	
9	2.827	-411	2.827	18.460	18.460	-.000	
		331	2.826	18.468			
4	2.742	411	2.744	19.039	19.050	-.011	
		450	2.744	19.039			
		-421	2.739	19.075			
2	2.726	360	2.728	19.154			
		151	2.728	19.157	19.170	-.013	
1/2	2.689	-341	2.687	19.459	19.450	.009	
1	2.370	180	2.370	22.193	22.190	.003	
		521	2.367	22.215			
2	2.298	640	2.298	22.927	22.920	.007	
1/2	2.287	-451	2.292	22.990	23.040	.050	R

I	d (meas.)	hkl	d (calc.)	theta (calc.)	theta (meas.)	theta diff.	
		4.51	2.247	23.456			
3	2.248	470	2.247	23.477	23.470	.007	
		361	2.244	23.477			
1/2	2.192	-271	2.188	24.152	24.100	.052	R
1	2.130	-461	2.130	24.843	24.850	-.007	
1/2	2.116				24.020		
1/2	2.095				25.300		
3	2.057				25.800		
1	2.033				26.120		
2	2.020				26.300		
1	2.010				26.450		
1	1.969				27.040		
1	1.949				27.340		
1	1.928				27.670		
1	1.917				27.840		
1	1.902				28.080		
1	1.889				28.290		
1	1.871				28.580		
2	1.838				29.140		
2	1.824				29.390		
1	1.798				29.850		

TABLE 59

Stannite Cu_2FeSnS_4 (Mine LaFab., Bolivia)

Tetragonal: I $\bar{4}2$ m $\lambda = Co_{k\alpha} = 1.7902$

Refined parameters (Å): a = 5.457 ± .002, c = 10.794 ± .005

Conditions for non-extinction: hkl h+k+l = 2 n
hhl l = 2 n
okl k+l = 2 n
hoo h = 2 n

Unheated sample from the Nonius camera

I	d (meas.)	hkl	d (calc.)	theta (calc.)	theta (meas.)	theta diff.
1/2	5.401	002	5.397	9.547	9.540	.007
1/2	3.851	110	3.859	13.414	13.440	-.026
10	3.141	112	3.139	16.569	16.560	.009
3	2.731	200	2.728	19.152	19.130	.022
2	2.699	004	2.698	19.372	19.370	.002
5	1.928	220	1.929	27.643	27.660	-.017
6	1.917	204	1.919	27.810	27.840	-.030
6	1.645	312	1.644	32.997	32.970	.027
3	1.631	116	1.630	33.297	33.290	.007
2	1.570	224	1.569	34.774	34.760	.014
1	1.453	314	1.454	38.004	38.020	-.016

TABLE 60

Stannite Cu_2FeSnS_4

Tetragonal: I $\bar{4}2m$ $\lambda = Cu_{k\alpha} = 1.5405$

Refined parameters (Å): a = 5.466 ± .002, c = 10.841 ± .003

Conditions for non-extinction: none

Theta tolerance = .067

Temperature: 490° C

I	d (meas.)	hkl	d (calc.)	theta (calc.)	theta (meas.)	theta diff.	
2	5.427	002	5.420	8.169	8.160	.009	
10	3.142	112	3.147	14.167	14.190	-.023	
2	2.722	200	2.733	16.369	16.440	-.071	R
1/2	2.231	212	2.228	20.221	20.200	.021	
9	1.929	220	1.933	23.428	23.530	-.042	
		204	1.924	23.593			
9	1.647	312	1.647	27.885	27.880	.005	
1/2	1.572	224	1.574	29.308	29.340	.032	
4	1.365	400	1.367	34.308	34.350	-.042	
6	1.254	332	1.253	37.914	37.900	.014	
7	1.115	424	1.114	43.732	43.690	.042	
5	1.051	512	1.052	47.089	47.130	-.041	
4	.924	532	.924	56.494	56.470	.024	
3	.864	620	.864	63.023	63.060	-.037	

TABLE 61

Zincian Stannite $Cu_2(Zn,Fe)SnS_4$ (Snowflake mine, B.C.)

$\lambda = Co_{K\alpha} = 1.7902$

Tetragonal: $I\bar{4}2m$

Refined parameters (Å): $a = 5.424 \pm .004$, $c = 10.89 \pm .012$

Conditions for non-extinction: hkl $h+k+l = 2n$
hhl $l = 2n$
okl $k+l = 2n$
hoo $h = 2n$

Unheated sample from the Nonius camera

I	d (meas.)	hkl	d (calc.)	theta (calc.)	theta (meas.)	theta diff.
1/2	5.481	002	5.447	9.458	9.400	.058
1	4.871	101	4.855	10.624	10.590	.034
1/2	3.843	110	3.835	13.497	13.470	.027
10	3.135	112	3.136	16.585	16.590	-.005
1/2	3.025	103	3.017	17.256	17.210	.046
4	2.715	200	2.712	19.273	19.250	.023
1/2	2.374	211	2.368	22.214	22.150	.064
5	1.922	204	1.922	27.761	27.750	.011
5	1.917	220	1.918	27.826	27.840	-.014
4	1.640	116	1.641	33.055	33.080	-.025
4	1.634	312	1.636	33.172	33.210	-.038
1	1.566	224	1.568	34.812	34.850	-.038

TABLE 62

Zincian Stannite $Cu_2(Zn,Fe)SnS_4$

Tetragonal: I $\bar{4}2m$ $\lambda = Cu_{k\alpha} = 1.5405$

Refined parameters (Å): $a = 5.447 \pm .003$, $c = 10.913 \pm .002$

Conditions for non-extinction: hhl h+k+l = 2n
hhl l = 2n
0kl k+l = 2n
h00 h = 2n

Theta tolerance = .024

Temperature: 607° C

I	d (meas.)	hkl	d (calc.)	theta (calc.)	theta (meas.)	theta diff.	
2	4.870	101	4.874	9.093	9.100	-.007	
10	3.146	112	3.147	14.169	14.170	-.001	
2	3.029	103	3.025	14.751	14.730	.021	
4	2.730	004	2.728	16.399	16.390	.009	
1	2.384	211	2.377	18.904	18.850	.054	R
9	1.929	204	1.927	23.554	23.530	.024	
9	1.645	116	1.645	27.925	27.920	.005	
1/2	1.577	224	1.573	29.312	29.240	.072	R
1/2	1.512	206	1.513	30.613	30.630	-.017	
3	1.364	008	1.364	34.377	34.380	-.003	
6	1.252	316	1.251	38.015	37.970	.045	R
6	1.113	228	1.113	43.784	43.790	-.006	
4	1.050	11.10	1.050	47.187	47.190	-.003	

TABLE 63

Enargite $3Cu_2S \cdot (As,Sb)_2S_5$ (Ouray Co., Colorado)

$\lambda = Co_{k\alpha} = 1.7902$

Orthorhombic: Pnm 2

Refined parameters (Å): a = 6.409 ± .002, b = 7.436 ± .006, c = 6.141 ± .002

Conditions for non-extinction: okl k+l = 2 n
oko k = 2 n
ool l = 2 n

Theta tolerance = .034

Unheated sample from Nonius camera

I	d (meas.)	hkl	d (calc.)	theta (calc.)	theta (meas.)	theta diff.
9	3.203	200	3.204	16.221	16.230	-.009
9	3.067	002	3.070	16.950	16.960	-.010
10	2.842	201	2.841	18.366	18.360	.006
6	2.217	202	2.217	23.813	23.810	.003
5	1.852	320	1.852	28.897	28.900	-.003
2	1.847	132	1.847	28.990	28.980	.010
8	1.724	203	1.725	31.259	31.280	-.021
1	1.602	400	1.602	33.964	33.970	-.006
6	1.585	322	1.586	34.358	34.380	-.022
3	1.551	401	1.550	35.266	35.240	.026
1	1.536	004	1.535	35.667	35.650	.017

TABLE 64

Tennantite $(Cu,Zn,Fe)_{12}As_4S_{13}$
Cubic: $I\bar{4}3\ m$ $\lambda = Cu_{k\alpha} = 1.5405$
Refined parameters (Å): a = 10.281 ± .006
Conditions for non-extinction: hkl h+k+l = 2n
hhl l = 2n
Theta tolerance = .052
Temperature: 590° C. Formed from heatin enargite in an open system

I	d (meas.)	hkl	d (calc.)	theta (calc.)	theta (meas.)	theta diff.	
1/2	3.622	220	3.635	12.234	12.280	-.046	
10	2.966	222	2.968	15.043	15.050	-.007	
3	2.570	400	2.570	17.439	17.440	.001	
2	2.426	330	2.423	18.534	18.510	.024	
1	2.101	422	2.099	21.533	21.510	.023	
5	2.015	510	2.016	22.460	22.470	-.010	
3	1.881	521	1.877	24.228	24.170	.058	R
9	1.821	440	1.817	25.076	25.020	.056	R
6	1.554				29.710		
1/2	1.288				36.730		

TABLE 65

Cubic phase of unknown composition formed from heating enargite in an open system.

Refined parameters (Å): 5.711 ± .002 $\lambda = Cu_{k\alpha} = 1.5405$
Theta tolerance = .029
Conditions for non-extinction: none
Temperature: 610° C

I	d (meas.)	hkl	d (calc.)	theta (calc.)	theta (meas.)	theta diff.	
3	3.295	111	3.297	13.510	13,520	-.010	
3	2.854	002	2.855	15.650	15.660	-.010	
10	2.018	022	2.019	22.426	22.440	-.014	
5	1.723	113	1.722	26.573	26.550	.023	
1/2	1.433	004	1.428	32.650	32.510	.140	R

TABLE 66

Emplectite $Cu_2S \cdot Bi_2S_3$ (Johanngeorgenstadt, Saxony)
Orthorhombic: P nam $\lambda = Co_{k\alpha} = 1.7902$
Refined parameters (Å): a = 6.149 ± .0009, b = 14.539 ± .003,
c = 3.925 ± .0008
Conditions for non-extinction: okl k+l = 2n
hoo h = 2n
oko k = 2n
ool l = 2n
Unheated sample from the Nonius camera

I	d (meas.)	hkl	d (calc.)	theta (calc.)	theta (meas.)	theta diff.	
5	7.273	020	7.270	7.073	7.070	.003	
4	4.695	120	4.695	10.991	10.990	.001	
1	3.631	040	3.635	14.256	14.270	-.014	
10	3.224	111	3.226	16.110	16.120	-.010	
8	3.128	140	3.129	16.222	16.630	-.008	
7	3.072	200	3.075	16.925	16.940	-.015	
8	3.048	031	3.050	17.067	17.080	-.013	
2	3.003	210	3.008	17.311	17.340	-.029	R
3	2.833	220	2.832	18.426	18.420	.006	
1	2.734	131	2.732	19.123	19.110	.013	
2	2.597	230	2.596	20.167	20.160	.007	
1/2	2.444	141	2.447	21.460	21.480	-.020	
1	2.421	201	2.420	21.705	21.700	.005	
6	2.336	051	2.336	22.527	22.530	-.003	
1	2.293	221	2.296	22.941	22.980	-.039	R
2	2.254	160	2.254	23.393	23.400	-.007	
6	2.165	231	2.165	24.417	24.420	-.003	
1/2	1.973	320	1.973	26.982	26.980	.002	
4	1.962	002	1.962	27.140	27.150	-.010	
1/2	1.900	260	1.903	28.055	28.120	-.065	R
6	1.861	251	1.860	28.762	28.750	.012	
2	1.818	080	1.817	29.506	29.500	.006	
5	1.803	311	1.802	29.768	29.780	-.012	
3	1.785	340	1.785	30.088	30.100	-.012	
2	1.759	171	1.759	30.587	30.580	.007	
1	1.713	261	1.712	31.514	31.500	.014	
3	;/663	142	1.662	32.577	32.570	.007	
3	1.655	202	1.655	32.761	32.750	.011	
2	1.565	360	1.565	34.887	34.890	-.003	
1	1.538	400	1.537	35.608	35.600	.008	

TABLE 67

Cuprobismutite $Cu_2S \cdot Bi_2S_3$

Monoclinic: C2/m $\lambda = Cu_{k\alpha} = 1.5405$

Refined parameters (Å): a = 17.660 ± .025, b = 3.928 ± .005,
c = 15.198 ± .030, β = 100°6' ± 6'

Conditions for non-extinction: hkl h+k = 2n
h0l h = 2n
0k0 k = 2n

Theta tolerance = .061

Temperature: 410° C. Formed from heating emplectite above 390° C.
Compare this refinement with Table 68

I	d (meas.)	hkl	d (calc.)	theta (calc.)	theta (meas.)	theta diff.	
9	3.607	-403	3.605	12.337	12.330	.007	
9	3.458	-112	3.465	12.844	12.870	-.036	
7	3.231	204	3.236	13.770	13.790	-.020	
10	3.101	-113	3.097	14.403	14.380	.023	
2	2.945	-601	2.943	15.173	15.160	.013	
6	2.845	-313	2.855	15.650	15.710	-.060	
7	2.733	-114	2.730	16.390	16.370	.020	
1	2.553	602	2.555	17.544	17.560	-.016	
6	2.176	-207	2.166	20.835	20.730	.105	R
6	2.107	-515	2.106	21.453	21.440	.013	
6	2.018	514	2.016	22.459	22.440	.019	
		406	2.016	22.466			
2	1.828	023	1.827	24.930	24.920	.010	

TABLE 68

Cuprobismutite $Cu_2S \cdot Bi_2S_3$

Orthorhombic $\lambda = Cu_{k\alpha} = 1.5405$

Refined parameters (Å): a = 17.423 ± .008, b = 14.952 ± .009, c = 3.959 ± .003

Conditions for non-extinction: none

Theta tolerance = .038

Temperature: 410° C. Formed from heating emplectite above 390° C. Compare this refinement with Table 67

I	d (meas.)	hkl	d (calc.)	theta (calc.)	theta (meas.)	theta diff.	
9	3.607	201	3.604	12.340	12.330	.010	
9	3.458	240	3.435	12.957	12.870	.087	R
7	3.231	221	3.247	13.724	13.790	-.066	R
10	3.101	031	3.100	14.387	14.380	.007	
2	2.945	150	2.947	15.149	15.160	-.011	
6	2.845	610	2.851	15.676	15.710	-.034	
7	2.733	331	2.735	16.359	16.370	-.011	
1	2.553	540	2.549	17.589	17.560	.029	
6	2.176	800	2.178	20.711	20.730	-.019	
6	2.107	701	2.107	21.441	21.410	.001	
6	2.018	560	2.027	22.333	22.440	-.107	R
5	1.732	10·10	1.731	26.428	26.410	.018	
4	1.682	181	1.682	27.250	27.250	.000	
2	1.616	770	1.621	28.371	28.470	-.099	R
3	1.461	681	1.461	31.823	31.820	.003	
2	1.432	272	1.432	32.537	32.540	.003	
		742	1.431	32.560			

TABLE 69

Cuprobismutite $Cu_2S \cdot Bi_2S_3$

$\lambda = Co_{K\alpha} = 1.7902$

Monoclinic: C2/m

Refined parameters (Å): a = 17.646 ± .007, b = 3.935 ± .003,
c = 15.258 ± .005, β = 100°31' ± 2.3'

Conditions for non-extinction: hkl h+k = 2 n
hol h = 2 n
oko k = 2 n

Theta tolerance = .048

Formed from heating emplectite to 390° C, quenched, and X-rayed at room temperature on the Nonius camera.

I	d (meas.)	hkl	d (calc.)	theta (calc.)	theta (meas.)	theta diff.	
2	6.283	-202	6.268	8.210	8.190	.020	
1	5.206	202	5.222	9.869	9.900	-.031	
1	5.021	003	5.001	10.311	10.270	.041	
3	4.374	-401	4.386	11.776	11.810	-.034	
1/2	4.091	-402	4.092	12.634	12.640	-.006	
2	3.848	110	3.827	13.489	13.450	.039	
1	3.703	-204	3.697	14.012	13.990	.022	
8	3.624	-403	3.620	14.317	14.300	.017	
6	3.465	-112	3.474	14.933	14.970	-.037	
8	3.238	204	3.234	16.067	16.050	.017	
2	31.30	-404	31.134	16.596	16.620	-.024	
2	3.115	311	3.114	16.706	16.700	.006	
10	3.090	-312	3.103	16.765	16.840	-.075	R
1	2.944	-601	2.941	17.720	17.700	.020	
1/2	2.878	312	2.879	18.116	18.120	-.004	
6	2.858	-313	2.865	18.208	18.250	-.042	
9	2.726	-603	2.728	19.152	19.170	-.017	
1/2	2.684	205	2.688	19.450	19.480	-.030	
1/2	2.555	602	2.547	20.578	20.510		
1/2	2.528	-206	2.528	20.733	20.740	-.007	
1/2	2.331	-315	2.328	22.614	22.580	.034	
1	2.297	206	2.094	22.970	22.940	.030	
1/2	2.194	-802	2.193	24.091	24.080	.011	
6	2.173	-207	2.175	24.302	24.330	-.028	
		800	2.169	24.376			
1	2.135	-116	2.135	24.792	24.790	.002	
2	2.105				25.160		
2	2.094				25.310		
1	2.046				25.940		
1/2	2.008				26.480		
2	1.996				26.640		
1/2	1.943				27.430		
1	1.895				28.180		
1/2	1.881				28.410		
1/2	1.869				28.610		

TABLE 70

Phase X $3Cu_2S \cdot 5Bi_2S_3$

$\lambda = Cu_{k\alpha} = 1.5405$

Monoclinic: C2/m

Refined parameters (Å): a = 13.072 ± .026, b = 4.005 ± .007,
c = 14.687 ± .092, β = 99°18' ± 24'

Conditons for non-extinction: none

Theta tolerance = .088

Temperature: 480° C. Formed from heating emplectite.

I	d (meas.)	hkl	d (calc.)	theta (calc.)	theta (meas.)	theta diff.	
6	3.613	203	3.598	12.362	12.310	.052	
10	3.458	302	3.461	12.860			
		-112	3.451	12.895	12.870	.025	
2	3.309	112	3.317	13.426	13.460	-.034	
7	2.955	204	2.961	15.076	15.110	-.034	
1	2.178	-601	2.178	20.706	20.710	-.004	
7	2.112	-406	2.103	21.480	21.390	.090	R
2	1.976	602	1.976	22.943	22.940	.003	
3	1.908	-221	1.908	23.813	23.810	.003	
1/2	1.828	222	1.827	24.928	24.920	.008	

TABLE 71

Wittichenite $3Cu_2S \cdot Bi_2S_3$

Orthorhombic: $P2_12_12_1$ $\lambda = Cu_{k\alpha} = 1.5405$

Refined parameters (Å): a = 7.723 ± .005, b = 10.295 ± .012, c = 6.741 ± .004

Conditions for non-extinction: none

Theta tolerance = .026

Temperature: 480° C. Formed from heating emplectite.

I	d (meas.)	hkl	d (calc.)	theta (calc.)	theta (meas.)	theta diff.	
3	3.864	200	3.861	11.506	11.498	.008	
6	3.613	210	3.615	12.301			
		121	3.615	12.302	12.310	-.008	
2	3.116	130	3.136	14.219	14.310	-.091	R
7	2.955	112	2.959	15.090	15.110	-.020	
10	2.843	131	2.843	15.718	15.720	-.002	
1/2	2.650	122	2.649	16.906	16.900	.006	
1	2.278	222	2.277	19.770	19.760	.010	
1	2.178	321	2.179	20.703	20.711	-.008	
7	2.112	113	2.112	21.394	21.390	.004	
1/2	1.828	411	1.827	24.941	24.921	.020	
		133	1.826	24.943			

TABLE 72

Wittichenite $3Cu_2S \cdot Bi_2S_3$

Orthorhombic: $P2_12_12_1$ $\lambda = Co_{k\alpha} = 1.7902$

Refined parameters (Å): a = 7.691 ± .005, b = 10.343 ± .005, c = 6.701 ± .004

Conditions for non-extinction: h00 h = 2n
0k0 k = 2n
001 l = 2n

Theta tolerance = .041

Formed from heating emplectite to 490° C, quenched, and X-rayed at room temperature on the Nonius camera

I	d (meas.)	hkl	d (calc.)	theta (calc.)	theta (meas.)	theta diff.	
2	5.623	011	5.624	9.158	9.160	-.002	
2	4.548	111	4.540	11.372	11.350	.022	
1	3.851	200	3.846	13.460	13.440	..020	
7	3.619	121	3.614	14.341	14.320	.021	
7	3.602	210	3.604	14.379	14.390	-.011	
2	3.356	002	3.350	15.495	15.470	.025	
3	3.184	012	3.187	16.310	16.330	-.020	
6	3.084	220	3.086	16.862	16.870	-.008	
7	2.949	112	2.945	17.697	17.670	.027	
10	2.858	131	2.848	18.320	18.250	.070	R
3	2.644	122	2.641	19.812	19.790	.022	
1	2.584	040	2.586	20.254	20.270	-.016	
1	2.399	231	2.397	21.926	21.910	.016	
3	2.269	222	2.270	23.226	23.240	-.014	
1/2	2.057	330	2.057	25.792	25.790	.002	
2	1.996	150	1.998	26.622	26.640	-.018	
1/2	1.929	203	1.931	27.609	27.640	-.031	
4	1.894	322	1.894	28.195	28.210	-.015	
2	1.823	250	1.822	29.430	29.410	.020	
		133	1.823	29.438			

TABLE 73

Phase X $3Cu_2S \cdot 5Bi_2S_3$

Monoclinic: C2/m $\lambda = Co_{k\alpha} = 1.7902$

Refined parameters (Å): a = 13.075 ± .009, b = 4.006 ± .003,
c = 14.705 ± .009, β = 99°20' ± 4'

Conditons for non-extinction: hkl h+k = 2n
hol h = 2 n
oko k = 2n

Theta tolerance = .068

Formed from heating emplectite to 490° C, quenched, and X-rayed at room temperature on the Nonius camera

I	d (meas.)	hkl	d (calc.)	theta (calc.)	theta (meas.)	theta diff.
1	4.490	202	4.474	11.542	11.500	.042
7	3.619	004	3.627	14.285	14.320	-.034
7	3.602	203	3.600	14.400	14.390	.010
10	3.456	-112	3.453	15.022	15.010	.012
1	3.139	-402	3.143	16.548	16.570	-.022
1/2	2.897	005	2.902	17.966	18.000	-.034
6	2.824	-205	2.823	18.483	18.480	.003
3	2.644	-313	2.640	19.822	19.790	.032
1/2	2.612	312	2.619	19.984	20.040	-.056
1	2.508	403	2.502	20.958	20.910	.048
1	2.399	-206	2.396	21.938	21.910	.028
3	2.177	-601	2.179	24.255	24.280	-.025
3	2.110	-406	2.106	25.154	25.100	.054
2	2.095	-603	2.095	25.292	25.300	-.008
2	1.996	-604	1.997	26.625	26.640	-.015
2	1.985	-514	1.985	26.805	26.800	.005
		021	1.984	26.815		
4	1.958	315	1.957	27.220	27.210	.010
1/2	1.929	022	1.931	27.619	27.640	-.021
1/2	1.910	-221	1.908	27.970	27.950	.020
2	1.823	-208	1.825	29.373	29.410	-.037